ANCR-1032

NASA CR-120824

PHASE I TOPICAL REPORT

FLOWING GAS, NON-NUCLEAR EXPERIMENTS ON THE GAS CORE REACTOR

J. F. Kunze
D. H. Suckling
C. G. Cooper

Prepared for
NATIONAL AERONAUTICS AND SPACE ADMINISTRATION
Contract C-59718B

R. E. Hyland, NASA-Lewis
Technical Project Manager

Date Published - February 1972

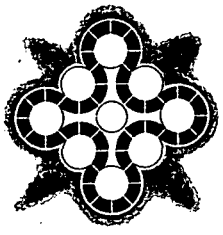

Aerojet Nuclear Company

NATIONAL REACTOR TESTING STATION
Idaho Falls, Idaho - 83401

Printed in the United States of America
Available from
National Technical Information Service
U. S. Department of Commerce
5285 Port Royal Road
Springfield, Virginia 22151
Price: Printed Copy $3.00; Microfiche $0.95

1. Report No.	2. Government Accession No.	3. Recipient's Catalog No.
NASA CR-120824		

4. Title and Subtitle	5. Report Date
PHASE I TOPICAL REPORT FLOWING GAS, NON-NUCLEAR EXPERIMENTS ON THE GAS CORE REACTOR	February 1972
	6. Performing Organization Code

7. Author(s)	8. Performing Organization Report No.
J. F. Kunze, D. H. Suckling, and C. G. Cooper	ANCR-1032
	10. Work Unit No.
9. Performing Organization Name and Address	
Aerojet Nuclear Company Idaho Falls, Idaho 83401	11. Contract or Grant No. C-59718B
	13. Type of Report and Period Covered
12. Sponsoring Agency Name and Address	Contractor Report
National Aeronautics and Space Administration Washington, D.C. 20546	14. Sponsoring Agency Code

15. Supplementary Notes

Technical Project Manager, R. E. Hyland, Advanced Concepts Branch, NASA Lewis Research Center, Cleveland, Ohio 44135

16. Abstract

Flow tests have been conducted on models of the gas core (cavity) reactor. Variations in cavity wall and injection configurations were aimed at establishing flow patterns that give a maximum of the nuclear criticality eigenvalue. Correlation with the nuclear effect was made using multigroup diffusion theory normalized by previous benchmark critical experiments. Air was used to simulate the hydrogen propellant in the flow tests, and smoked air or argon or freon to simulate the central nuclear fuel gas. All tests were run in the down-firing direction so that gravitational effects simulated the acceleration effect of a rocket. Results showed that acceptable flow patterns with high volume fraction for the simulated nuclear fuel gas and high flow rate ratios of propellant to fuel can be obtained. Using a "point" injector for the fuel, good flow patterns are obtained by directing the outer gas at high velocity along the cavity wall, using louvered or oblique-angle-honeycomb injection schemes.

17. Key Words (Suggested by Author(s))	18. Distribution Statement
Gas Core Reactor Flow Patterns Nuclear Criticality	Unclassified - Unlimited

19. Security Classif. (of this report)	20. Security Classif. (of this page)	21. No. of Pages	22. Price*
Unclassified	Unclassified	92	$3.00

* For sale by the National Technical Information Service, Springfield, Virginia 22151

ACKNOWLEDGEMENTS

Acknowledgement is made to J. H. Lofthouse, R. R. Jones, H. G. Miller, and Dr. R. C. Young for their significant contributions to various phases of the experiment.

TABLE OF CONTENTS

TABLES

TABLE OF CONTENTS

(Cont'd)

TABLE OF CONTENTS

(Cont'd)

TABLE OF CONTENTS

(Cont'd)

1.0 SUMMARY

Result of a flow-experiment program on the open cycle gas core concept are discussed in this report. The program was designed to study conditions that achieve the volume fractions of central gas (uranium) that makes criticality in a gas core reactor possible. The results from prior critical experiments on gas-core reactors were used as the basis for selecting the type of flow patterns that would be optimum. The flow test apparatus was designed for ease of modifications, such that the cavity walls and inner gas injector could be readily modified with minimum expense.

Results described in the document cover experiments through August 1971, and included tests on a variety of small (18-inch diamter) configurations and on larger 36-inch diameter configurations. The latter size is nominally the minimum cavity sphere that can be expected to go critical in the presence of hydrogen, and at high temperature conditions.

The conclusions from these flow tests are favorable to the overall open cycle concept. High volume flow ratios (> 100/1) of inner to outer gases can be achieved with good flow patterns. The central gas under these best conditions can be shown to occupy net volume fractions of approximately 50% in the "two-dimensional" tests and 35% in the three dimensional tests. Gravity, acting in the direction of the exhaust nozzle, has been used to simulate acceleration effects in the rocket. Where the inner gas is of higher density than the outer, it was found to be significantly more difficult to obtain the desired flow patterns when gravitational effects were present (gases of different density).

2.0 INTRODUCTION

The open cycle co-axial flow gas core concept[1] is shown in Figure 2.1. This concept has been studied experimentally in a number of laboratories. The flow patterns, with high ratios of outer to inner gas flow rates, have been studied previously in cylindrical geometry experiments[2,3]. Critical experiments to study the reactor physics characteristics of a dilute gas core surrounded with hydrogen and a low absorption moderator (heavy water) have also been reported[4,5]. The ideal geometry for criticality is a sphere, with large volume fraction of central fissile material in the gaseous cavity. In 1969, Lanzo[6] performed the first spherical geometry flow experiments and found that flow patterns could be attained that ostensibly would create a configuration capable of attaining nuclear criticality with gas pressures in the cavity which would not be impractical for an operating system (less than 1000 atm pressure). Since that time, a series of flow experiments on spherical or pseudo-spherical chambers have been conducted at Aerojet Nuclear, with direct consideration being given to establishing those conditions which are nuclearly feasible as well as economically practical. The goals are minimum cavity pressures, maximum propellant to nuclear fuel flow rate ratios, minimum reactor size, and, more recently, overall low flow rates to correspond to low thrust conditions for the application rocket.

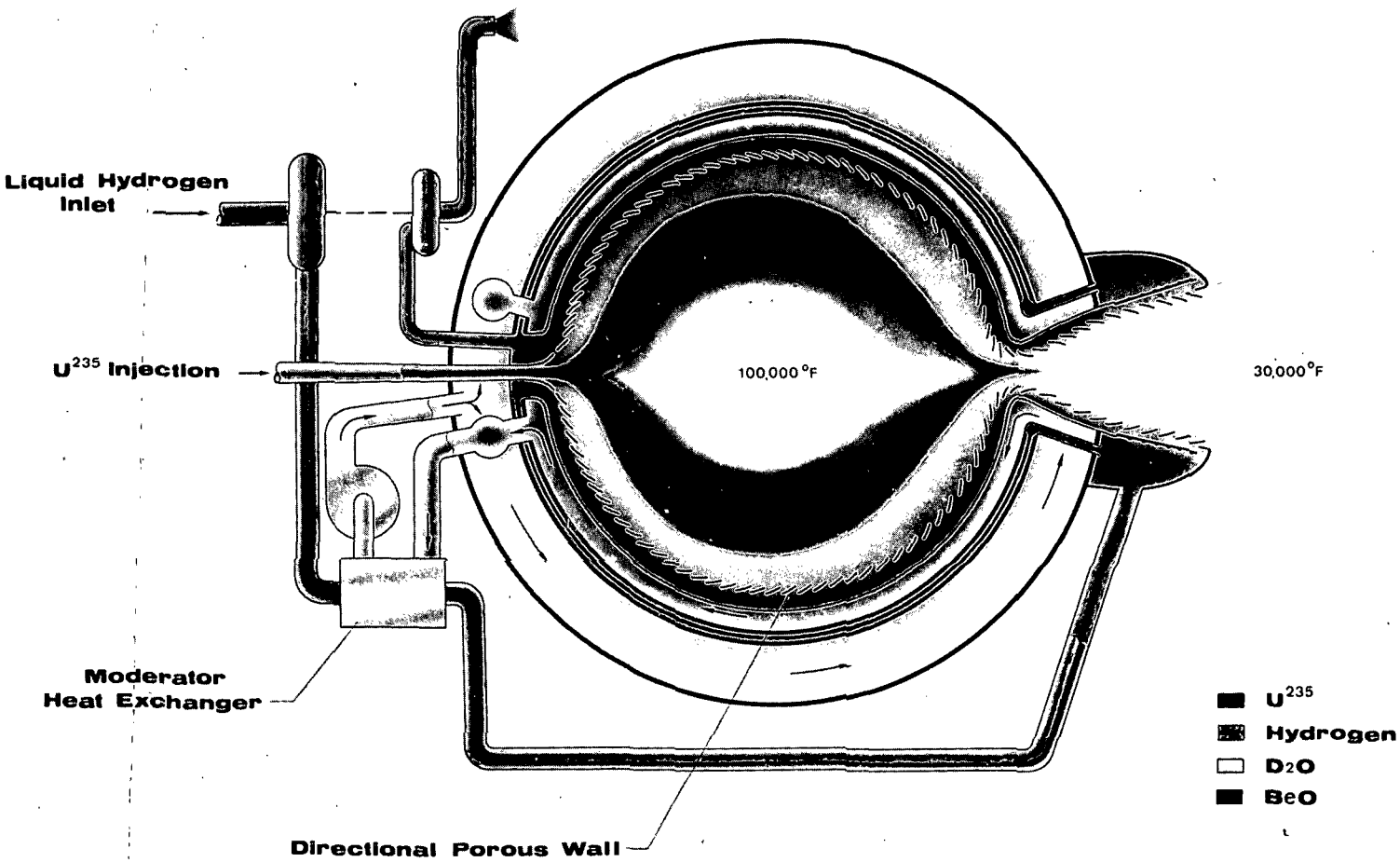

Fig. 2.1 Open Cycle Gas Core Concept

3.0 TEST APPARATUS

The apparatus for the flow tests was designed so that modifications to the cavity shape, walls, the injector, and the exhaust nozzle could be made relatively easily and inexpensively. The important consideration was ease of disassembly. Fine adjustments to the flow into various regions of the cavity could be accomplished by installing baffles or flow restrictors, but precise measurement of flow rates could be made only on the total inner gas flow and total outer gas flow.

The apparatus is shown in Figure 3.1. The outside flow was provided by a large blower feeding an 8-inch pipe into which was installed an interchangeable orifice for monitoring a wide range of flow rates, from 50 cfm to 1500 cfm. The monitoring section of the pipe was sufficient to eliminate end effects for the orifice measurements (see Appendix A). The outer gas then entered the test box through a number of baffles and finally a grid plate, such that all areas of the cavity walls experienced the same pressure and velocity-of-approach conditions. The cavity wall was then installed inside the test box. Figures 3.2 and 3.4 show typical setups. In this configuration the main cavity wall was perforated metal sheet (Figure 3.7) on which were installed louvers also made from perforated sheet metal. The characteristics of the perforated sheets used in the various experiments is given in Table 3.1. For some tests, "Scott Foam" (Figure 3.7) was installed on the walls and/or louvers at selected locations in order to redistribute flow. In other tests, the walls and louvers were replaced by a honeycomb wall (Figures 3.3 and 3.7); and finally in the truly spherical cavity tests, neither the walls nor louvers had perforations (Figure 3.5). Instead thin plexiglas sheets were formed into overlapping spherical curves to provide louvers, and to give complete visual access to events inside the cavity. These solid walls did not provide for simulation of transpiration cooling. However, it had previously been shown that a small amount of transpiration cooling had little or no effect on the flow patterns.

For the so-called "two-dimensional" tests, the cavity shape was flat in the direction perpendicular to the viewing direction. This arrangement facilitated viewing and interpretation of the tests and made the construction of a number of different cavity shapes relatively simple. The flat end walls, which were also walls of the test box, did perturb the flow patterns. However, this end perturbation extended only a few inches from the viewing wall surface, and at least qualitatively did not compromise the interpretation of the test results. The more appropriate tests were those with truly three-dimensional curvature. In these, all of the cavity walls were internal to the walls of the test box.

The inner gas was provided by a smaller blower--or by facility compressed air, or by a gas bottle in the case of argon or freon. This flow was introduced into a smoke-mixing box, where smoke from an oil-heater-smoke-generator was introduced. In this large 30 cubic foot box the smoke was mixed with the central gas by the injected oil-droplet smoke jet and/or by means of a small circulating fan.* With smoke demands of between 1 and 6 cubic feet per

---

* Subsequently it was found desirable to circulate the smoke as little as possible, since circulation appeared to hasten the process of agglomeration, resulting in rapid loss of smoke density before the smoke even left the mixing box.

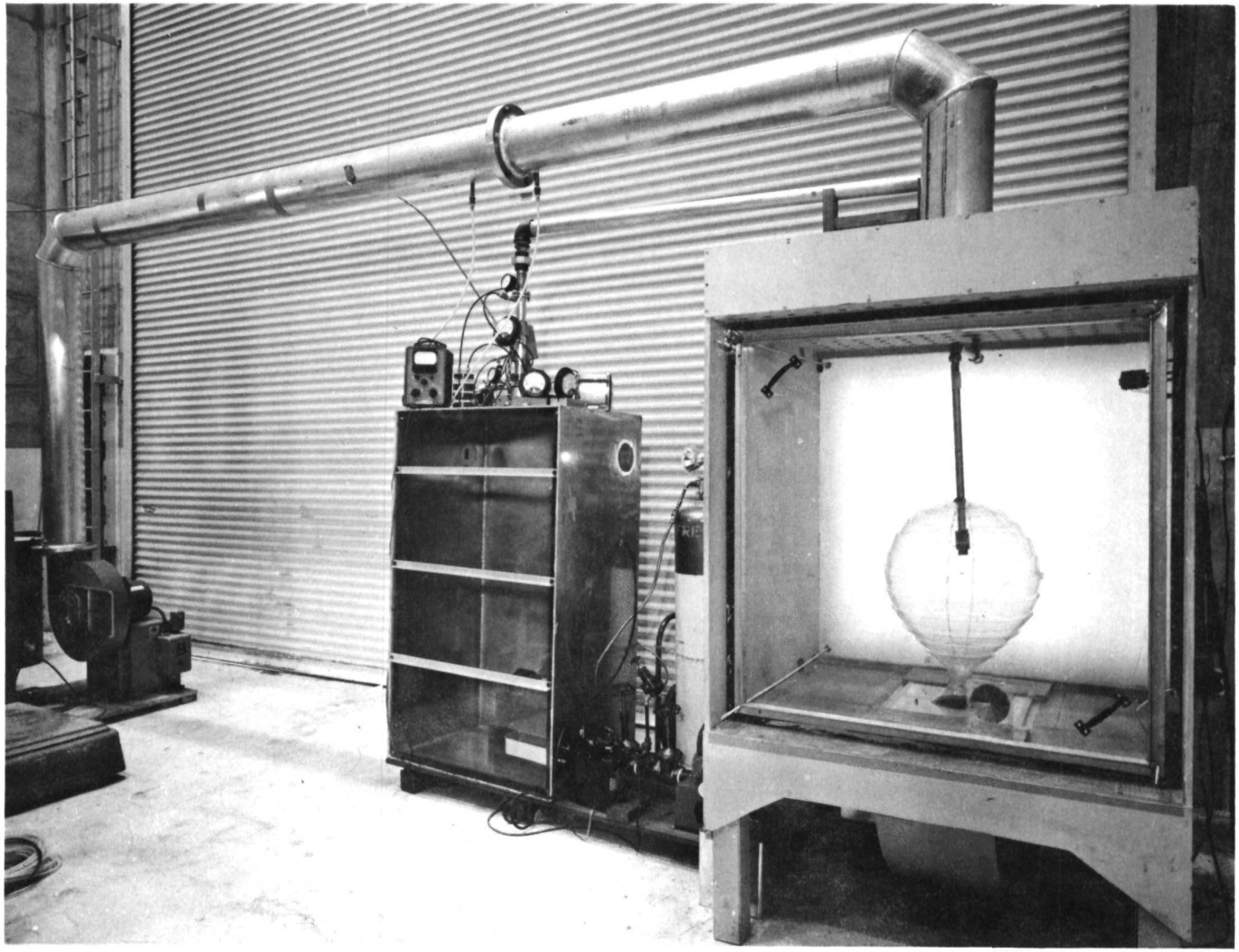

Fig. 3.1 Experimental apparatus showing blowers, smoke-mixing box, and test box

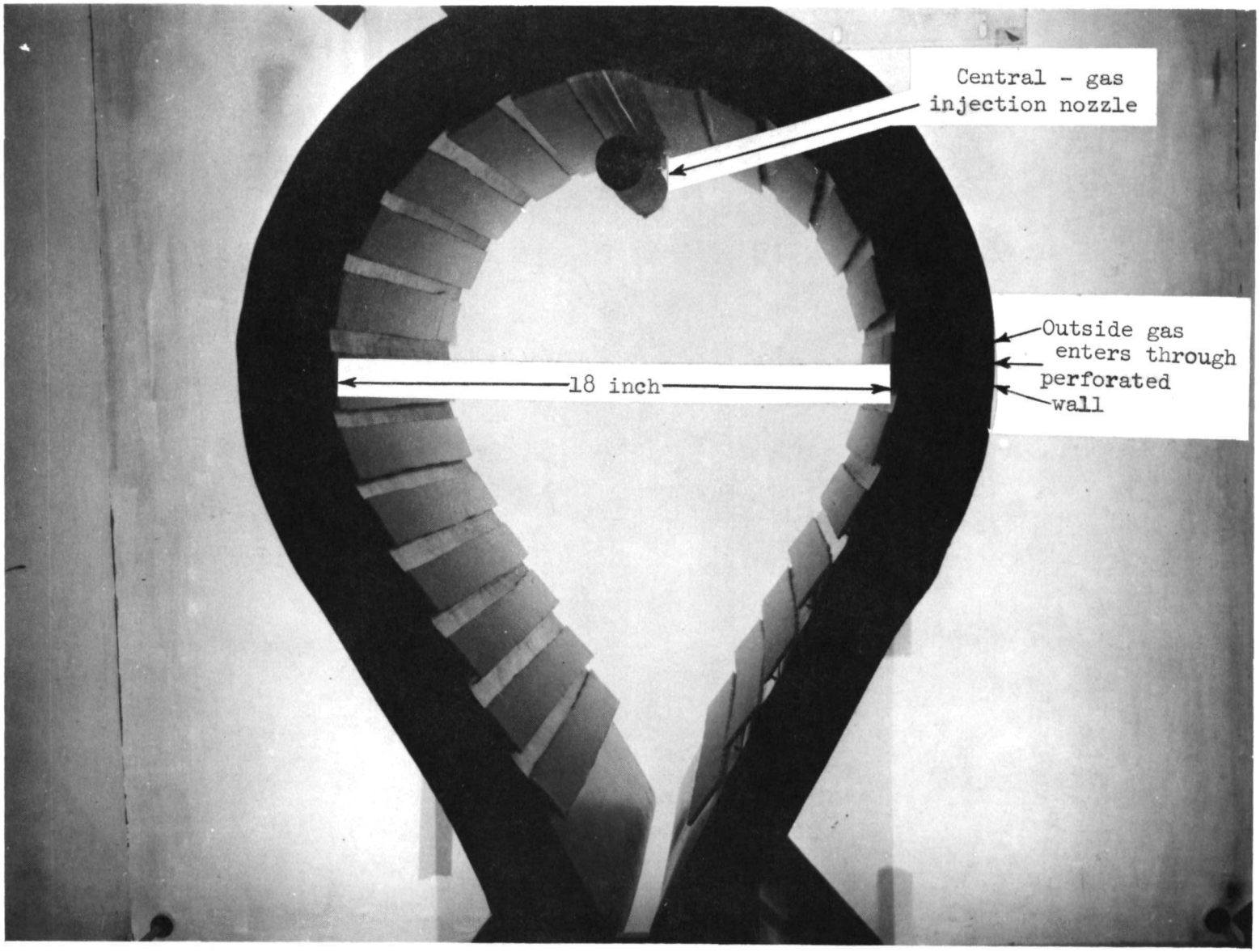

Fig. 3.2 View of 18" cavity, showing louvers with foam covering

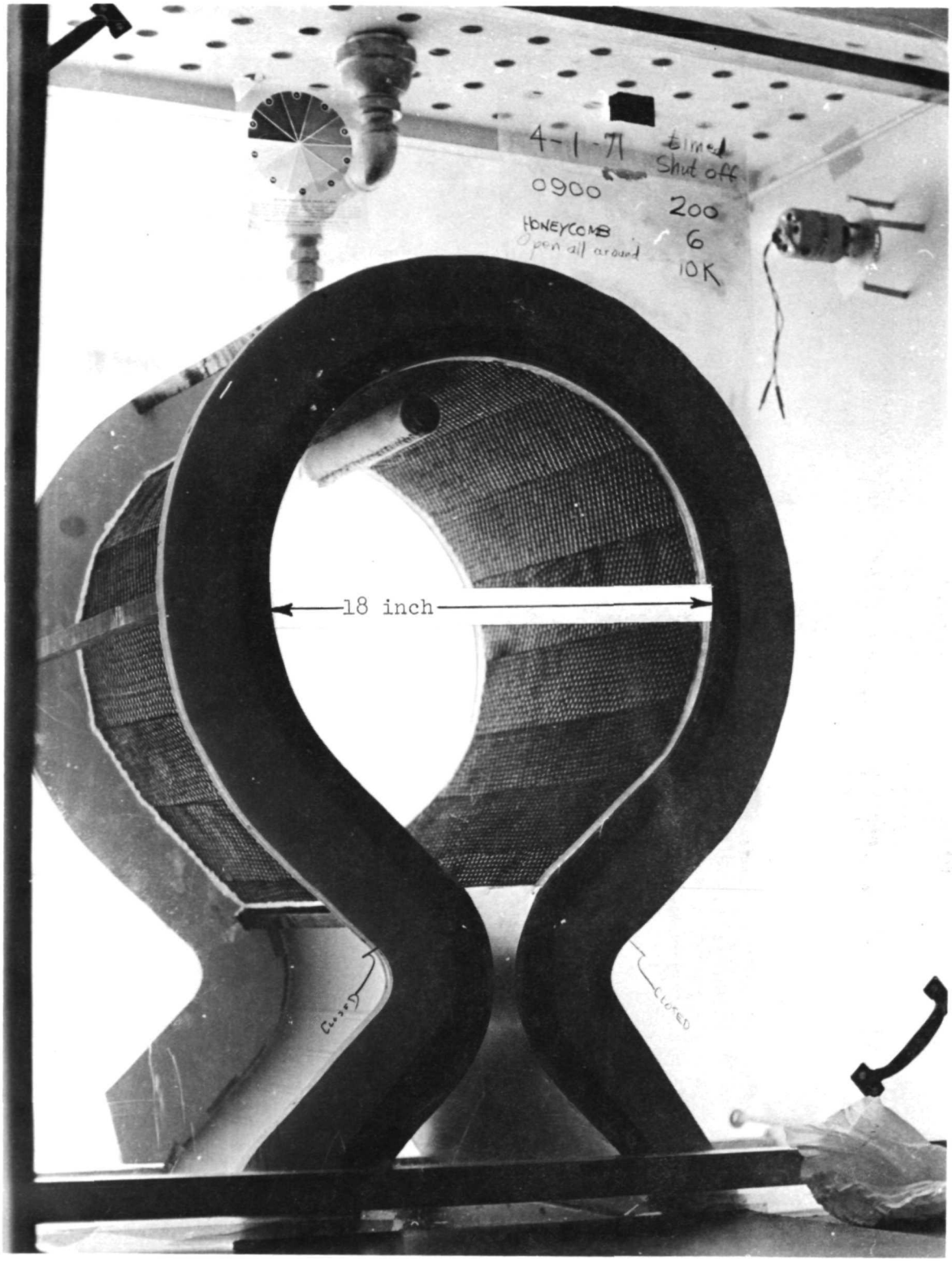

Fig. 3.3 View of 18" diameter cavity with "honeycomb"wall. Honeycomb angle is 20° to the tangent of the wall

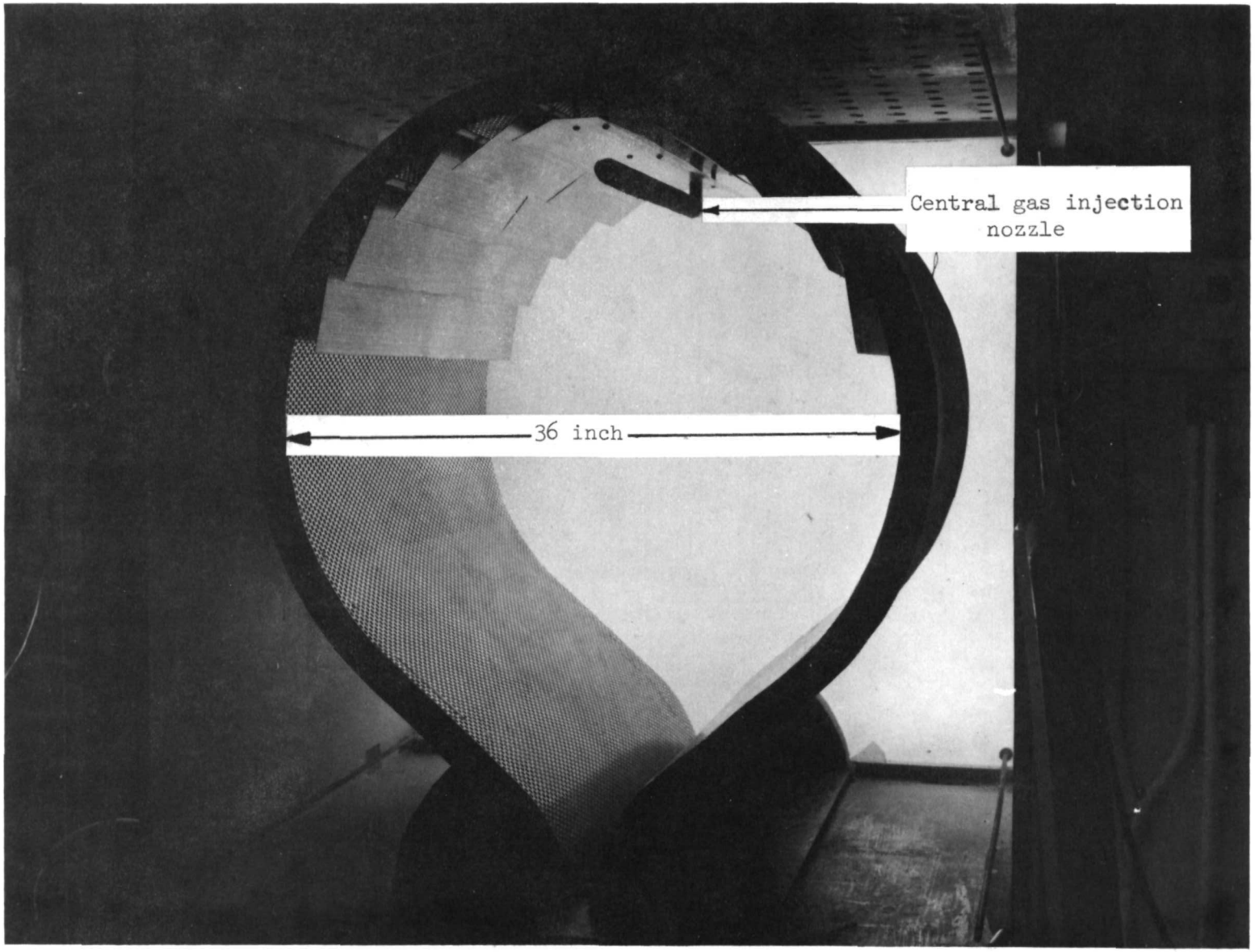

Fig. 3.4 View of three-ft diameter cavity with louvers on upper third of wall

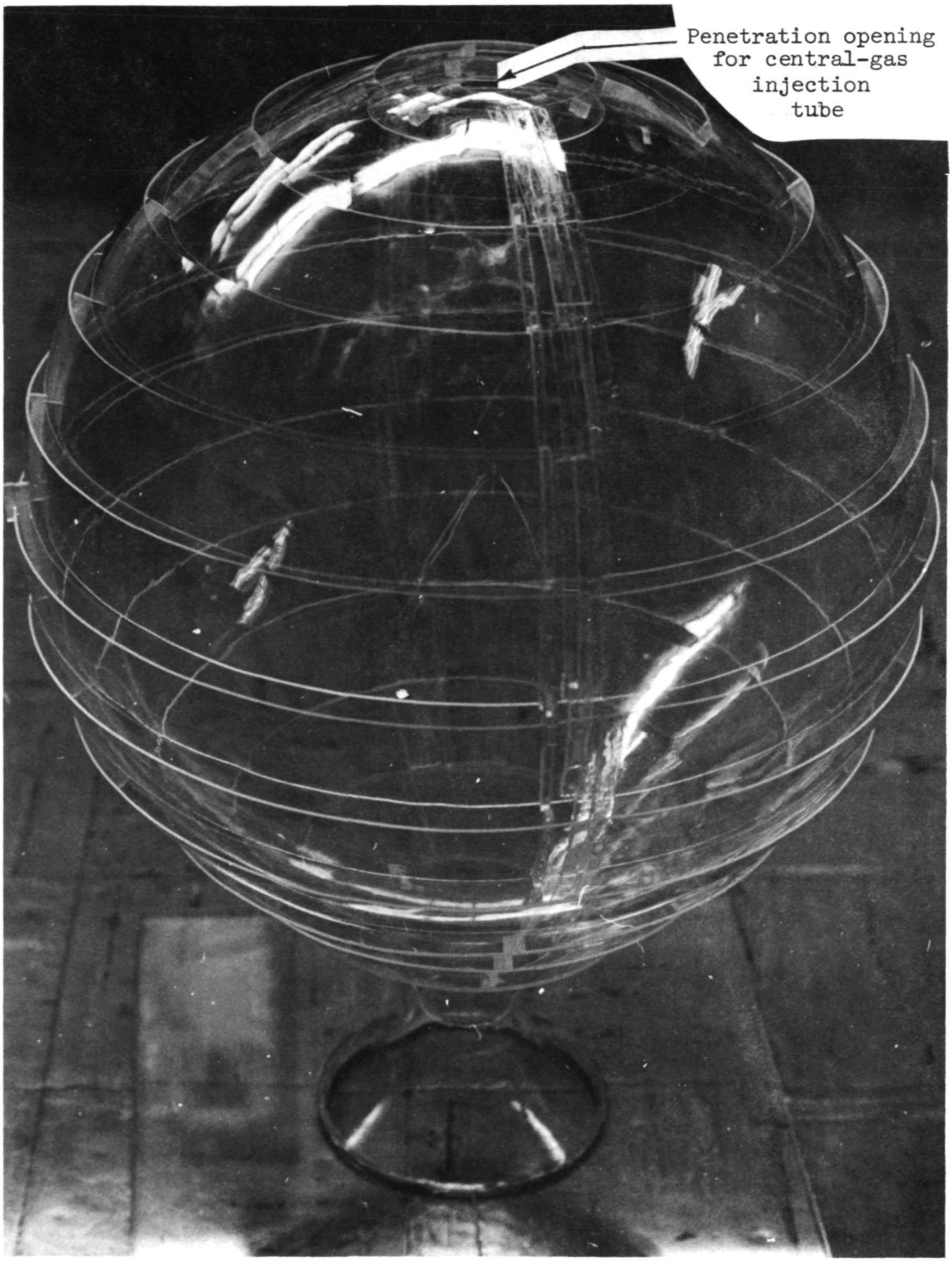

Fig. 3.5 View of 18" spherical cavity with 18-inch minor diameter. Unperforated walls & louvers

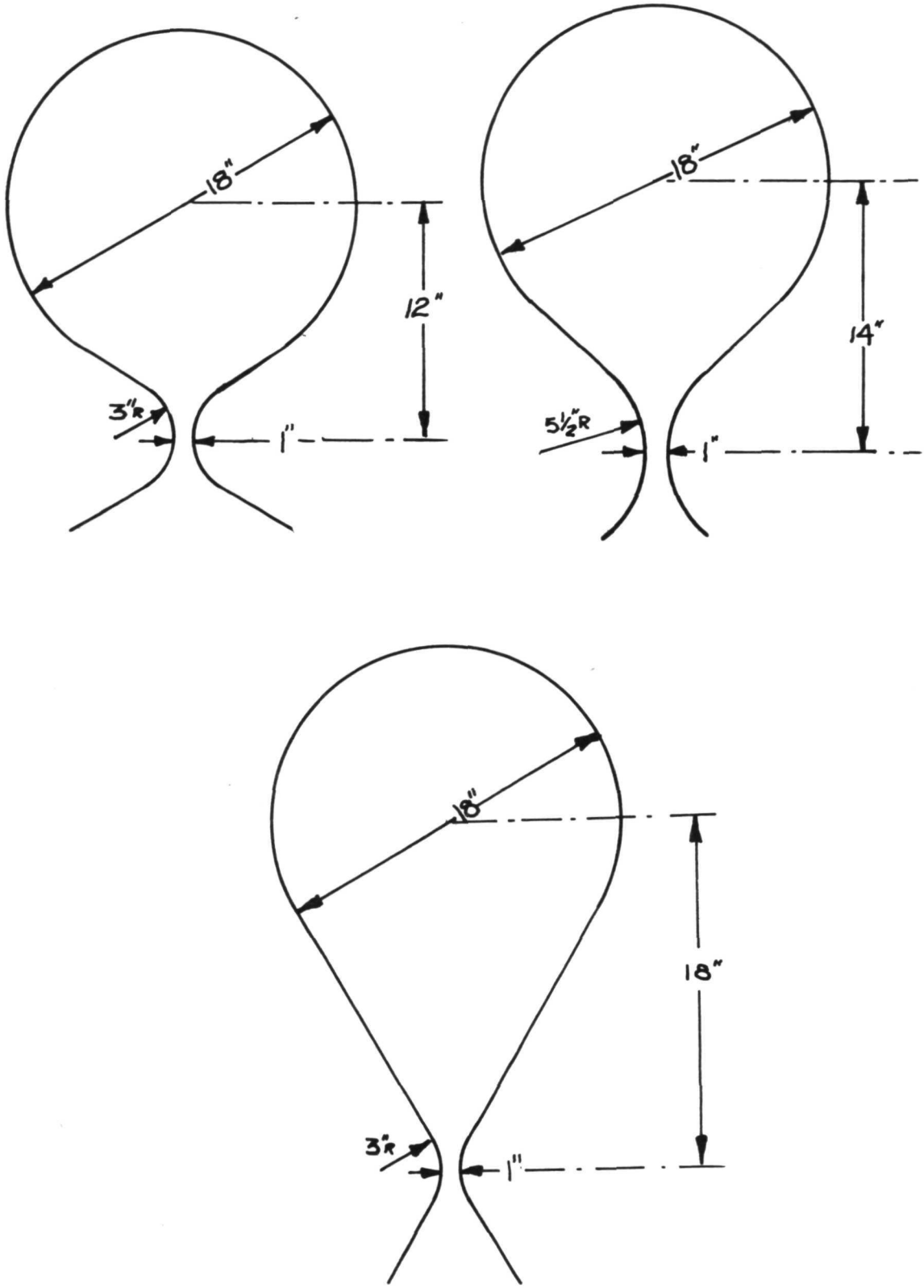

Fig. 3.6 Three different cavity shapes tested for the effect on flow patterns

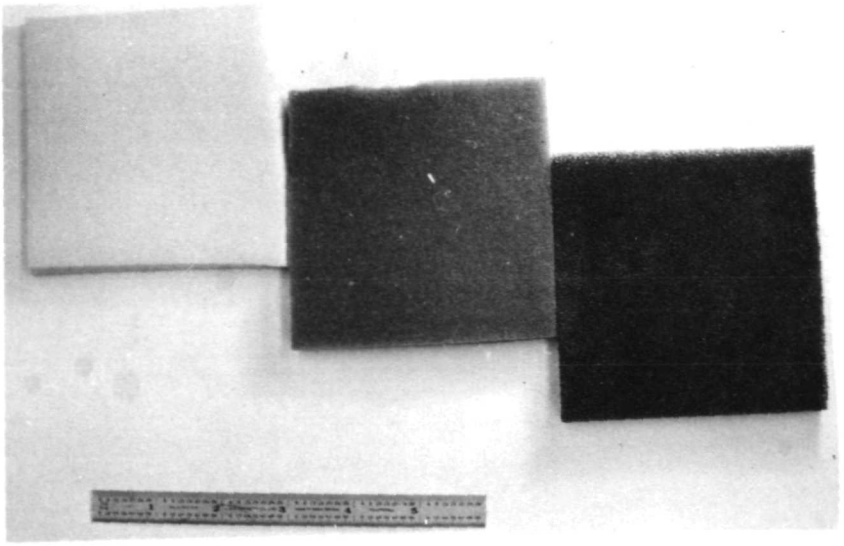

"Scott Foam"

80, 60, and 30 pores per lineal inch

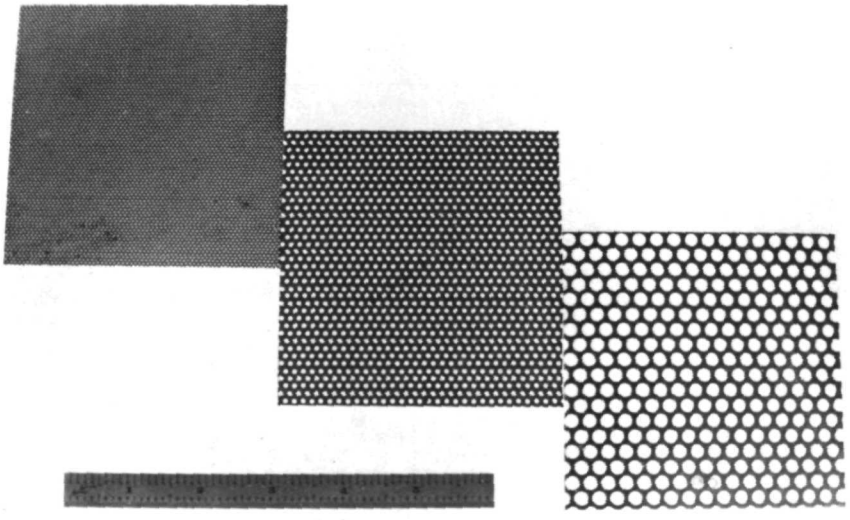

Screen Material

0.024 inch dia. by 18% open, 0.0625 inch dia by 22% open, 0.183 inch dia. by 50% open

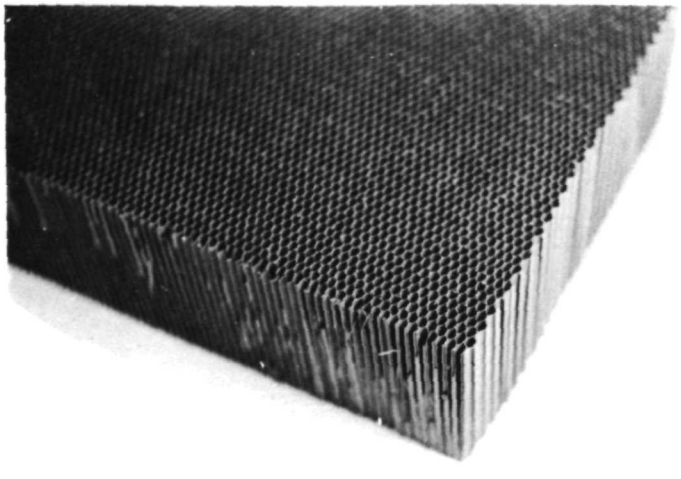

Honeycomb

nominal 0.25 inch across flats of hexagonal cell, 6 inches long

Fig. 3.7 Special materials used for cavity walls and injectors

Table 3.1

Characteristics of Walls and Louvers of Cavity

18-inch diameter cavities (all three shapes)	Walls: 0.024 in. diameter holes 18% open Louvers*: 0.024 in. diameter by 18% open, and 0.0625 in. diameter by 22-1/2% open
18-inch diameter honeycomb-walled cavity	1/4 in. (nominal) hexagonal honeycomb, aligned at 20° to the wall tangent.
36-inch diameter cavity	Walls: 0.3125 in. diameter holes, 47% open Louvers*: 0.0625 in. diameter holes 22-1/2% and 30% open

* Louvers were variously used "as-is", covered with foam, or completely sealed with plastic.

Characteristics of Scott** Foam Used to Restrict Flow Through Walls and Louvers

Type	Flow Velocity Through 1-inch Thickness	
	Δp=0.5 inches H_2O	Δp=0.25 inches H_2O
80 pores per linear inch	220 ft/min	140 ft/min
60 pres per linear inch	370	230
30 pores per linear inch	730	470

** Data furnished by Scott Paper Company, Chester, Pa.

minute, the large box provided a smoke accumulator such that relatively constant density smoke flow could be achieved for reasonable periods of time. The output from the smoke box was at the top. Also at the top was a light-beam smoke-density monitor. This was used to establish uniform smoke densities for all tests for the smoke entering the pipe on its way to the test chamber. In this pipe was a long orifice flow measuring section. The smoke was then directed down to the injection nozzle inside the cavity.

The central gas injection conditions were designed to simulate injection conditions in an operating high temperature cavity. There it is assumed that the uranium will be fed into the cavity as a fine powder, small pellets, or a thin wire. As the solid uranium contacts the very hot gaseous conditions of the cavity, the solid will quickly vaporize, essentially exploding. Thus, point injection conditions needed to be simulated in these flow tests. In the three-dimensional tests this could easily be simulated by using a thin pipe with a small diffuser on the end. In the two-dimensional tests however, it was necessary to elongate the pipe such that the central gas entered over a length of pipe approximately equal to the cavity width.

The outer gas, after entering through the walls of the cavity, was discharged along with the small amount of inner gas through a nozzle in the bottom of the cavity. A nozzle exit path of about 5 L/D ratio was provided. Of the various cavity shapes tested, the three basic ones are shown in Figure 3.6. Initially, a relatively round cavity with an unaccentuated nozzle exit was installed. The nearly perfectly round shape is the most compatible for nuclear criticality considerations. Following these tests, a relatively accentuated elongated nozzle was designed, and that cavity shape is shown in the middle of Figure 3.6. Finally, a so-called modified round shape, as shown on the right of Figure 3.6, was adopted for most of the remaining tests. This basic shape was used in the large 36-inch diameter cavity as well as in the spherical cavity.

4.0 TEST PROCEDURES

The procedures for operating the tests were relatively straight forward. Constant flow was established in both the outer and inner gas circuits. The flow rates were monitored visually on differential pressure meters. Flow rates were adjusted by means of valves at each air source, i.e., the blower or the gas bottle. The only adjustments provided beyond this point were at the walls of the cavity, where Scott foam or plastic sheet was used to partially or fully restrict air flow through certain portions of the cavity wall. Typical pressure-drop versus flow curves are shown in Figure 4.1. Appendix A shows the standard fluid flow formulas used to derive these curves and gives the relationship for flow in the inner gas circuit of air vs. argon vs. freon. Thus, the basic data for each test were the two flow rates and photographs of the flow patterns.

Supplementary data consisted of flow velocity measurements within the cavity. These were made with hot wire anemometers. Such measurements were made without the inner gas flowing, since its flow velocity inside the cavity and its perturbing effect on the outer gas flow were too small to measure with a standard anemometer. More important supplemental information was obtained by scanning the photographs with a densitometer in order to determine smoke densities throughout the cavity. To obtain satisfactory pictures for densitometer scanning, time exposures were taken. These averaged-out the time dependent fluctuations in the smoke density. In order to obtain photographs which could be scanned for density and readily converted to smoke density, it was necessary to operate the photographic film on the linear portion of the log density exposure curve. To establish the best combination of exposure smoke density and development time, wedge tests of smoke density were made. For these tests a wedge-shape was installed in the test region, and photographs of this wedge filled with smoke were subsequently scanned by the densitometer. That combination which gave the most linear density trace along the wedge was chosen as the standard condition. Henceforth, all inlet smoke conditions were established to be the same as those for the selected most linear wedge test result. The inlet smoke conditions were monitored at the top of the smoke mixing box by means of a light beam and photo cell which penetrated the full width of the box.

The time exposure photographs were scanned on an automatic scanning densitometer. Traces were obtained radially across the cavity at a number of different longitudinal locations. The resultant traces were normalized for smoke densities varying between 0 and 100%. The 100% value was established as the density at the outlet of the injection nozzle. For the two-dimensional cavity tests, the effective density through the cavity could easily be interpreted directly from the smoke density traces, and the isodensity lines could be directly plotted accordingly.

In the case of the three-dimensional cavity with chord lengths varying across the scan, density interpretations could not be directly made. The density had to be unfolded from the observed density traces. The unfolding scheme is equivalent to solving for the coefficients in a matrix of simultaneous equations. The method used and computer program for the unfolding scheme are shown in Appendix C. Furthermore, background corrections were made in the data reduction program so as to correct for the varying attenuation of the walls of the Plexiglas sphere and of variations in lighting conditions. Thus, the three-dimensional tests required a rather involved process to obtain the radial smoke density function. For the two-dimensional tests the process was quite simple, since chord-viewing-

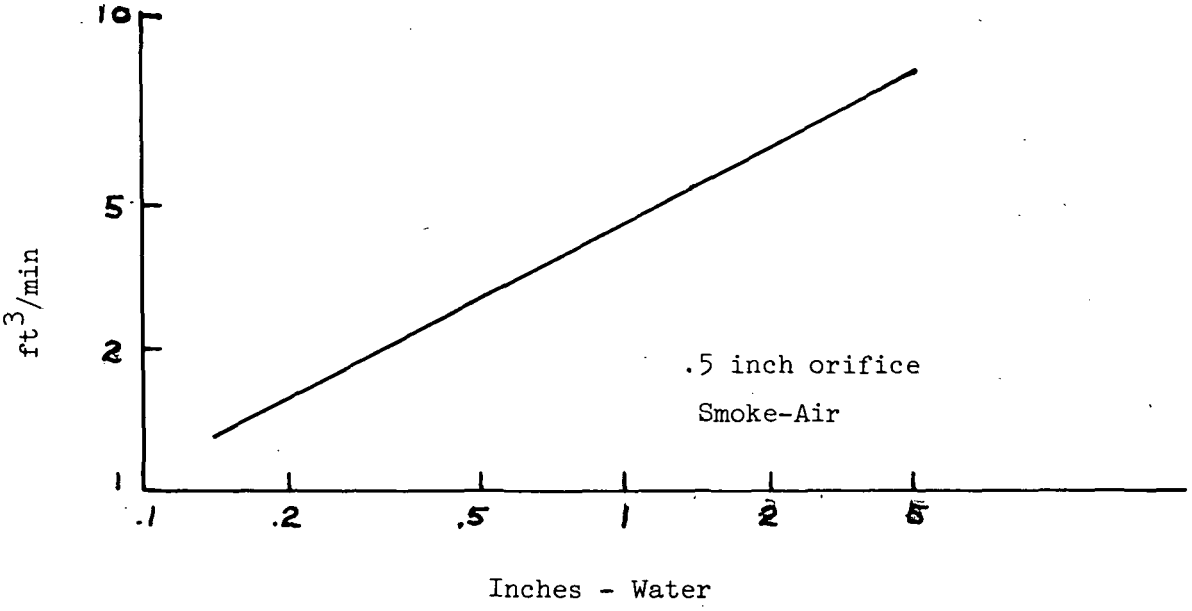

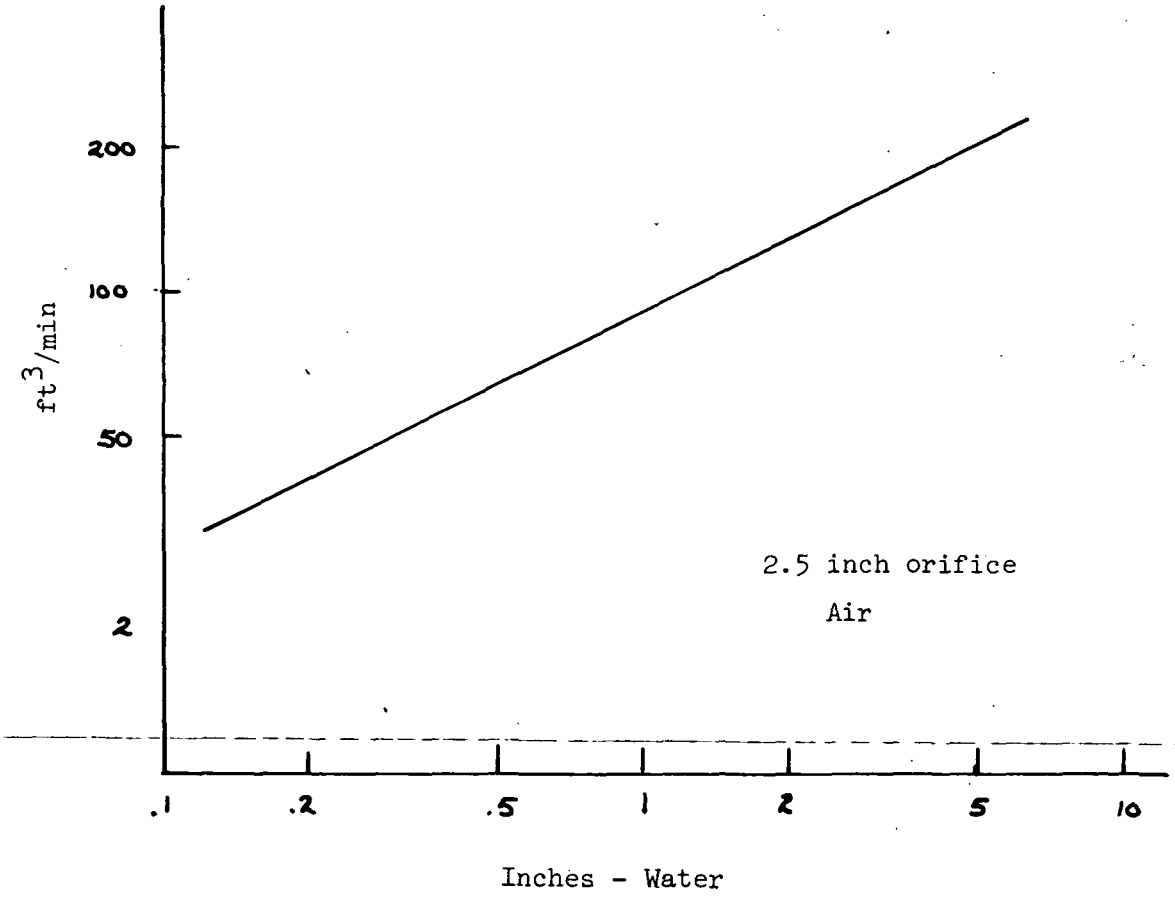

Fig. 4.1(a) Flow rate vs pressure drop through orifice. Upper curve for inner gas flow. Lower curve for outer gas flow

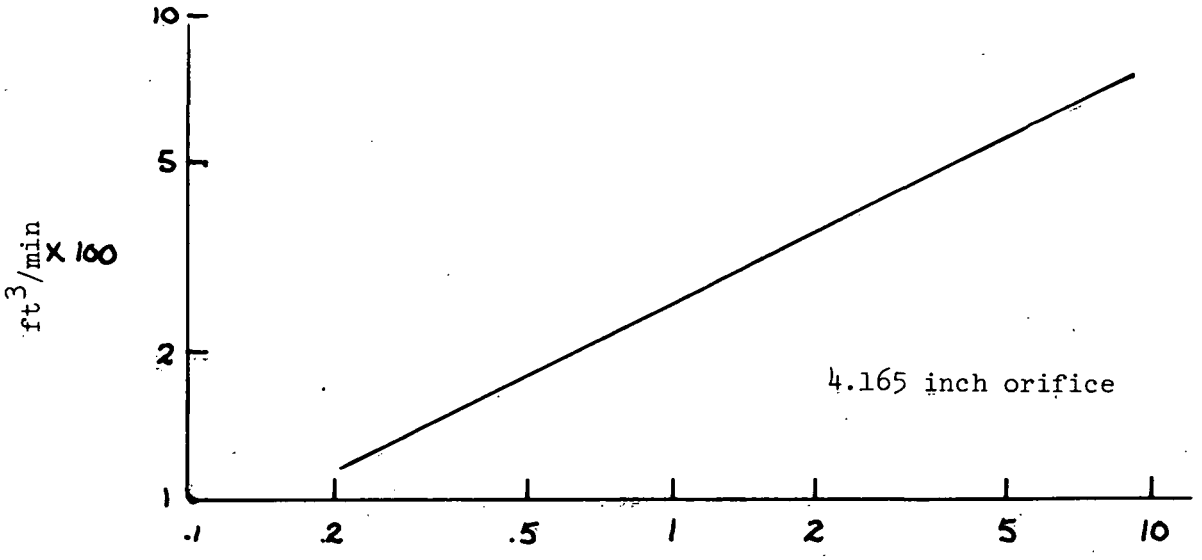

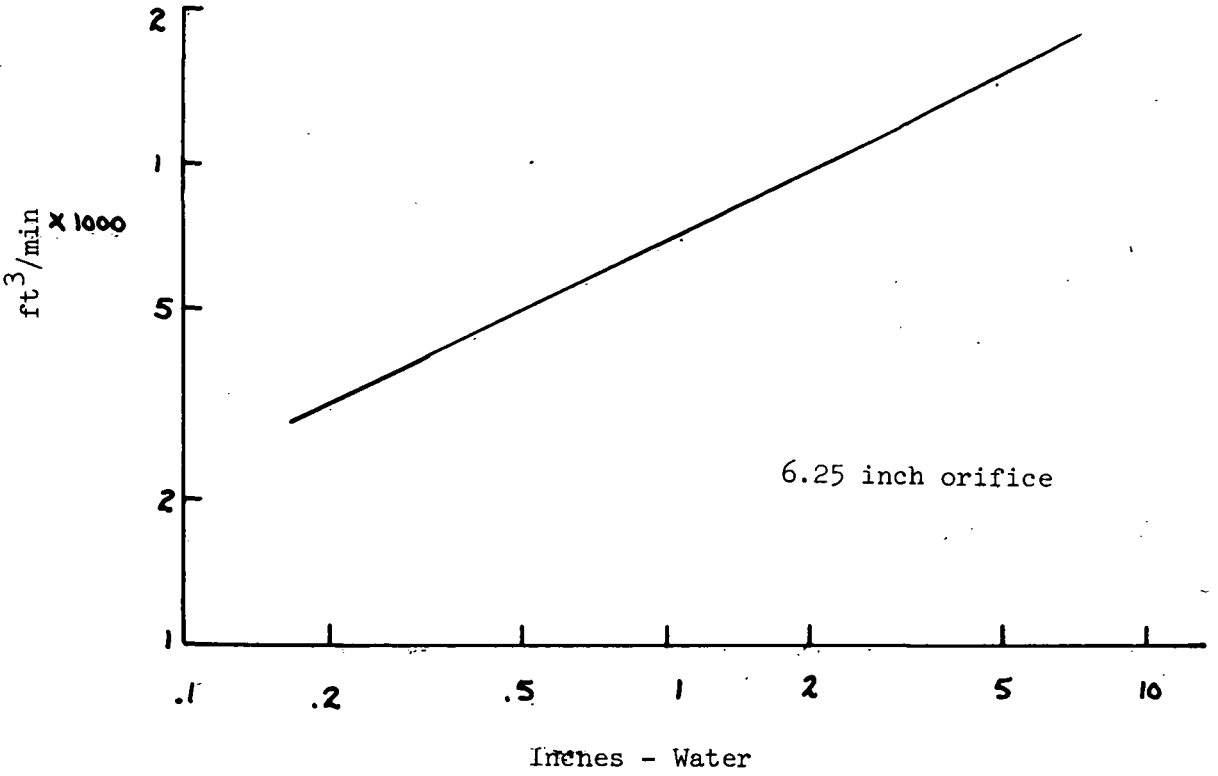

Fig. 4.1(b) Flow rate vs pressure drop through orifice

length and background effects were essentially constant. However, the end wall effects distorted the two-dimensional results and made these density measurements only semi-quantitative.

5.0 TEST RESULTS AND DISCUSSION

5.1 Injection Nozzle Effects and Expansion of Inner Gas

The initial testing was performed with the round shaped cavity (See Figure 3.6). The injection nozzle used in the original test was similar to that employed by Lanzo in the work reported in Reference 6. This showerhead injection nozzle with a perforated wall cavity and no louvers gave test conditions shown as in Figure 5.1. Effectively large volumes of smoke were obtained within the cavity. The actual size of the smoke volume was largely determined by the efficiency of the showerhead in spraying the smoke out over the cavity volume. For the low flow conditions nominally projected for the application rocket, such a shower spray is probably not a condition that could be created in the high temperature rocket. Hence, subsequent series of tests used the point injection-type of nozzle simulating the conditions from a series of pellets injected as point sources or of a single rapidly injected wire. These two nozzles are shown in Figure 5.2, the showerhead on the top and the point injection high velocity nozzle on the bottom. Typical results with the high velocity injection nozzle are shown at the bottom of Figure 5.1. In these tests the injection velocity from the central nozzle was 5-ft per second at the 2 cfm flow rate. Essentially, very high inner smoke volumes were obtained. Mixing was considerable, caused by the turbulence of the high injection velocity of the inner gas. However, along the cavity wall, there was pure outer gas. The flow of the outer gas through the perforated walls easily provided cooling for these walls, and kept the mixed inner gas away, as would be needed in the high temperature applications. However, despite the success of these initial tests, their pertinence to the actual situation for high temperature operating conditions is debatable. It is not known how explosive the vaporization of the uranium pellets or wire will be. However, it appears that the injection conditions simulated in these first tests created an initial radial injection velocity far in excess of that which can be expected from the vaporization of small spheres of uranium metal. Hence, the injection nozzle for all subsequent tests was redesigned similar to that shown in Figure 5.3. This "low-dispersal" injection nozzle contained Scott foam on its periphery, which essentially reduced the injection velocity to 0--less than 0.15 ft/sec even at an inlet flow condition of 6 cfm. Note, however that for the three-dimensional tests, the injector area was much smaller, and injection velocities were about 6 times higher for the same volume flow rates than in the two-dimensional tests.

Before abandoning the high injection velocity tests, studies were made of the flow patterns with varying heights of the injection nozzle. These results are shown in Figure 5.4. It is apparent that if vaporization with high velocity occurs from the injected pellets near the top of the cavity, uranium fills most of the cavity. If the effective point of vaporization is more than 1/3 the distance from the top to the bottom of the cavity, then uranium has a more difficult time filling the cavity before it is swept out the exhaust nozzle.

With a low velocity injection nozzle, it was immediately obvious that methods had to be found to expand the inner gas to a large volume within the cavity. One such method of expansion would be direct entrainment into the outside gas stream. This is not entirely satisfactory because it also results

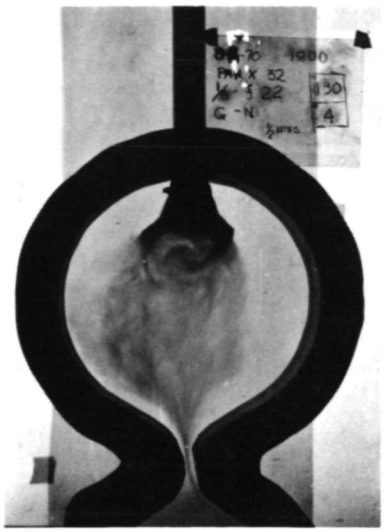

"Shower-head" injector
130 cfm outer, 4 cfm inner

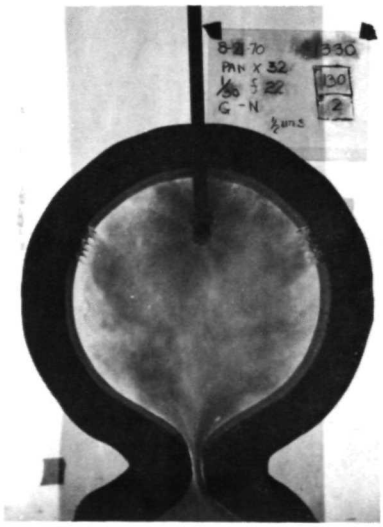

One-inch diameter cylindrical injector containing pinholes, giving an effective open area of only 1%
130 cfm outer, 2 cfm inner

Fig. 5.1 Typical tests with central gas injectors having high dispersal characteristics

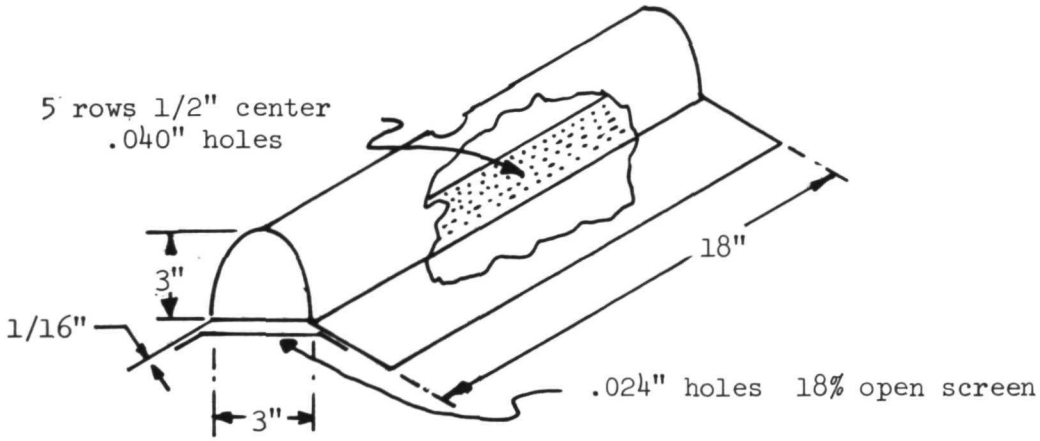

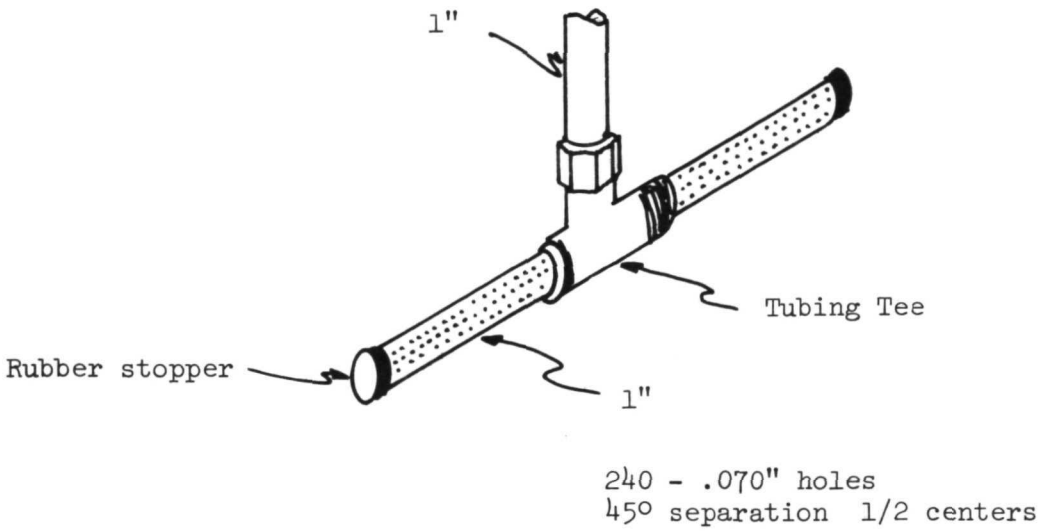

Fig. 5.2 "High dispersal" injectors

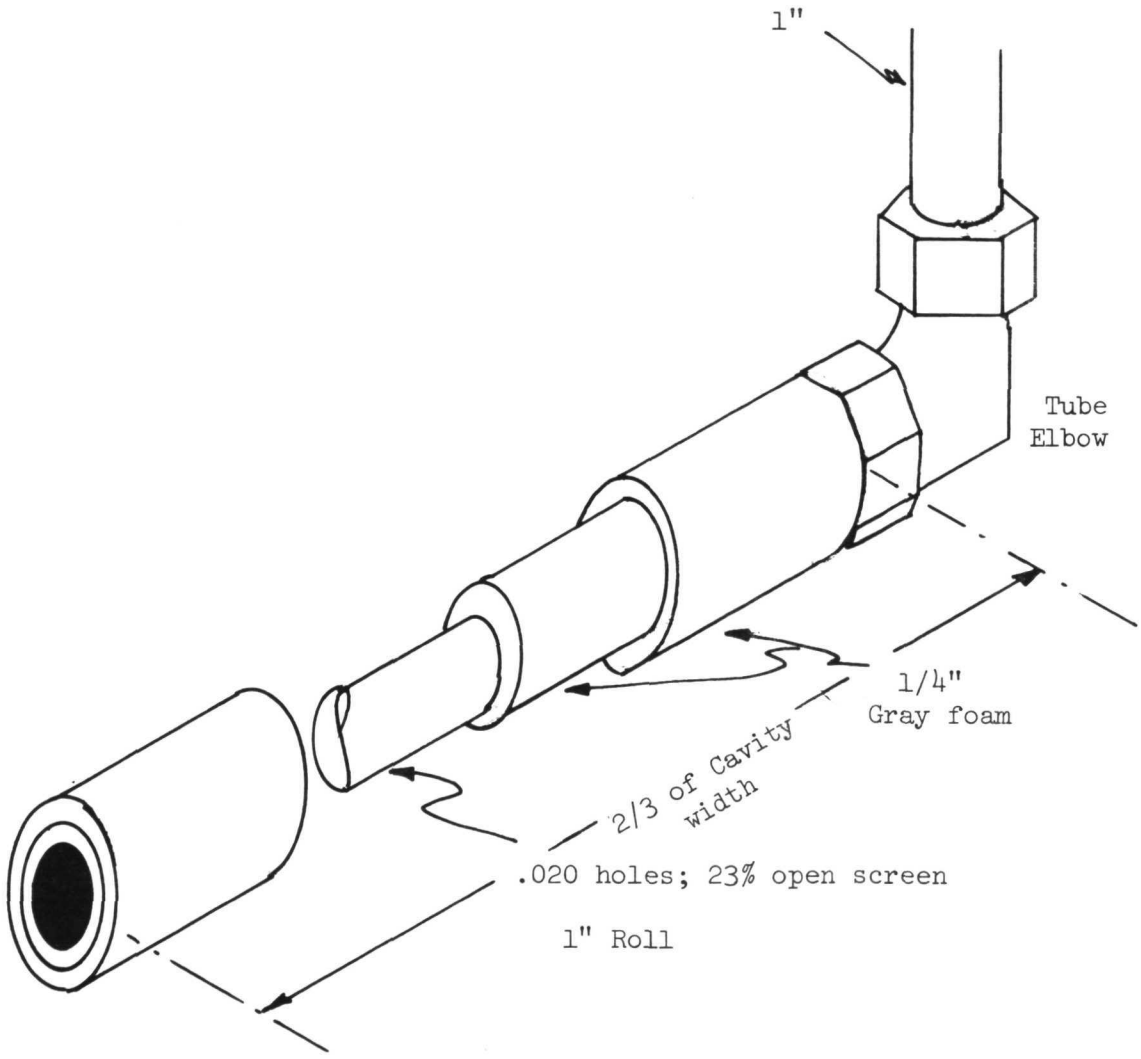

Fig. 5.3 "Low-dispersal", low velocity injector

2 3/8" from Top

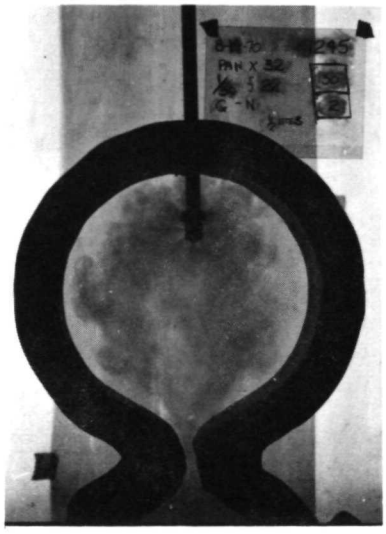

4" from Top

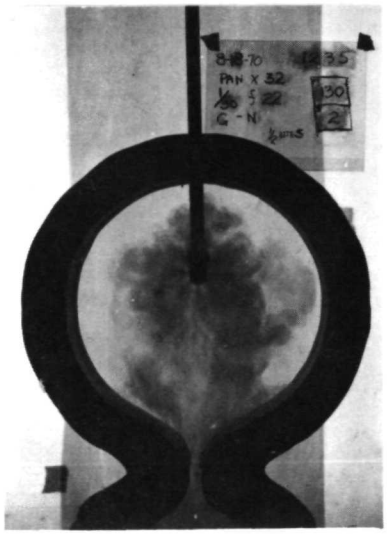

6 3/4" from Top

Fig. 5.4 High velocity injector results at varying injector nozzle position. All outer flows 130 cfm, inner 2 cfm

in considerable mixing in the two gases. A preferable method is to utilize velocity shear forces, which can effectively and uniformly expand the inner gas out to a region near to the cavity wall. Velocity shear forces of the right direction do not exist with a cavity wall consisting of merely perforations, giving only a radial velocity component. Hence, in order to set up a radial shear, a tangential flow is needed, requiring the installation of louvers along the cavity wall. The louvers directed the flow of the outside gas tangentially along the wall of the cavity, and simultaneously created shear forces. By moving the central injection nozzle near to the location of significant shear forces, the central gas could be pulled out to a relatively large volume in the cavity. Typical results are shown in Figure 5.5. In this figure it can be seen that the shear forces are adequate, and expansion of the inner gas occurs even with the injection nozzle being as far as 5-1/2 in. below the top of the cavity. However, a careful examination of the photographs for those injection positions much below 2 in. shows that shear forces are probably not the dominant mode of expansion for the center gas, but that recirculation patterns result in the major method of dispersing the smoke. Such recirculation patterns can easily be seen in motion pictures of the flow. The recirculation appears to develop near the exhaust nozzle opening, proceeds upwards along the centerline towards the injection nozzle, and folds outward to the cavity wall near the top of the cavity. In the elongated cavity, recirculation was more apparent than in the other shapes; and in the three-dimensional configuration, recirculation was most obvious.

Figure 5.6 shows the effect of lowering the injection nozzle in the modified round cavity. At positions below 2-inches from the top of the cavity, velocity shear appears to have become impotent, and the central gas is not expanded at all. Neither is it dispersed much by recirculation. Comparison between this and Figure 5.5 for the elongated cavity implies that there is some benefit to be derived from achieving recirculation which will in turn result in better dispersal of the center gas. However, the velocity shear effect set up in the region of the injection nozzle is the more effective expansion mode, and results in less mixing of the two gases.

The amount of velocity shear can be varied in the region near the injection nozzle by directing more or less flow through the nearby wall. This effect can be observed in Figure 5.7, of the honeycombed configuration. With uniform flow around the entire wall, as in the two pictures on the top , center-gas expansion is satisfactory even with the injection nozzle as low as 2-1/4 inches from the top. However, when more flow is directed through the upper 20% of the wall, as seen in the two bottom pictures, expansion is enhanced. The upper left shows greater expansion than in either of the two pictures on the top. Even when the injection nozzle was lowered to 4-1/2 inches from the top of the cavity, expansion was appreciable. In fact, the lower position actually produced as good if not better overall central gas expansion and density than the 1-3/4 inch injector position. Apparently, the latter position is too close and perhaps actually contacts too much of the high velocity outer gas stream, resulting in too much entrainment and a resulting degradation of overall density.

Study of the effect of the injector position on flow patterns in the large 36-inch cavity yielded similar conclusions. Figure 5.8 shows results of 4

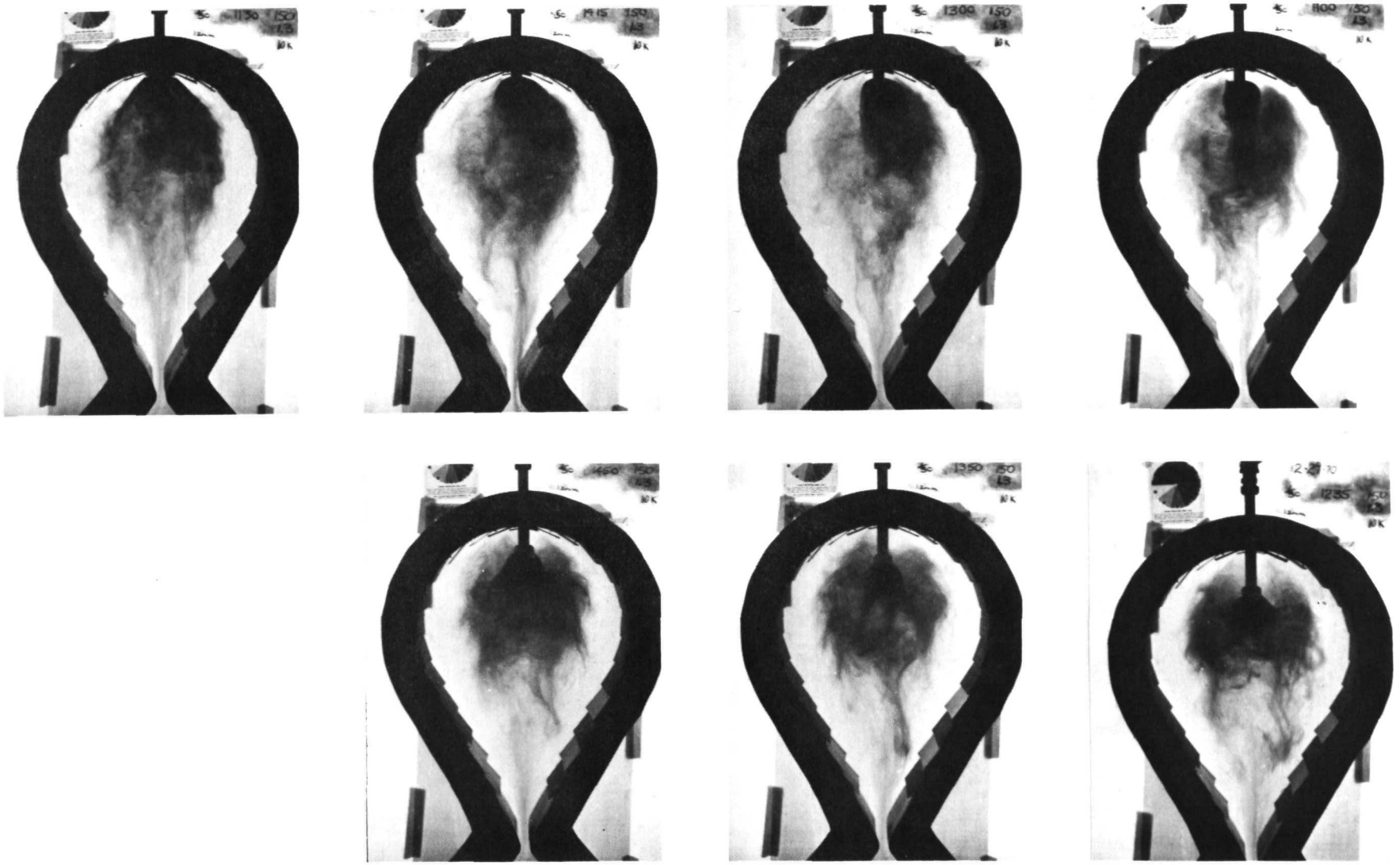

3 1/2" 4 1/2" 5 1/2"

Fig. 5.5 Effect of injector nozzle position on flow patterns. All flows are 150 cfm outer, 1.3 cfm inner.

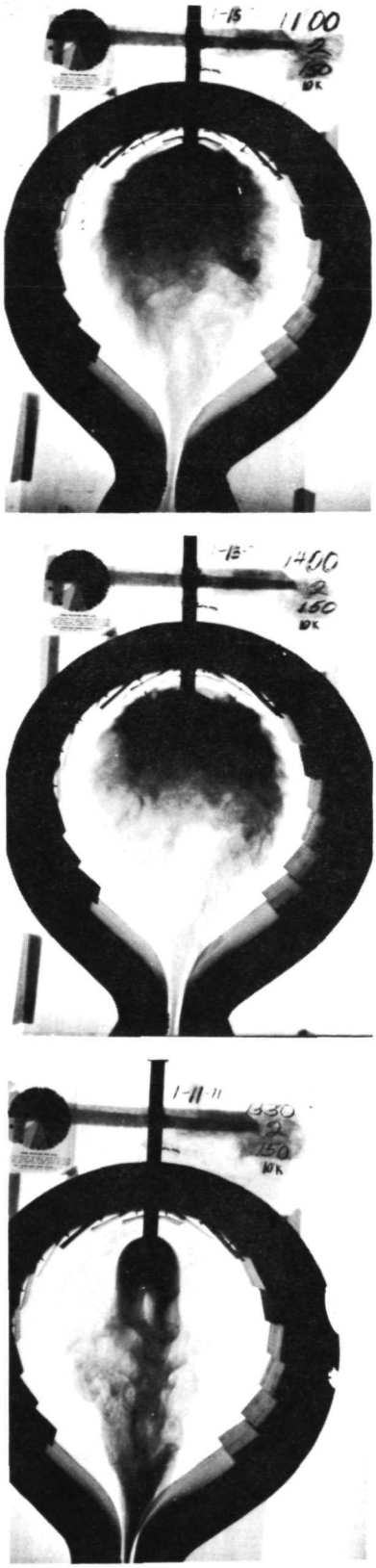

1 1/2"

2"

2 1/2"

Fig. 5.6 Injector position effects with modified round configuration 150 cfm outer, 2 cfm inner

No Foam

1 1/2"

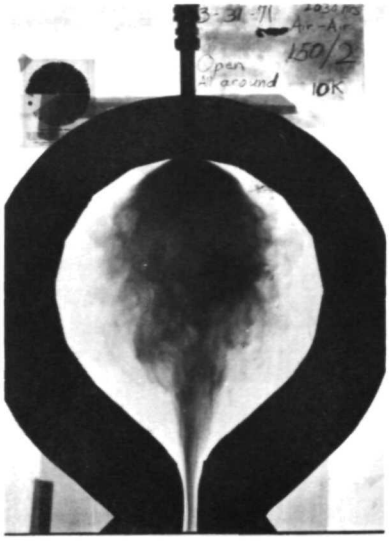

2 1/4"

Foam restriction on outside of cavity
except on the lower 80% of the cavity wall

1 3/4"

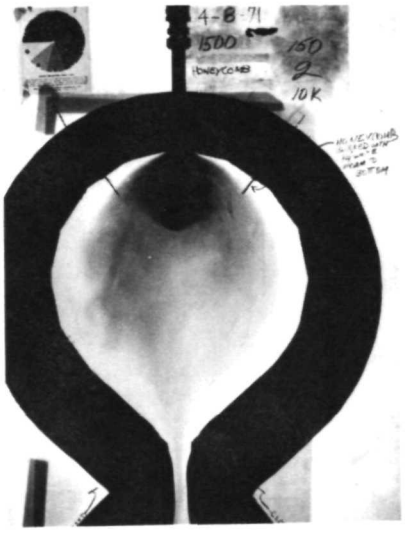

4 1/2"

Fig. 5.7 Injector position effects - Honeycomb cavity
150 cfm outer, 2 cfm inner

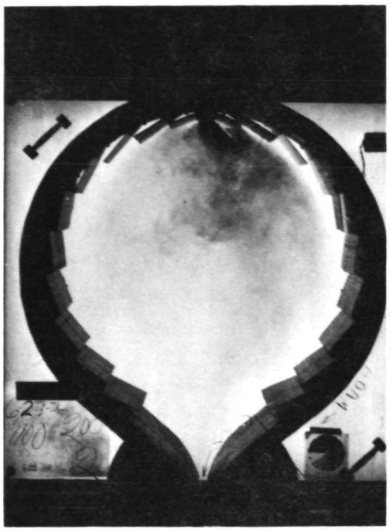

Injector 1" from top

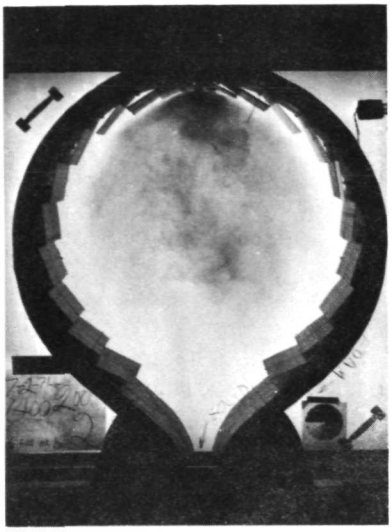

Injector 2" from top

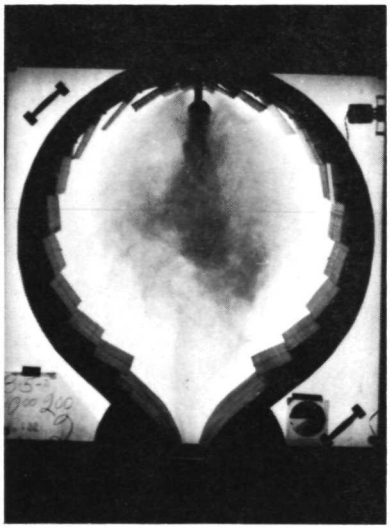

Injector 3" from top

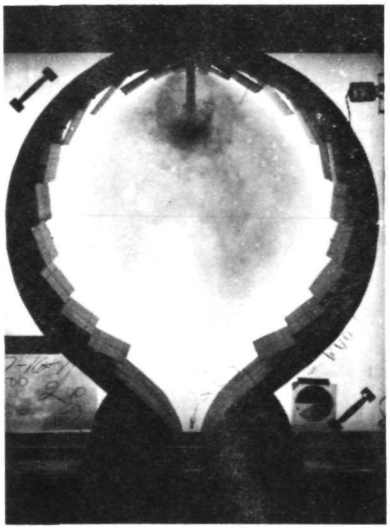

Injector 7" from top

Fig. 5.8 Injector position effects in 3 1/2 ft cavity
550 cfm outer, 2 cfm inner

different injector positions with 550 cfm outer gas flow. The overall quality of these flow patterns are poorer than those shown in pictures of the smaller cavity tests, but the flow rate ratio is quite large, 225 to 1. Note, with the nozzle at 1 and 2 in. from the top of the cavity, expansion of the outer gas is significant. At the 3 in. position expansion is far less satisfactory. But when the nozzle is moved down to 7 in., expansion now appears to have improved. This improvement is believed to be due largely to the fact that the nozzle is now in the recirculation pattern.

With the spherically shaped cavity, results of different injector positions showed less overall dependence on injector position. In Figure 5.9, with flow rate ratios of 100 to 1, expansion appears quite adequate with nozzle positions down to as far as the center of the sphere. The upper left picture shows an extreme condition of the nozzle lowered essentially down toward the throat of the exhaust nozzle. Here of course, expansion by velocity shear is negligible, but the recirculation pattern is somewhat obvious in this photograph. Much of the smoke is swept directly out the nozzle. Yet a noticeable amount of the smoke moves back up the cavity due to the recirculation pattern described previously. Because of the three-dimensional geometry of the sphere, recirculation patterns are at least as strong in this modified round three-dimensional configuration as they were in the elongated two-dimensional cavity configuration.

Further evidence of the effect of velocity shear can be seen in Figure 5.10. With uniform flow through all louvers, expansion is mediocre, as shown in the top figure. However, when more flow is directed through the top louvers by placing foam restriction on the bottom 80% of the cavity, expansion is greatly improved. However, note that too much expansion can result in to rapid a loss of central gas feed from the region around the injector, leaving it insufficient to feed the center and lower part of the cavity.

5.2 Cavity Shape Effects

Three basic cavity shapes were studied. Initially a round cavity with a small elongation for an exhaust nozzle at one side was used. This is the shape most amenable to criticality. Secondly, a rather exaggerated elongated type cavity was employed. And finally, a modified round cavity having an elongation mid-way between the two initial shapes was employed. For the most part there was very little obvious difference between the outer gas flow patterns in the three basic cavity shapes. Figure 5.11 shows flows in these three basic shapes with no restrictions on any of the louvers and flow rates of 200 cfm in the outer gas and 6 cfm for the inner gas. In general, the round cavity shape gave results equally as good if not better than those of the other two cavity shapes, and certainly gave a rounder shape for the center gas volume. However, as noted before, recirculation patterns were most pronounced in the elongated cavity. Recirculation with resulting mixing is not necessarily an undesirable nuclear effect. For flow and containment considerations, recirculation is particularly useful when the effective injection position for the center gas is far below the top of the cavity. Furthermore, when gases of unequal densities are tested, recirculation appears to be almost essential to prevent the heavier center gas from moving directly down toward the exhaust nozzle.

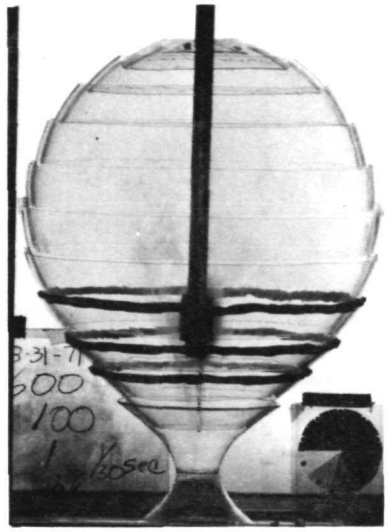

14.5"

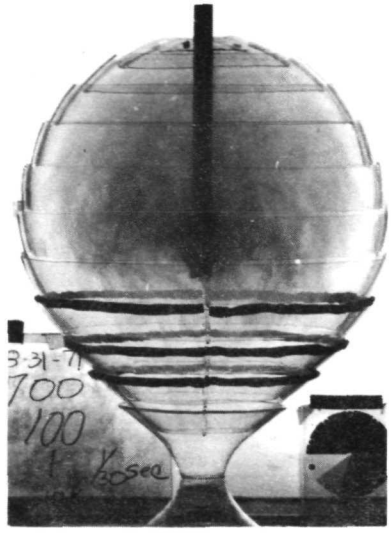

10"

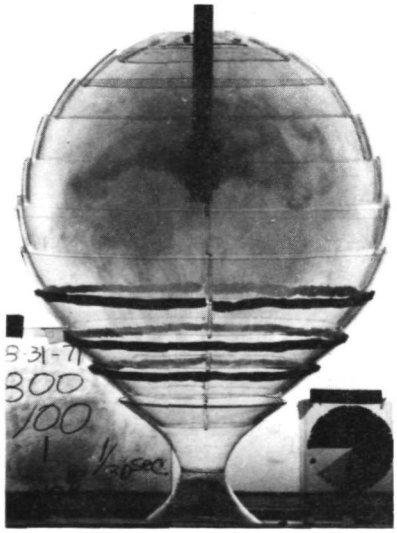

7"

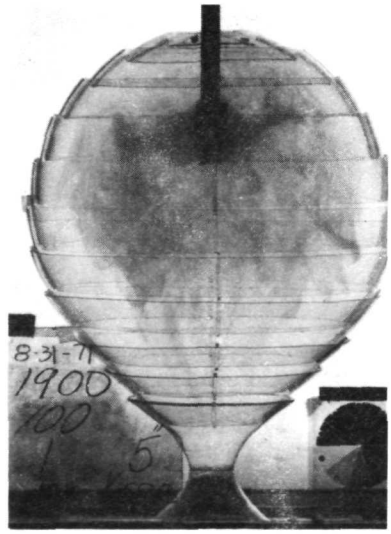

5"

Fig. 5.9 Injector position effects - spherical cavity
100 cfm outer, 1 cfm inner

No Foam

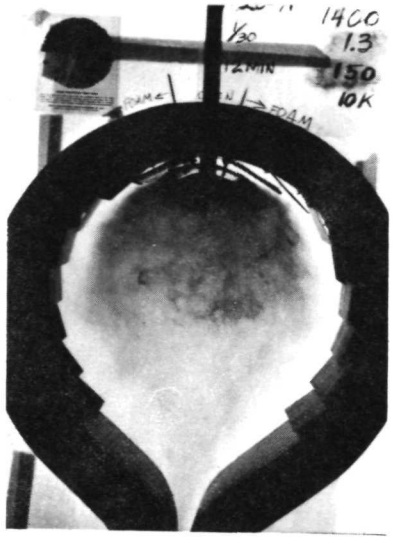

1/4" thick foam on outside of cavity from first louver on down

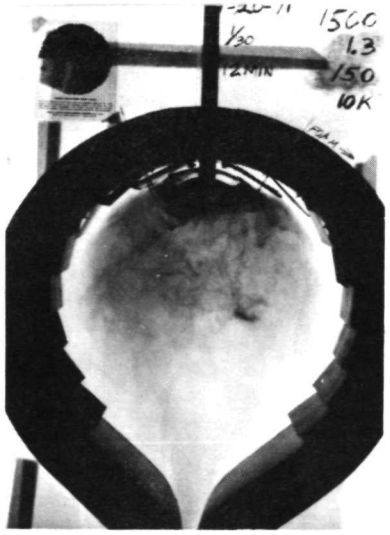

1/4" thick foam on outside of cavity from second louver on down

Fig. 5.10 Effect of tangential velocity near injection nozzle

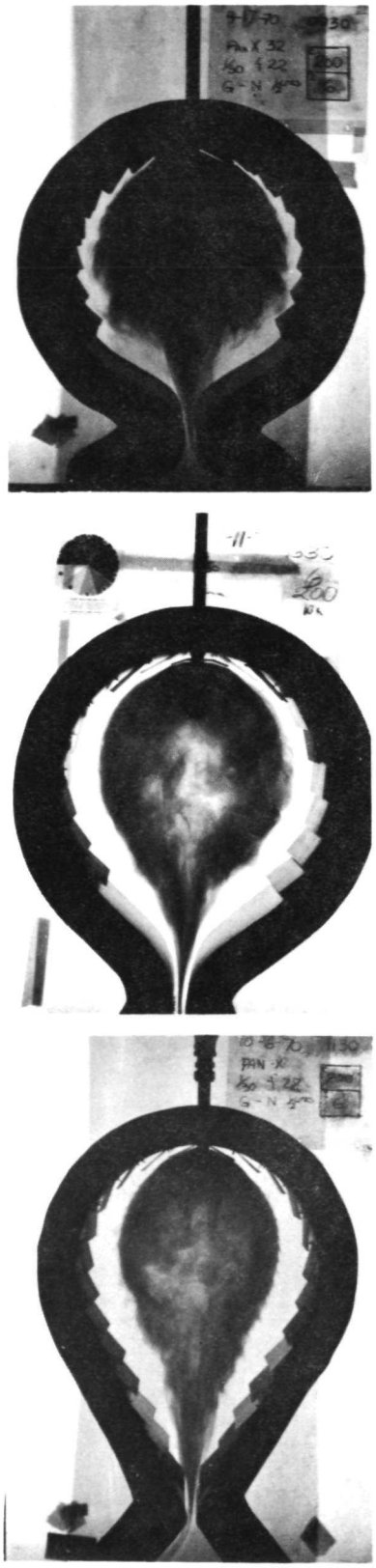

Round

Modified Round

Elongated

Fig. 5.11 Effect of cavity shape on flow. 200 cfm outer, 6 cfm inner

5.3 Exhaust Nozzle Effects

The effect of varying pressure drops though the exhaust nozzle was crudely studied by varying the opening of the exhaust nozzle in some of the two-dimensional tests. Typical results are shown in Figure 5.12, where the nozzle opening is varied from 2-1/4 square inches to 18 square inches with a flow of 100 cfm. These conditions correspond to pressure drops across the nozzle of 2.2 and 0.035 inches of H_2O, respectively. Examination of the photographic results show essentially very little difference in the primary flow patterns in the upper half of the cavity. Near the bottom half, however, the flow patterns are noticeably changed as the nozzle opening is reduced. Mixing and spreading of the inner gas into the outer gas stream is quite noticeable at these smaller openings. The cause of this effect, as seen in the upper view of Figure 5.12, is not fully understood at this time. It is expected, however, that the results may be somewhat misleading. At the high pressure drops encountered in these low area nozzle tests, leaks in the test box for the outer gas flow would not be unexpected. Note, that nozzle velocities even in the conditions of only a 2-1/4 square inch opening were far from choked flow conditions. Nozzle velocity in that case was less than 150 ft/sec.

5.4 Louver and Cavity Wall Effects

The need for installing louvers along the perforated cavity wall has been apparent in the previous discussions. The non-louvered wall functions effectively only if the center gas injection system is one of high velocity input, such that the center gas is initially expanded into the large cavity volume by the injector mechanism. Where low velocity injection schemes are employed for the center gas, expansion cannot occur without a mechanism such as velocity shear forces or direct entrainment into the tangential flowing stream. With merely perforated cavity walls containing no louvers, there is no tangential flow. Figure 5.13 strikingly shows the effect of an unlouvered cavity wall as seen in the upper two photographs of that figure. The lower two photographs show similar flow rate conditions but with louvers installed on the cavity walls. Note, in the lower right hand photograph, the nozzle position is further from the upper wall of the cavity than in any of the other three tests shown in Figure 5.13.

Despite a tangentially flowing stream of outer gas, the louvers in the actual gas core rocket application will need to have transpiration cooling. The louvers used in all tests to date, except those in the spherically shaped cavity, contained perforations. Typical open area of the louvers was 18% or 22%. However, too much transpiration flow through louver holes will create excessive inward radial velocity, and reduce the effectiveness of the velocity shear established by the tangential flow created by the louvers. Tests were conducted on the effect on inner gas volume of the inward radial velocity through the pores of the louvers. The upper photograph in Figure 5.14 shows the effect of foam lined louvers versus louvers whose bleed holes were unrestricted. Two effects result from the foam lining on the louver. First, the radial velocity component is reduced, allowing the center gas to approach the cavity wall much closer. Secondly, adding foam to both sides of the louver restricts the overall flow tangentially through that louver. By referring to the second and third photographs of Figure 5.14, it is apparent that the first effect is most predominant. Too much transpiration cooling resulting in high radial inward velocity

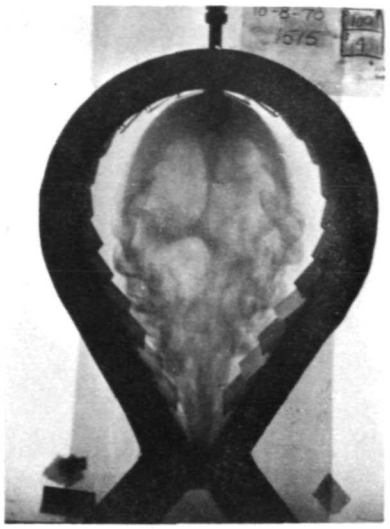

1/8" Nozzle Opening

18" long

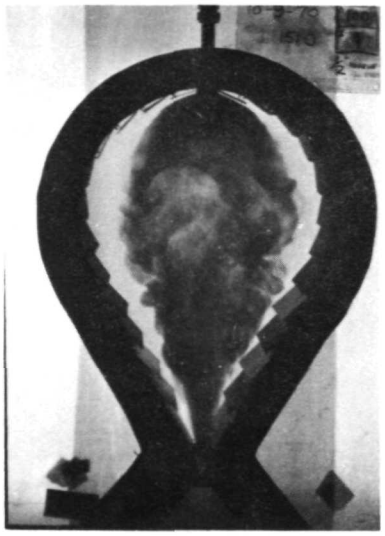

1/2" Nozzle Opening

18" long

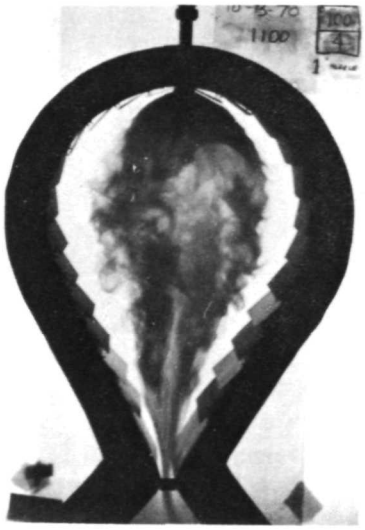

1" Nozzle Opening

18" long

Fig. 5.12 Effect of exhaust nozzle opening
100 cfm outer, 4 cfm inner

No Louvers

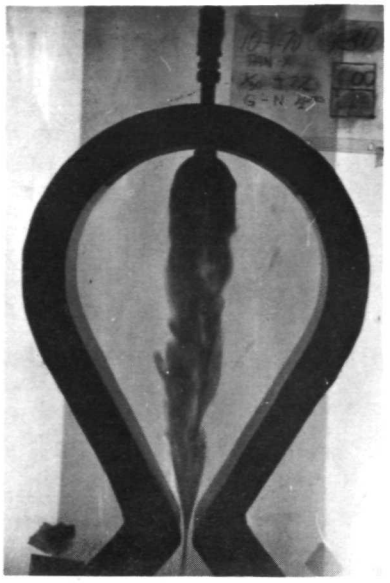

400 cfm outer, 4 cfm inner

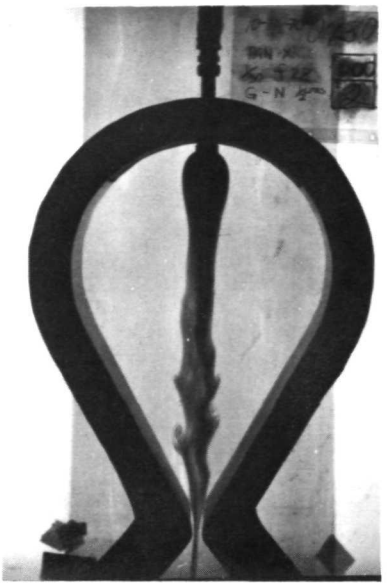

200 cfm outer, 2 cfm inner

With Louvers

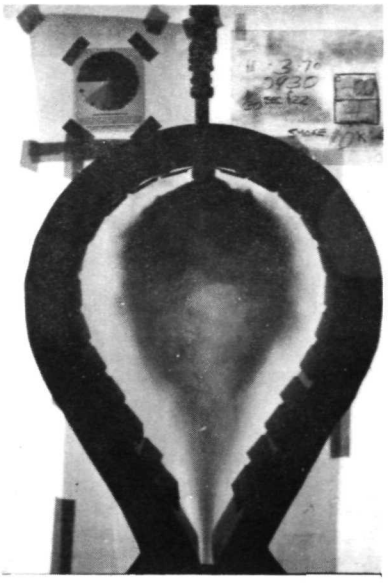

400 cfm outer, 4 cfm inner

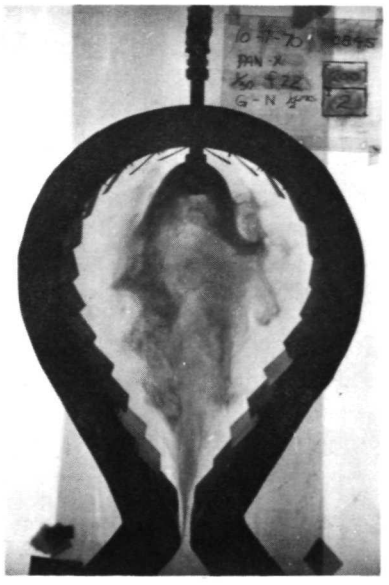

200 cfm outer, 2 cfm inner

Fig. 5.13 Louver effects

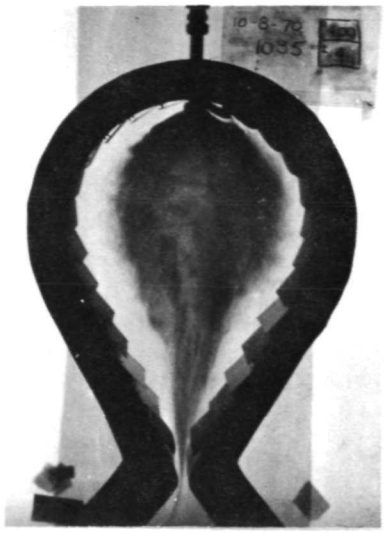

Foam lining on both sides of top four louvers on right hand side (effectively restricts flow through these louvers)

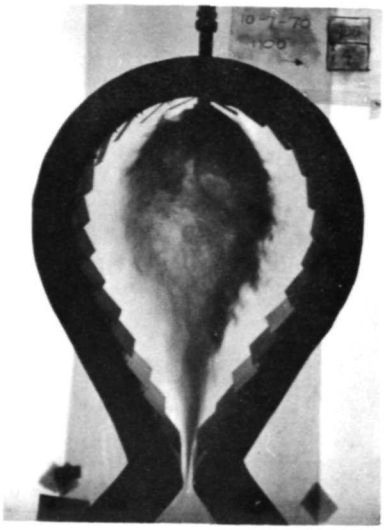

1/4" foam on right side wall along first five louvers

Louvers only, no foam

Fig. 5.14 Effect of foam lining

will reduce the expansion effect of the inner gas. With the foam lining on the louvers, as in the right hand side of the upper photograph, transpiration cooling is probably adequate for conditions resembling those that would exist in a high temperature operating gas core. Thus, it is concluded that transpiration cooling holes in the louvers should be reduced to the minimum amount necessary to cool the louvers and prevent melting in the high temperature environment.

Consideration was given to completely diffusing the flow as it left the louvers, and thereby possibly reducing the resulting turbulence in the tangential moving gas stream. Figure 5.15 shows the wall louver arrangement used, employing diffusers along the exits of the louvers. Essentially, no overall reduction in observed turbulence was seen. The photograph in Figure 5.15 is a closeup of the turbulence near a set of these diffused louvers. The turbulence appears to be even slightly greater than that near louvers without foam lining and diffusers. The thickness of the louver results in eddies as the gas moves past the louver and separation occurs. The eddies are greater for these thick foam-lined louvers than for the thin metal louvers.

A wall that would direct the flow tangentially with the maximum uniformity and with the minimum of wall surface discontinuities, presumably resulting in minimum sized eddies, would be a honeycomb wall. Figure 5.16 shows typical results of a honeycomb wall with the honeycomb tubes at an angle of 20° to the wall tangent. A comparison is also shown between the honeycomb wall configuration and the louvered wall configuration. By directing sufficient flow through the wall near the injection nozzle, adequate expansion of the inner gas can be obtained in either type of configuration. Turbulence was not necessarily less in the honeycomb configuration, however. It was concluded from the honeycomb tests that results with the honeycomb wall were not significantly better (in fact no noticeable improvement could really be observed) than with the louvered wall. Hence, subsequent tests on other cavity configurations were made with louvered walls, which were much simplier to construct than a honeycombed wall.

5.5 Velocity and Density Measurements

Velocity measurements taken throughout the two-dimensional cavities are shown in Figure 5.17, 18, and 19. High velocities are recorded near the walls. Near most of the interior of the cavity, velocities are generally small, giving rise to the slow recirculation patterns that occur in the interior regions. Velocity directions in these photographs are indicated by the arrows. The hot wire anemometer used for obtaining the measurements was rotated to obtain the maximum velocity (gradient of the velocity potential). However, the exact direction of this gradient, along the perpendicular to the wire, whether forwards or backwards, could not be deduced. Note, in Figure 5.19, the velocities obtained in the honeycomb wall show that high tangential velocities extended more toward the cavity center than was the case with the louvered walls. Presumably, this higher thickness of the turbulent tangential moving layer of outer gas can be reduced in the honeycomb configuration by reducing the angle of the honeycomb to the tangent of the wall. (The angle was 20° in these configurations.) Interestingly enough, a widening of the turbulent boundary layer could not generally be observed in the louvered configurations when the louver angle was increased. Extreme louvered angles were not employed, but variations of the angle between 5 and 15° from the tangent of the wall created no noticeable change in the flow patterns and hence in the apparent thickness of the boundary layer.

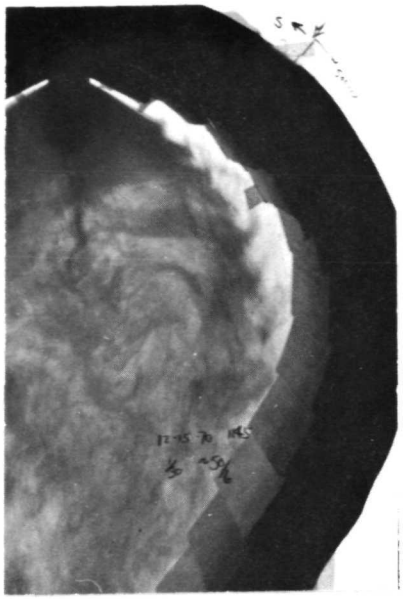

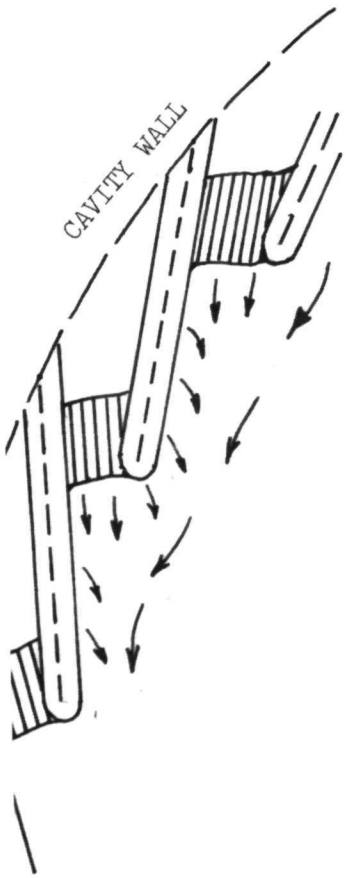

Louvers with porous wall.
Porous diffuser between

Fig. 5.15 Porous louvers and walls

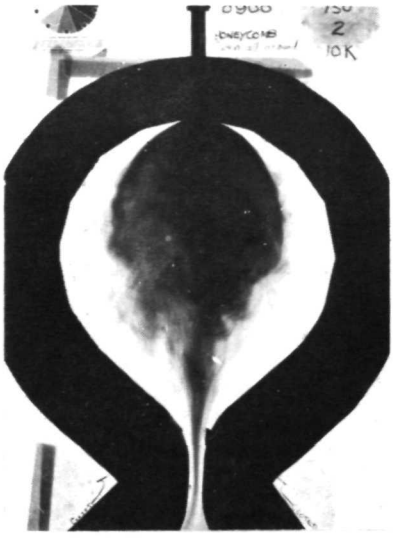

Honeycomb,
Open all around

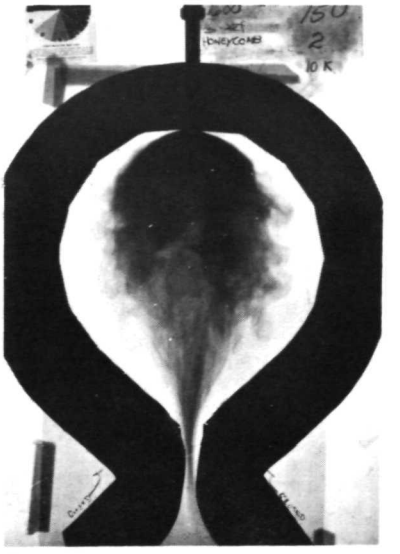

Honeycomb, 1/4" foam
starts 13" from top

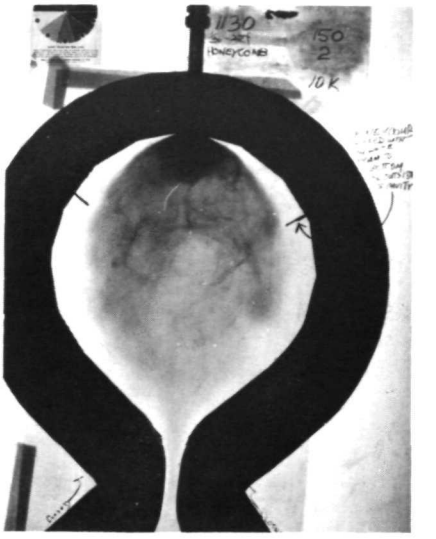

Honeycomb, 1/4" foam
starts at lines and
covers bottom 2/3 of
cavity

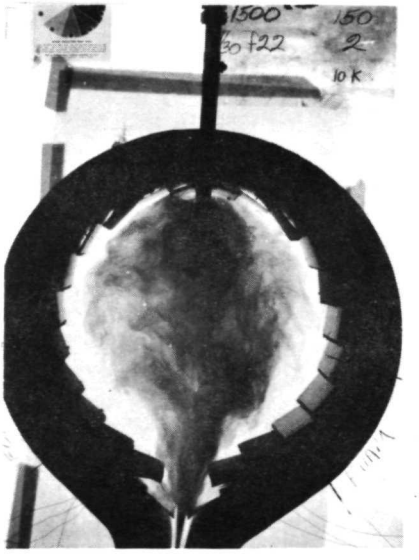

Louvers with no foam
restriction on wall.
Louvers 2,3,7,8,9,10
have 1/8" foam lining

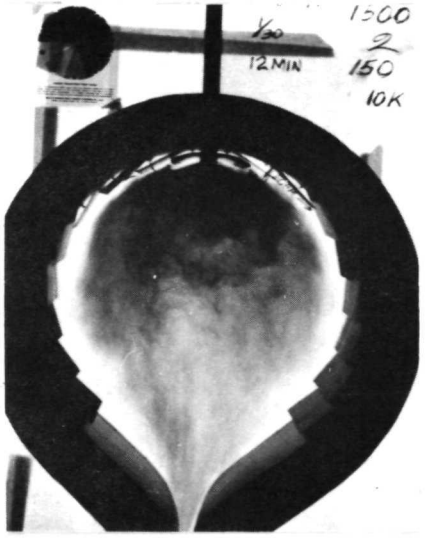

Louvers, foam restriction
except on top louver

Fig. 5.16 Honeycomb vs louvered walls

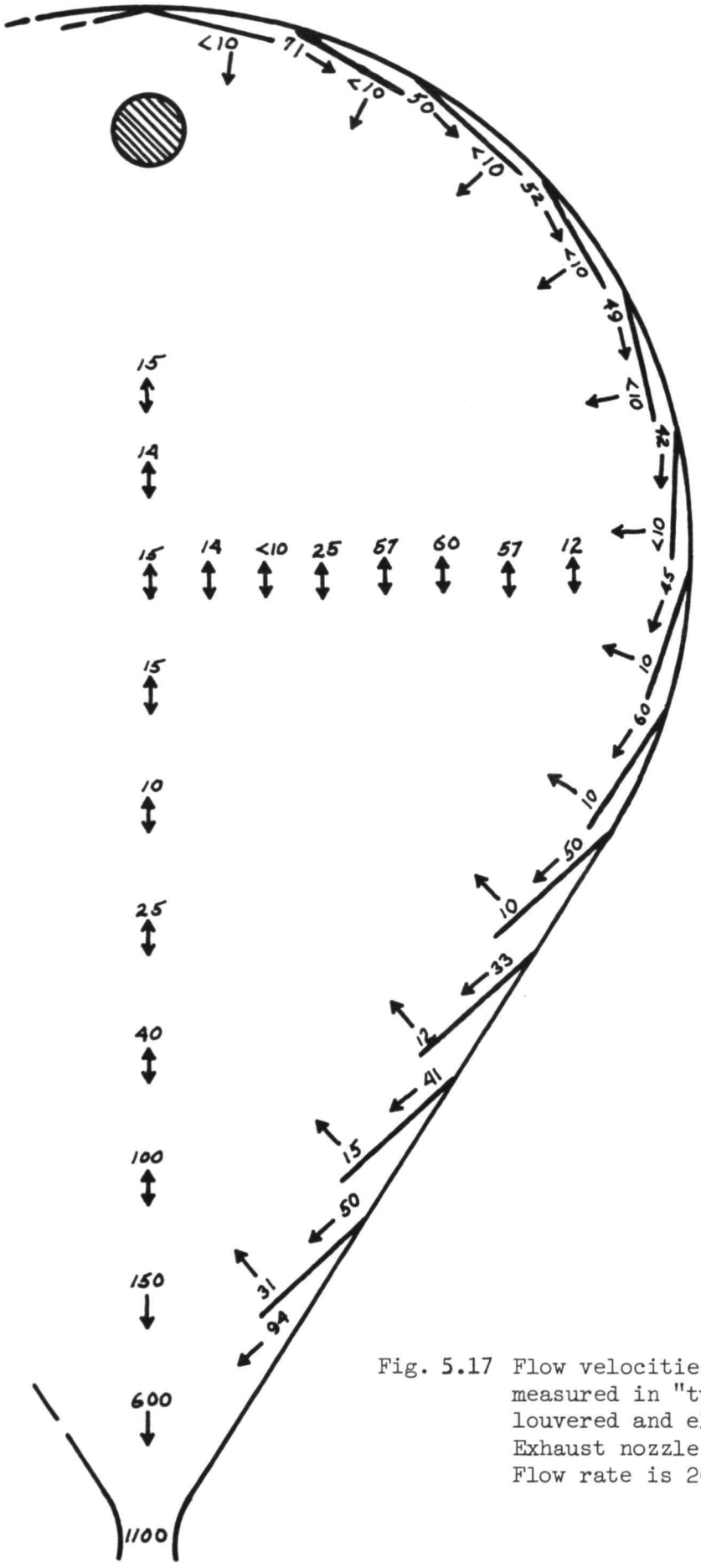

Fig. 5.17 Flow velocities (ft/min) as measured in "two-dimensional" louvered and elongated cavity. Exhaust nozzle opening is 7/8". Flow rate is 200 cfm, outer gas

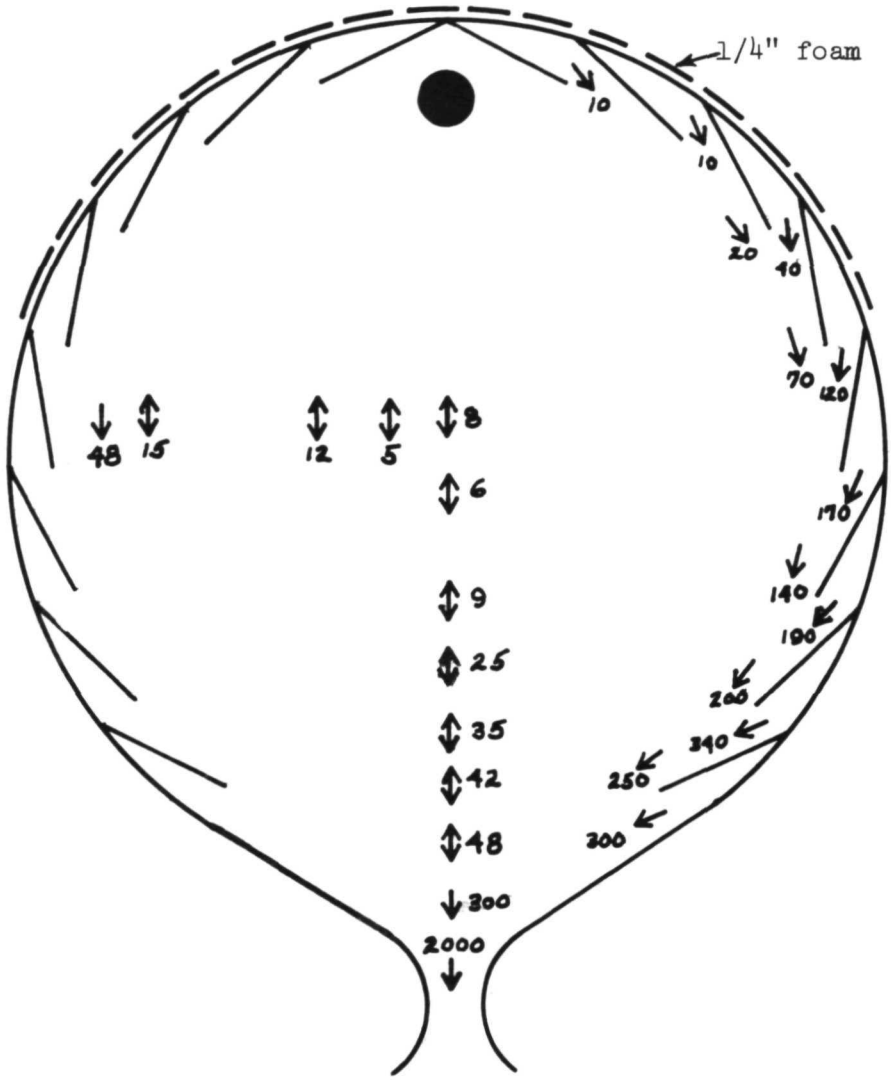

Fig. 5.18 Flow velocities (ft/min) as measured in the round "two-dimensional" cavity with louvered walls. Flow rate is 500 cfm, outer gas. Note, upper half of wall has restricted flow resulting from 1/4" foam covering

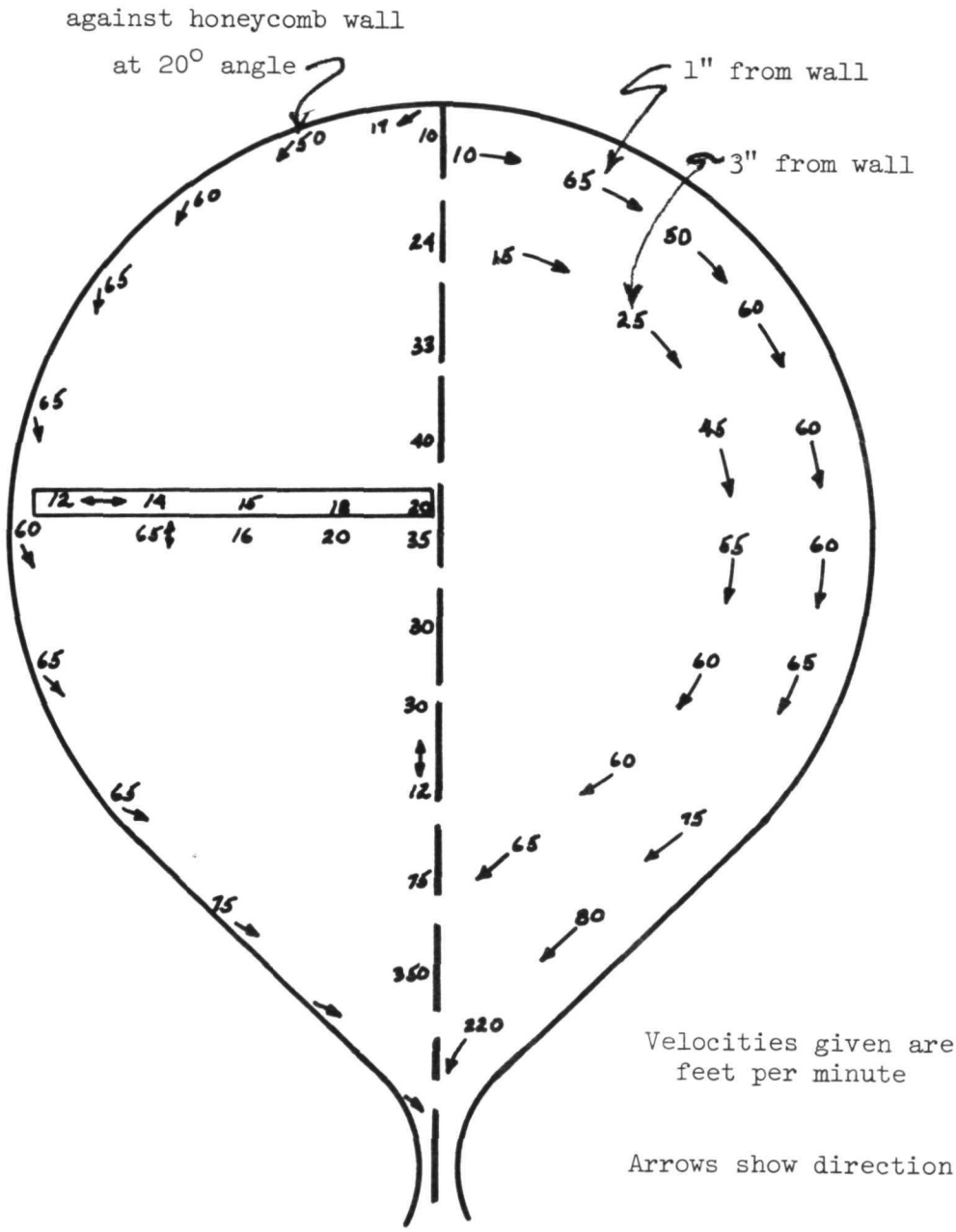

Fig. 5.19 Flow velocities as measured in "two-dimensional" honeycombed-wall configuration; no restrictions to flow. Flow rate is 200 cfm for outer flow.

Iso-density contours are shown in Figure 5.20 through 5.23. Shown are lines of constant density of the inner gas relative to the injection density. In Figure 5.20(a) are results with the elongated two-dimensional configuration. The leftside of the plot shows results with argon as the center gas, the right side with air as the center gas. Flow rate ratios for each half of the plot are approximately the same. Note, that the air results are much better expanded despite the lower overall flow rates. The air plot shows considerably more mixing of the center gas, with resultant dilution. On the other hand, the argon flow patterns show a general streaming of the inner gas towards the exhaust nozzle. Expansion is less than with the air, and hence densities in the very central portion of the cavity are overall higher than with the air case. The same general effects can be seen in Figure 5.20(b) of the honeycomb wall. In Section 5.9 calculations of these configurations reveal that it is more important to obtain high radius ratio expansion than high densities. Hence, the flow patterns obtained with the air as the center gas are much more effective in achieving nuclear criticality than those with the argon, despite the higher overall density in those regions that the argon occupies.

In Figure 5.21 are shown the results of two comparable conditions with air as the center gas. In the left half of the figure are shown the results with foam covering approximately the lower half of the cavity wall. In the right half are the results with foam covering most of the cavity wall except the region near the top at the critical expansion louvers. In this case expansion has been too severe for the right hand case, resulting in excessive entrainment of the center gas in the outside gas stream. Overall expansion of the two cases is approximately the same. Yet densities in the experiment on the right where entrainment was excessive are noticeably less than in the left hand case.

Figure 5.22 compares two different flow rate ratios. The outside gas flow is the same in both experiments. Hence, overall expansion is nominally the same. As expected, the lower inner gas flow rate results in noticeably reduced densities throughout the cavity. As shown in Section 5.9, both of these flow patterns will probably give only slightly different multiplications in a nuclear reactor system. Both have the same outer radius ratio of the inner gas. The lower overall density in the central (fuel) region of the cavity shown on the right will not create a significant penalty in reactivity.

Figure 5.23 shows iso-density plots in the spherical three-dimensional experiment. These results were obtained after the mathematical and unfolding process from the cordal adsorbtometer measurements. In this experiment, the center gas overall volume fraction was 1/3 of the total cavity volume. However, note that this 1/3 volume fraction was spread out over 70 to 80% of the volume of the cavity. Criticality with such a flow configuration is quite possible with low overall cavity pressures. The results shown in this figure are with air as the center gas. Results with argon show less overall expansion toward the cavity wall, as was observed with the two-dimensional tests. The net volume fractions shown for the "two-dimensional" tests are generally much higher than 1/3. This is simply because the inner volume fraction is proportional to the square of the fractional radius ratio in "two-dimensions" but to the cube of that quantity in three dimensions. To reduce the two dimensional net volume fraction approximately to the equivalent three dimensional configuration value, raise the result to the 3/2 power.

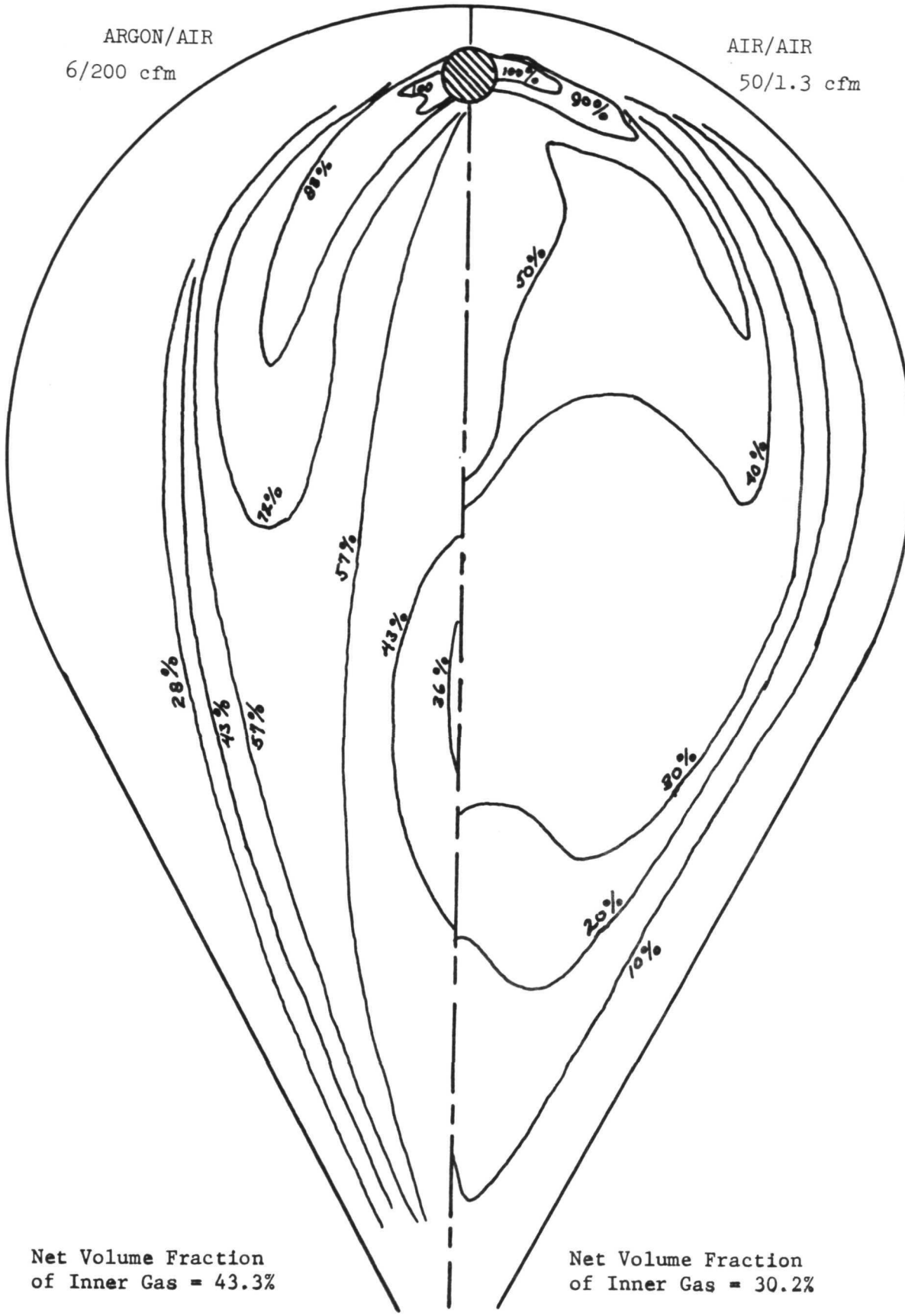

Fig. 5.20(a) Iso-density plot of an air/argon test (left of centerline) and of an air/air test (on the right). Percentages are of center gas inlet density. "Two-dimensional" elongated cavity.

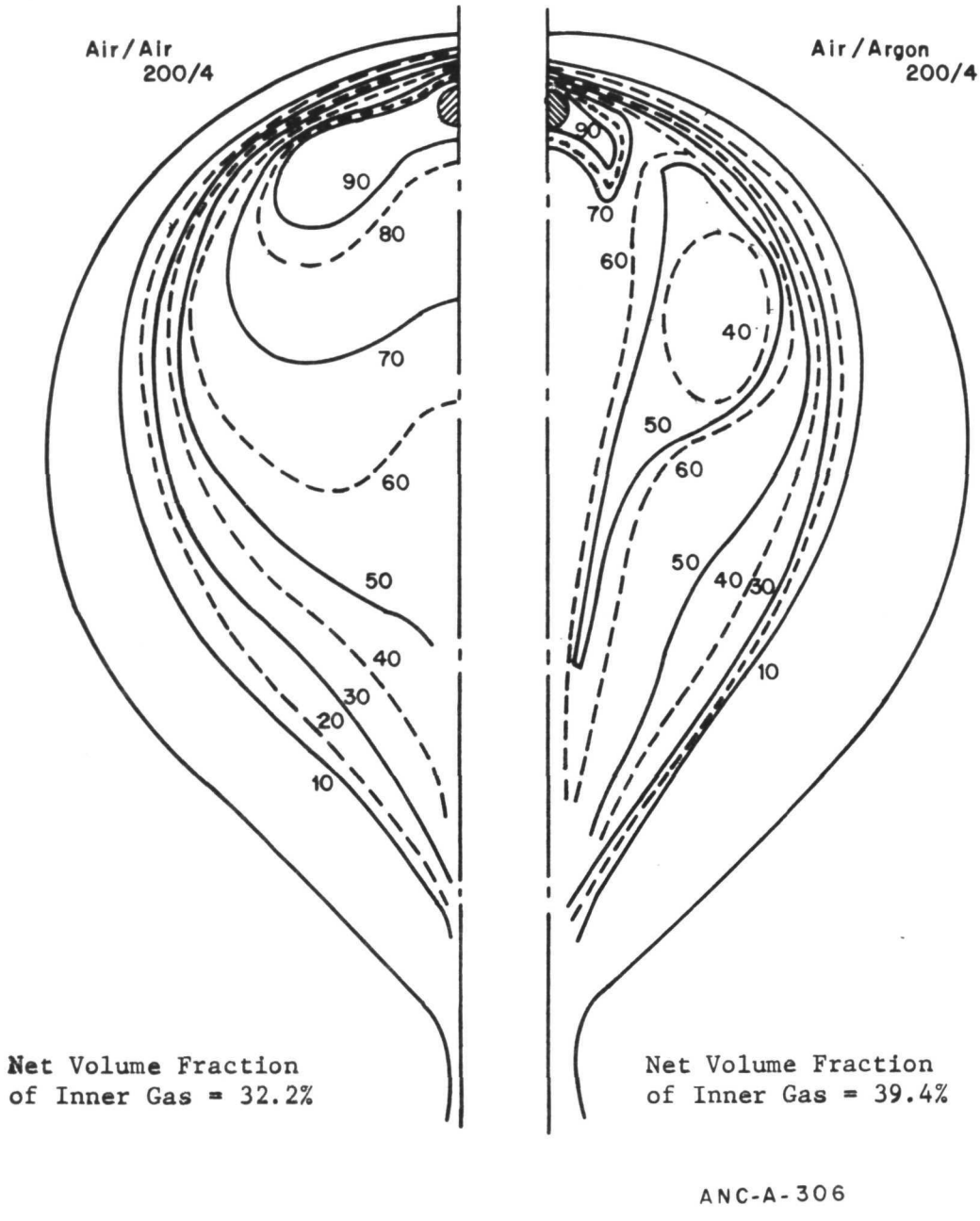

Fig. 5.20(b) Air vs argon. Iso-density lines, percentage of inner gas relative to 100% at the injection nozzle. Modified round cavity with honeycomb wall. No flow restrictions. 200 cfm outer flow, 4 cfm inner.

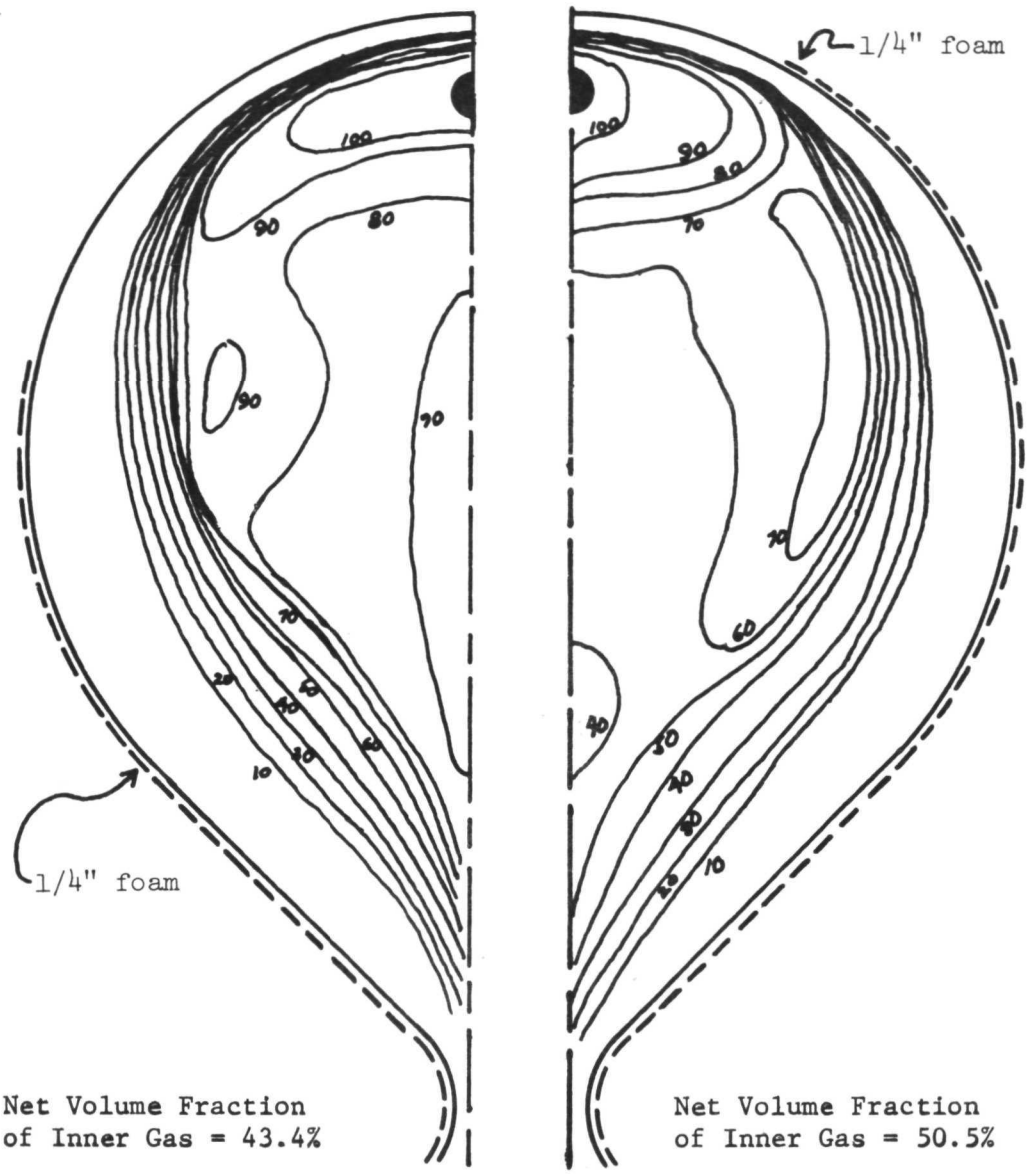

Fig. 5.21 Iso-density lines of center-gas density, relative to 100% at injection nozzle. Modified round cavity, "two-dimensional," with foam restriction as shown on each of two separate tests. Flows on both tests were 100 cfm outer, 6 cfm inner.

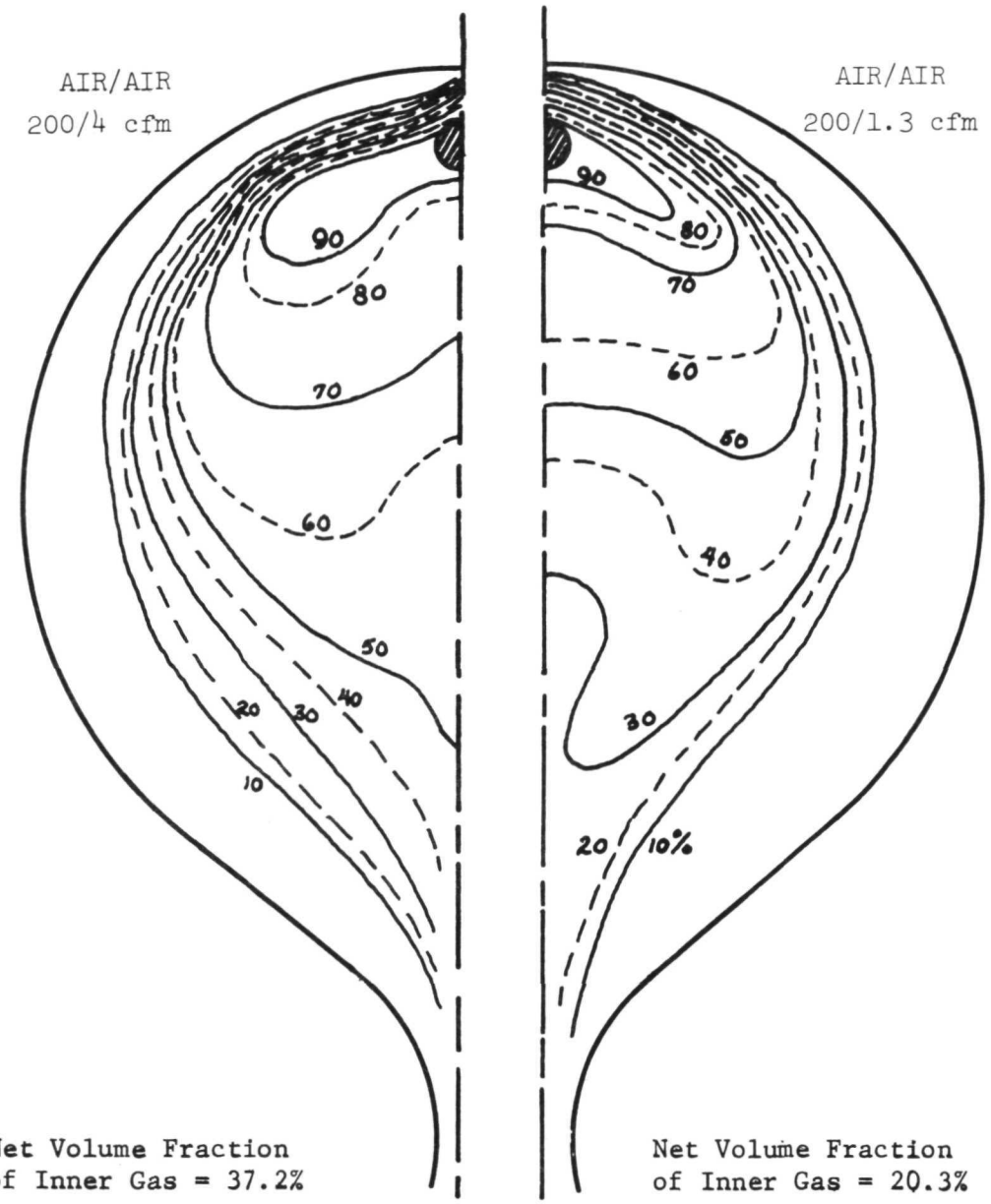

Fig. 5.22 Iso-density lines, percentage of inner gas relative to 100% at injection nozzle. Honeycombed wall. No flow restrictions.

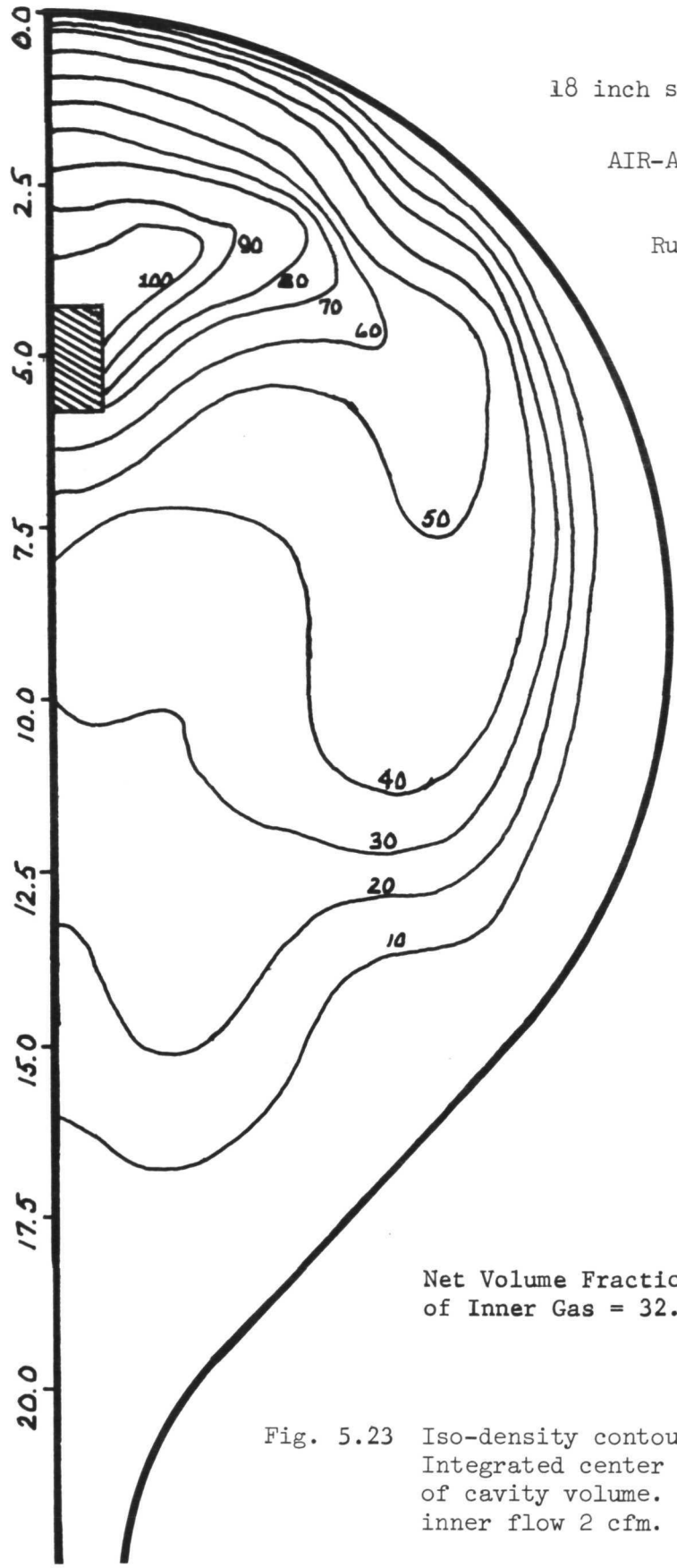

18 inch sphere

AIR-AIR

Run 8-31-71, 1900, 200:2

Injection nozzle 5 inches from top. Two inch exit nozzle with no other attenuation. Contour interval in % of center gas concentration, relative to 100% at injection nozzle.

Net Volume Fraction of Inner Gas = 32.1%

Fig. 5.23 Iso-density contours in spherical cavity. Integrated center gas concentration = 0.33 of cavity volume. Outer flow 200 cfm, inner flow 2 cfm.

5.6 Flow Rate Variations

The flow rates used in these tests were designed to scale those anticipated for the application gas core nuclear rocket. Though there are numerous missions proposed for an operating gas core nuclear rocket, it is appropriate to consider what the implications of the tests to date are for a typical mission. The recent applications proposed are for a rocket with a low thrust, in the neighborhood of 50,000 lb. For a cavity size of approximately 10 ft and rocket mass such that the acceleration is 0.01 to 0.02 g, the Reynolds† and Froude number conditions shown in Table 5-1 apply. The modified Froude number F*, shown in the table is the usual dimensionless Froude number divided by the square root of the fractional density difference between the two gases,

$$F^* = \sqrt{\frac{V^2}{L\,g} \cdot \frac{\rho_1}{|\rho_1 - \rho_2|}} \qquad \text{for gas No. 1}$$

In the flow testing, flow rates for the outer gas were varied from 50 to 600 cfm in the 18-inch diameter cavity, and from 200 to 1500 cfm in the 36-inch cavity. Inner gas flow rates were 1 to 6 cfm. It is apparent that the flow tests cover the Reynold's number region proposed for the reference rocket application. However, the modified Froude number in the tests conducted to date with argon generally just borders on the region of the application reactor.

Typical results covering the range of flow rates are shown in Figure 5.24 for the louvered modified round cavity. In general, all flow patterns look satisfactory except for the 50 cfm outer flow condition. In this case, the velocity shear forces are insufficient to expand the inner gas. In the case of 50 cfm outer flow to 6 cfm inner flow, the flow pattern looks quite satisfactory, primarily because the injection velocity for the inner gas was sufficient to expand it to a large volume without the aid of any fluid dynamic forces. At the 2 cfm inner gas flow rate, the injection velocity is essentially 0, and insufficient to push the gas up into the region where velocity shear will be able to create adequate expansion. Figure 5.25 shows similar results for the honeycombed wall cavity. Here again, differences in the injection velocity for the center gas are noticeable for those tests in which the outer gas velocities were marginal for producing expansion of the inner gas, i.e., the 50 cfm and 100 cfm conditions. However, at the 150 to 200 cfm conditions, sufficient velocity shear is developed around the injection nozzle. The center gas is expanded, and there is little difference between the flow patterns for different center gas flow rates. There is, however, a difference in the overall density of the center gas.

In Figure 5.26 can be seen the results of a range of flow rates in the large 36-inch diameter cavity. In this configuration, 200 cfm outer gas flow rates were so low that the velocity shear forces sufficient to expand the inner gas could not generally be obtained. However, by forcing virtually all of the outer gas flow through the upper louvers near the injection nozzle,

† Reynold's number for the outer gas were based on hydraulic diameters computed as twice the diametral thickness of the annular layer of fast-moving tangential flow ($4A/P = 4P \cdot \Delta r/P = 2\Delta D$, where P is the wetted outside wall perimeter).

Table 5-1

Comparison of Flow Variables

	Typical Low-Thrust Rocket Application		Tests Described in This Report: 18-inch Dia. Two-Dimensional Cavity	36-inch Dia. Two-Dimensional Cavity	18-inch Dia. Spherical Cavity
Reynolds Number					
Outer Gas	30,000		7000 to 100,000	2000 to 15,000	2000 to 8000
Inner Gas	600		50 to 1,800	120 to 500	800 to 3200
Modified Froude Number, F*	0.001 to 0.01	Air-Air	0.1 to 0.4	0.02 to 0.15	0.2 to 0.8
		Air-Argon(1)	0.03 to 0.15	0.005 to 0.04	0.05 to 0.2
For inner gas relative to outer gas density to inner gas density difference					

(1) To obtain Modified Froude number for the Freon-Air Tests, divide the Argon-Air results by 1.6

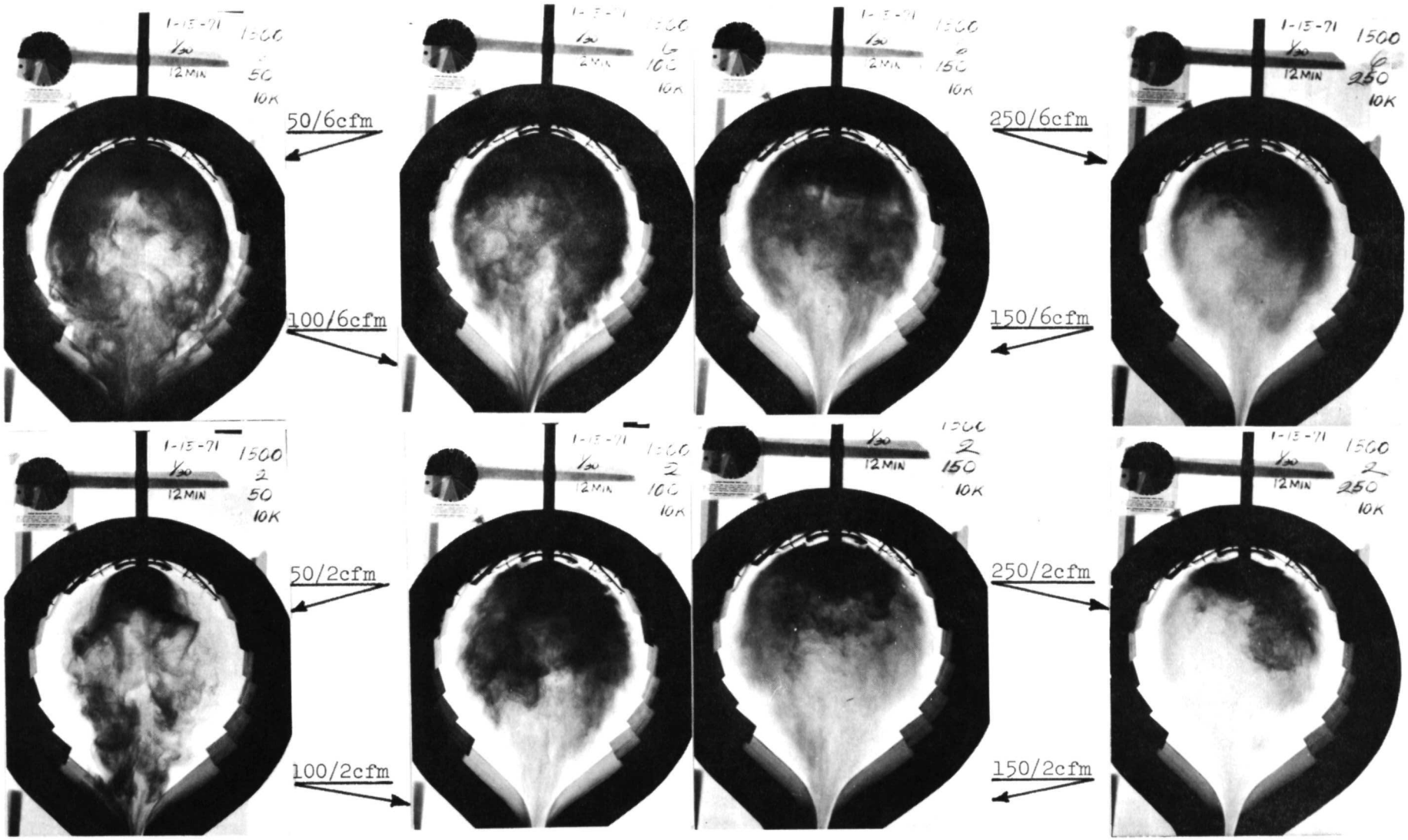

Fig. 5.24 Modified round 18" cavity with louvers. Flow contours vs flow rates. Noted are outer to inner flow rates

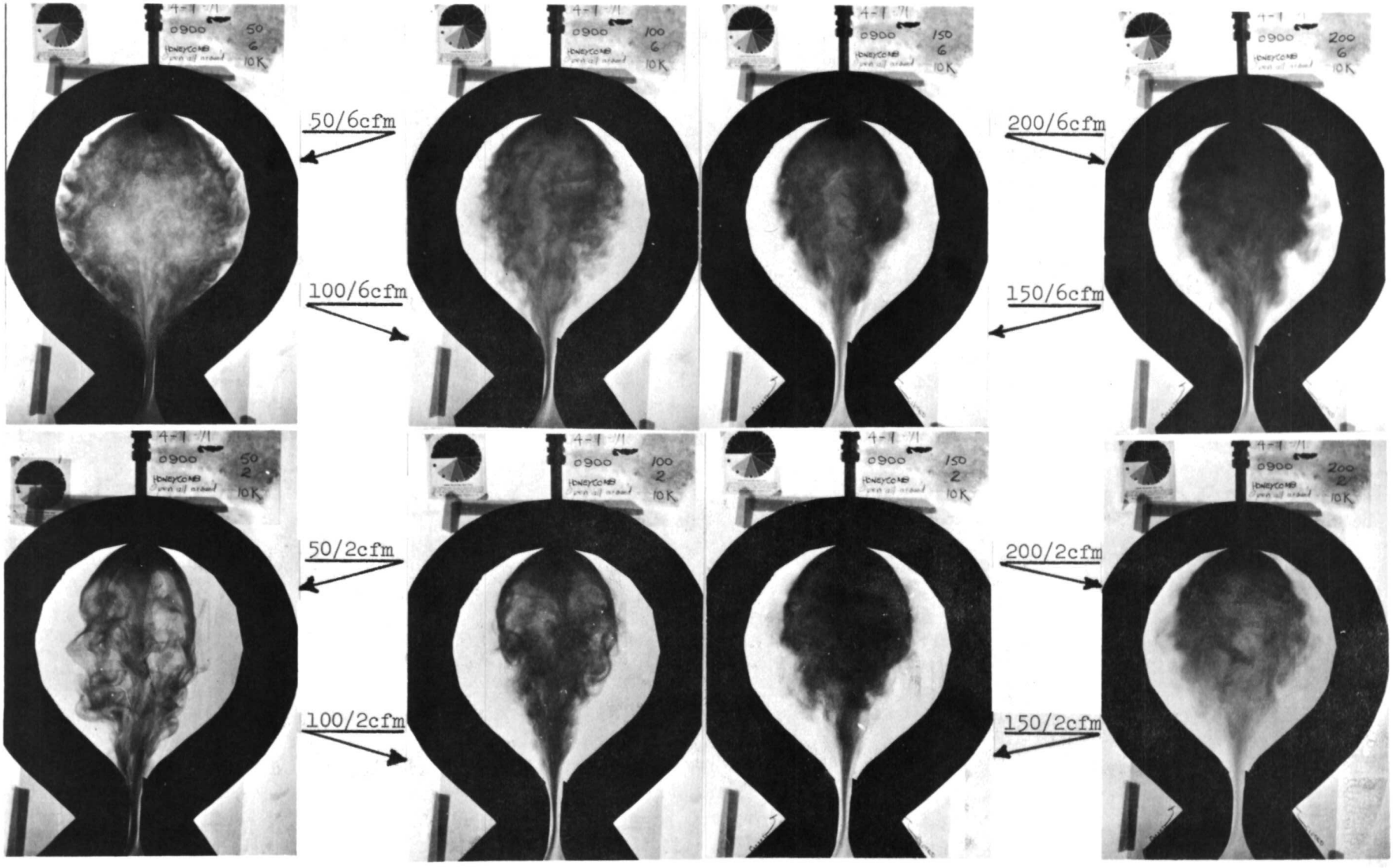

Fig. 5.25 Honeycomb wall. 18" dia. Flow contours vs flow rates. Noted are outer to inner flow rates

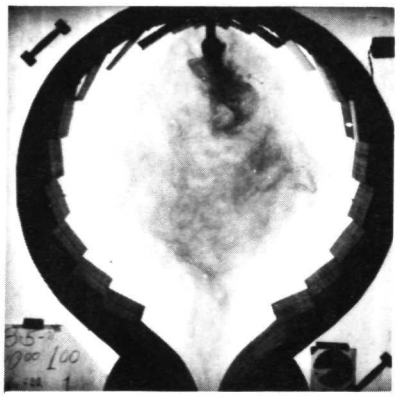

100/1

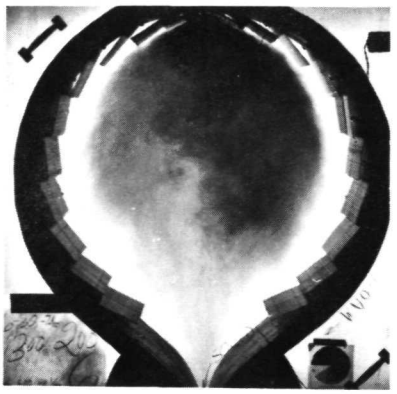

550/6

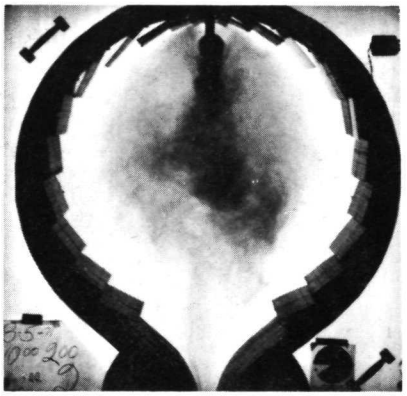

200/2

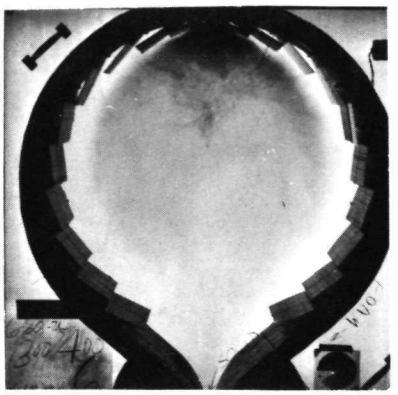

1100/6

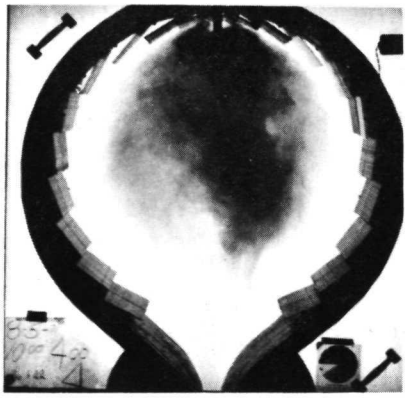

400/4

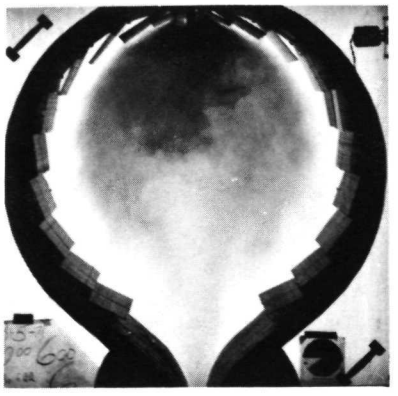

1550/6

Fig. 5.26 Large 36" diameter cavity. Flow contours vs flow rates. Noted are outer to inner flow rates in cfm

velocity shear expansion could be achieved. Results at much higher outer flow rates, without preferentially directing flow through the top louvers, were quite satisfactory, giving flow rate ratios of as high as 250 to 1 (lower right hand photograph of Figure 5.26). Note, this trick of directing more or less flow through the upper louvers appears to be a useful flow control scheme for regulating the volume of the inner gas. Tests were run with varied louver openings around mid-axis. Flow control regulation through these louvers appeared to have little effect on the size of the inner gas volume. Thus, it is important to regulate flow only through the top louvers.

Figure 5.27 shows the results of a range of flow rates in the spherical three-dimensional cavity. In this configuration, expansion of the inner gas is quite good in all but the very low outer flow rate conditions, below 100 cfm. The greater recirculation in the interior of the spherical cavity compared to that observed in the two-dimensional cavities was partly responsible for the obviously better inner gas expansion-density conditions.

5.7 Double Injector System

The single most basic general conclusion drawn from the various tests discussed previously is: appropriate flow patterns can be established in the gas core cavity to achieve high flow rate ratios of inner to outer gas, if mechanisms are found for initially expanding the inner gas to a large radius ratio. One type of scheme, tried in the earlier tests, is to inject the "fuel" so as to establish inner gas concentrations out to a large radius within the cavity. One such mechanism to do this is by using a high velocity spray injector device for the inner gas. If such high velocity injection conditions cannot be established in the actual application gas core rocket, then velocity shear and entrainment mechanisms must be utilized. However, an alternative mechanism is to have a number of injectors for the inner gas. These injectors would be located near the cavity wall and cover a large area at the cavity top just inside the fast moving turbulent tangential gas stream. The feasibility of such multiple injector systems in the high temperature operating application rocket has yet to be examined. However, some flow tests were conducted using a double injector model in order to determine if any anomalous flow patterns might result. The double injector system used is shown in Figure 5.28.

Typical results of the double injector system are shown in Figure 5.29, for several different locations and spacings of the injectors. These tests were conducted on the modified round cavity, where recirculation patterns were not too noticeable. In general, these results show that even with the double injector system, velocity shear effects are needed in order to get a uniform distribution of the center gas in the cavity. Without such an expansion mechanism, the center gas tends to accumulate near the injection points with large density gradients from there to other interior regions of the cavity. Such conditions are not desirable, as is shown in Section 5.9. Spotty regions of high density throughout the cavity are not as beneficial as uniform high densities near the outer radius of the fueled region (inner gas region). It appears that the double injector system is not the panacea that one might conclude from intuitive considerations. Instead, it appears preferable to rely on velocity shear and on recirculation flow patterns to distribute the inner gas into the volume and shape needed for nuclear criticality.

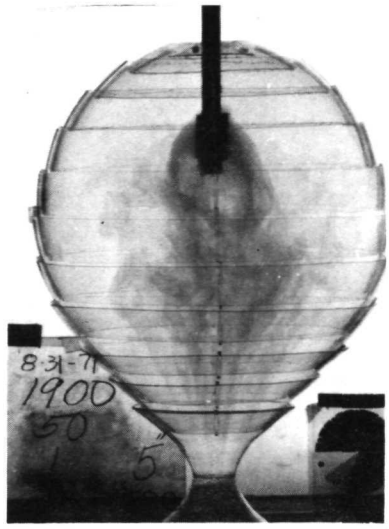

50 cfm/1 cfm

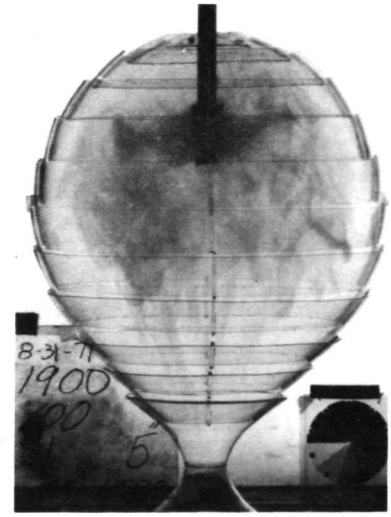

100 cfm/1 cfm

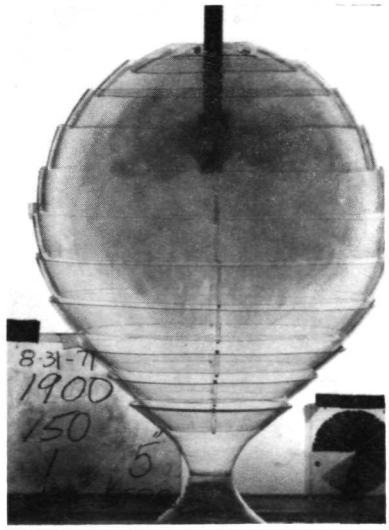

150 cfm/1 cfm

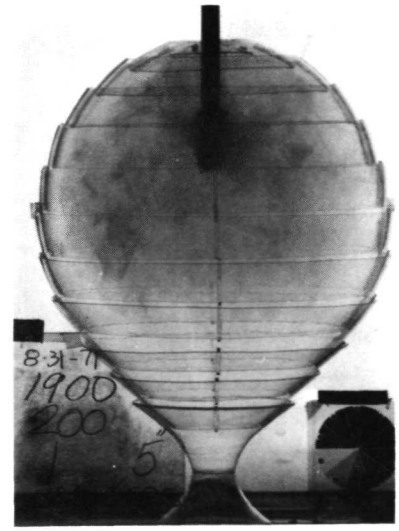

200 cfm/1 cfm

Fig. 5.27 Spherical 18-inch cavity. Flow contours vs flow rates. Noted are outer to inner flow rates

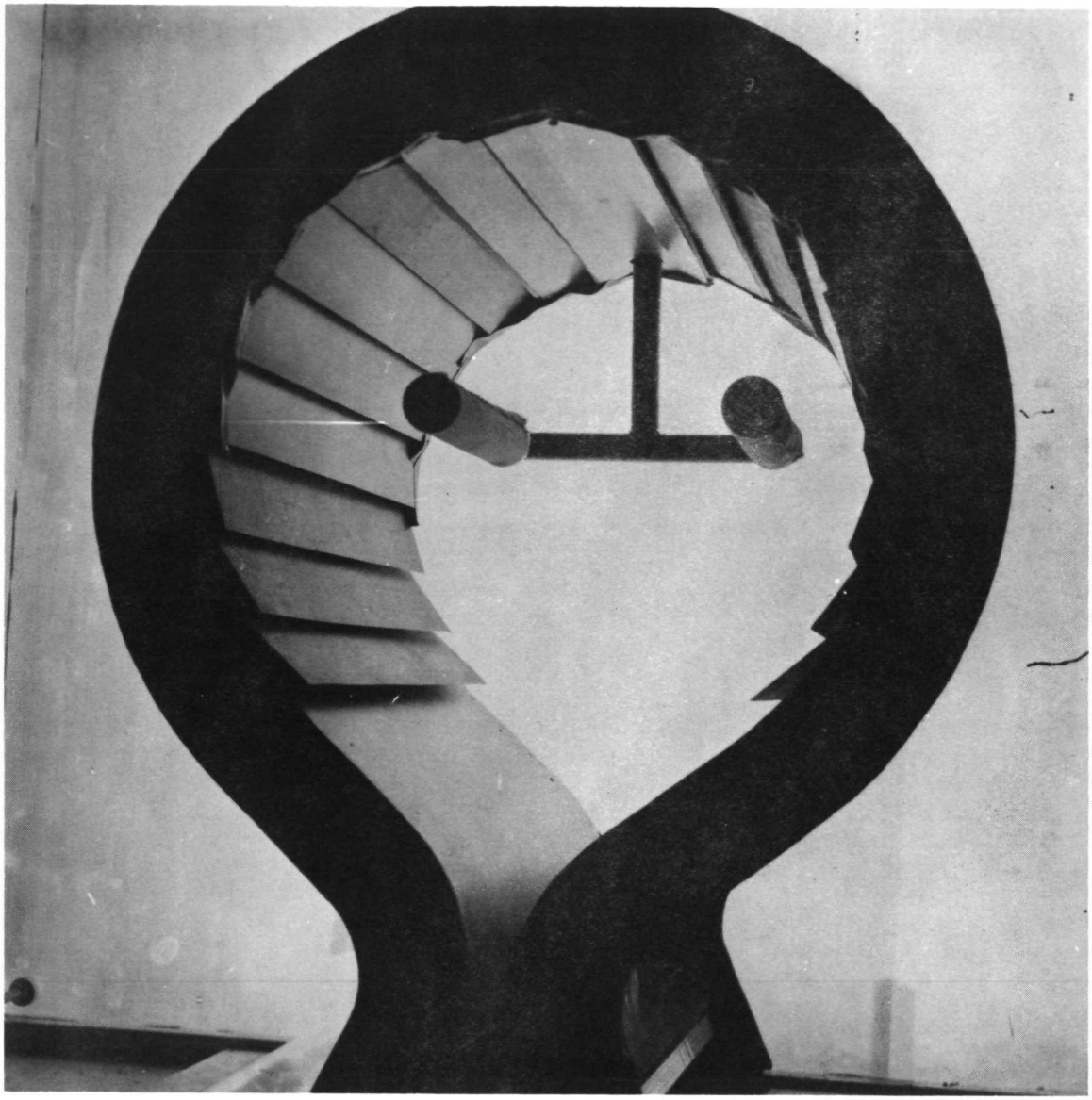

Fig. 5.28 Double injector nozzle in "Two-Dimensional" configuration

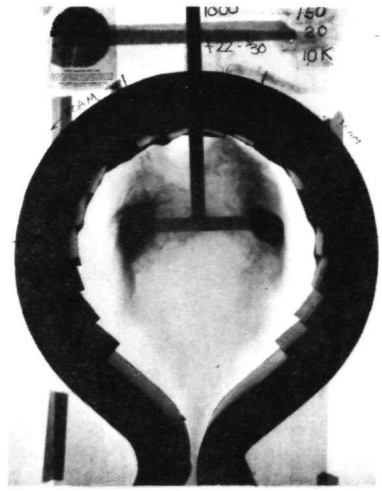

6 1/2" Down - 9" Apart

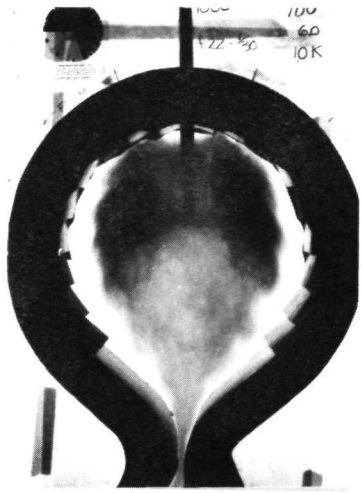

4 1/2" Down - 7" Apart

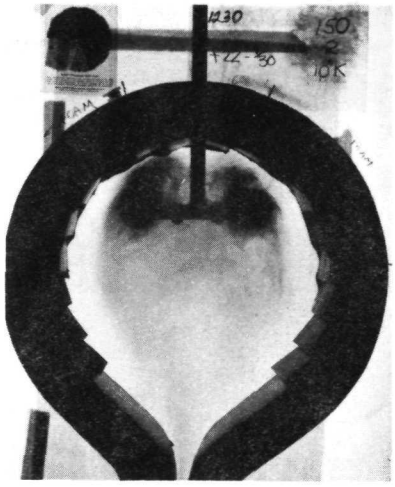

150/2 cfm

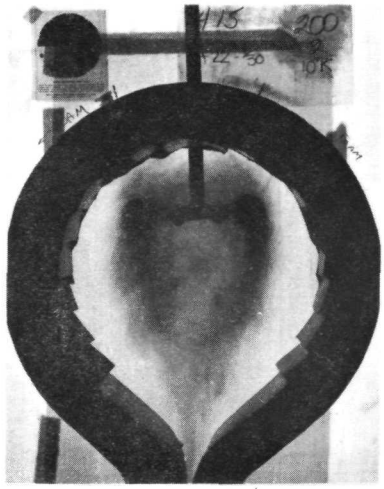

200/2 cfm

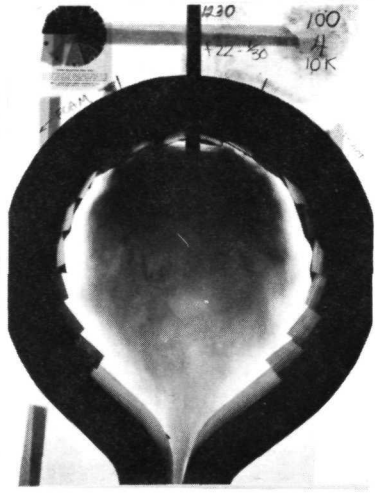

100/4 cfm

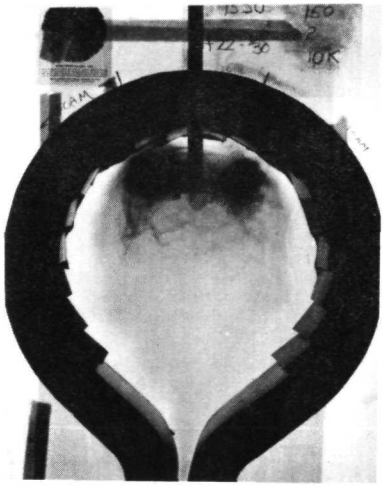

3 1/2" Down - 5" Apart

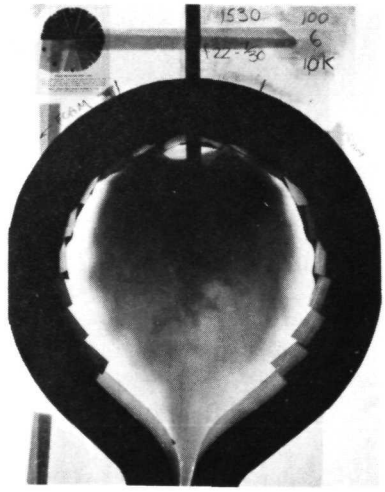

Fig. 5.29 Double injector tests. Noted are injector position from top and distance apart, as well as outer to inner flow rates

5.8 Gases With Density Differences

Experiments using air as both the inner and outer gas enable one to study only the effects of fluid dynamic forces. Gravitational effects are essentially identical on both gases, and hence are not observed. Measurements of the density of the smoked air show that it is only about 2% heavier than the unsmoked outer gas. Hence, very minor gravitational effects do occur in the air/air tests but are of little value in studying the real situation where factors of 4 to 20 in density difference appear between the hot fuel and the not-so-hot propellant. Argon, however, is 38% heavier than air, and with the slight added weight of the smoke the difference is approximately 40%. Furthermore, reference to Table 5.1 will show that the argon-air tests under a condition of 1.0 g of gravity approximately duplicates Froude number conditions of the proposed application for the gas core rocket. In that application there are density differences between the inner and outer gas of approximately a factor of 4 to 20, but the rocket acceleration is designed to be only 1 to 2% of normal gravity.

Typical results comparing tests with argon and with air as the center gas are shown in Figure 5.30. Since tests were in the downfiring direction, the gravitational force was in the same direction as the acceleration force would be in the rocket. The effect of gravity is quite obvious. The argon tends to move more directly downward towards the exhaust nozzle. Hence it is expanded less than the air, but gives generally greater center gas densities in the region that it occupies. This effect is readily seen in the iso-density plots of Figures 5.20(a) and (b). Note that the iso-density data is all referenced to the density right at the injection nozzle, where 100% density for the center gas exists. For reasons not fully understood, the injected argon is not nearly as dark as the air. Smoke appears to be filtered out in the injection nozzle preferentially more when high molecular weight gas is the carrier. Comparison of the air vs argon pictures will therefore be somewhat misleading when one attempts to deduce gas density from the general photographic density appearing in the picture.

Figures 5.31(a) and (b) show comparison between argon and air tests in the elongated two-dimensional cavity. These photographs are time exposures which integrate out short time scale variations in the inner gas density. These result from the slow circulation patterns in the cavity interior. Again, it is obvious that the velocity shear mechanisms are less effective in expanding the heavier argon gas. Figure 5.32 shows the results in the large 36-inch diameter cavity, at a flow rate ratio of approximately 100 to 1. With the conditions shown, velocity shear mechanisms are apparently quite adequate for expanding the inner gas. The argon test shows a noticeable asymmetry with most of the flow proceding toward the right side of the cavity. A similar situation seems to also exist in the air/air test. However, in the latter, recirculation is sufficient to substantially reduce the overall asymmetry. In the argon test, the recirculation is generally insufficient to overcome the gravitational effect, and argon was not redistributed around the interior of the cavity.

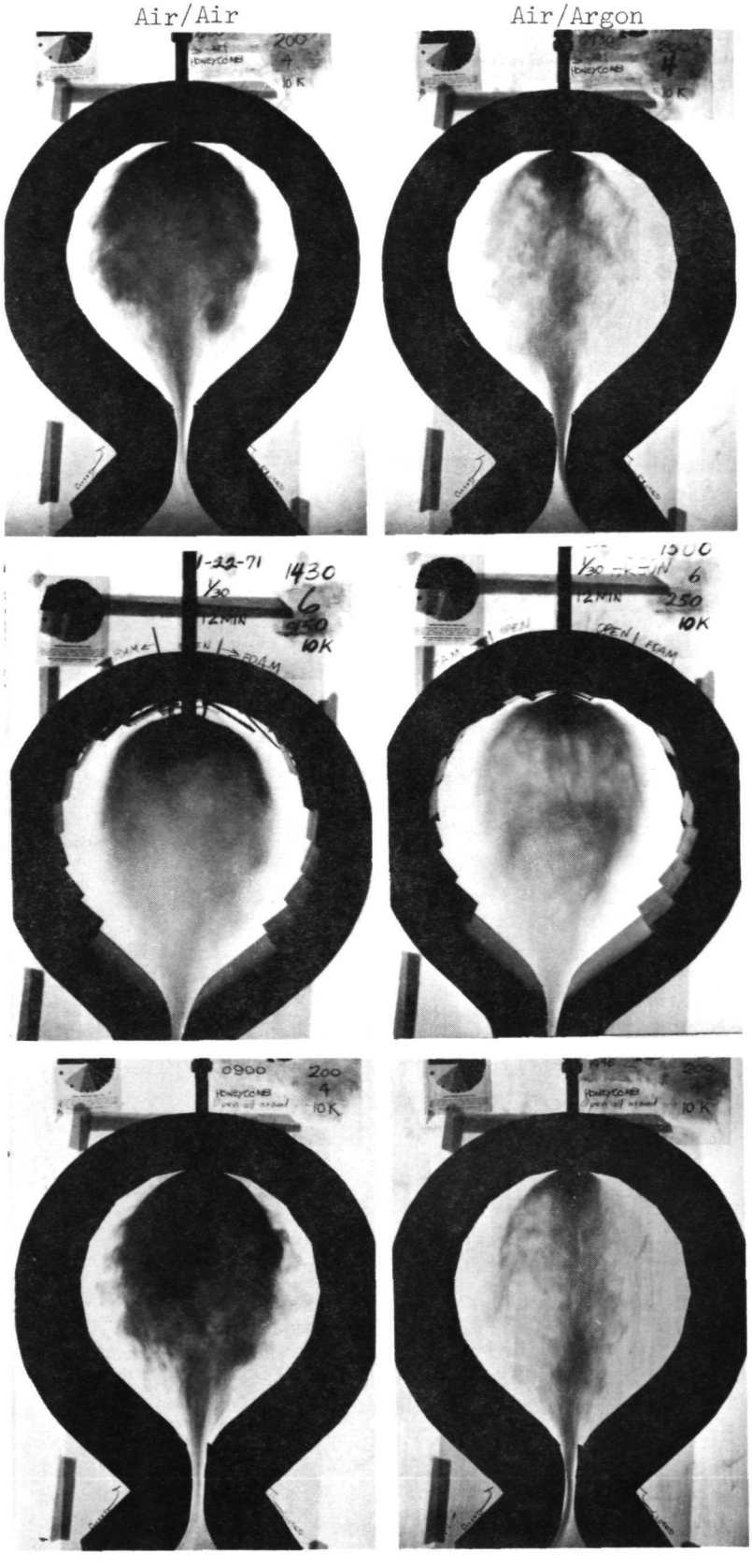

Fig. 5.30 Comparison of air vs argon as central gas. Shown are outer to inner flow rates in cfm.

Air/Air

Air/Argon

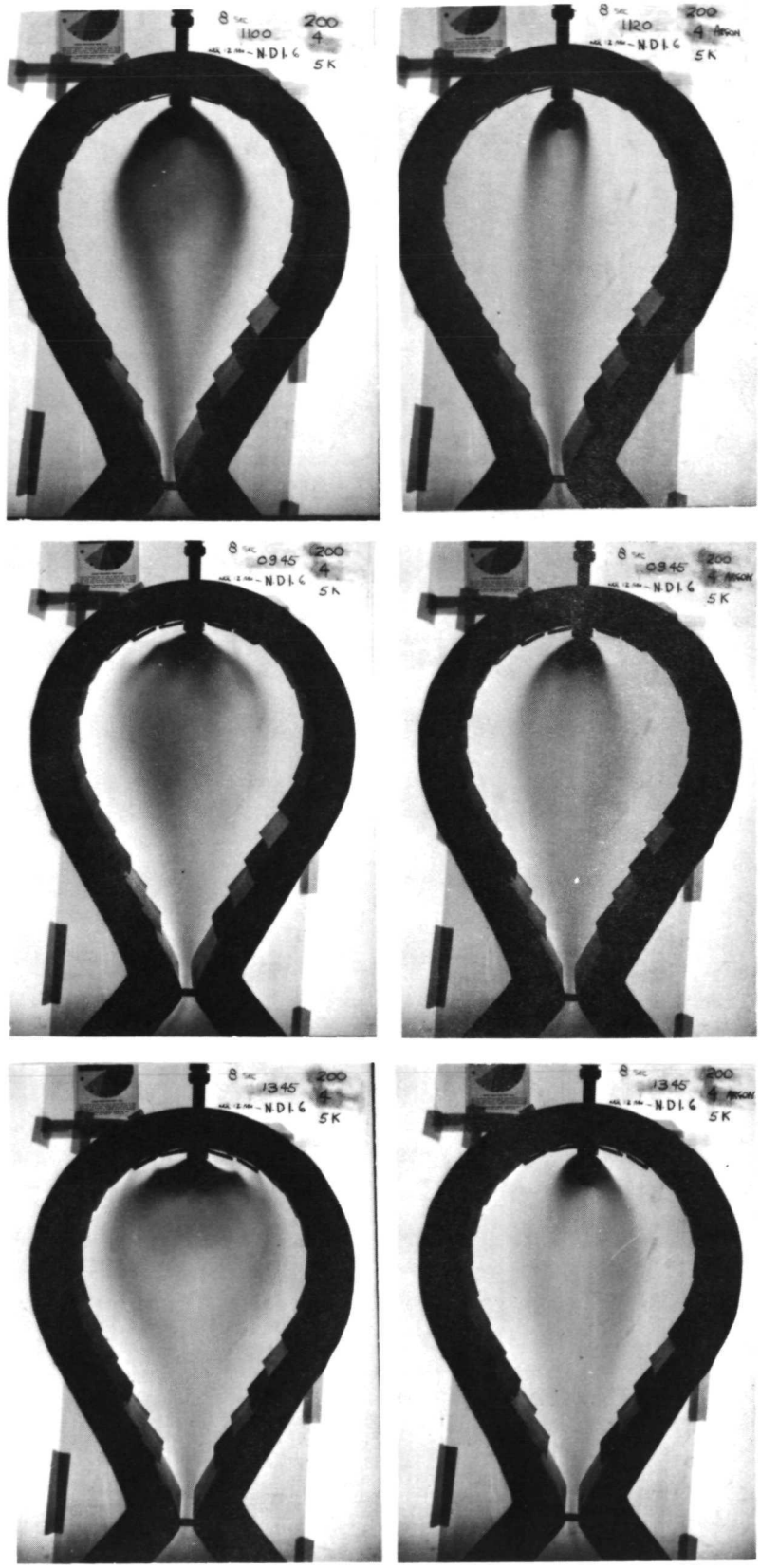

No foam restrictions

Foam on surface of top two louvers

Foam on top two louvers and extra 1-3/4" flow directing louver installed at very top of cavity

Fig. 5.31(a) Comparison of air vs argon as central gas. All flows 200 cfm outer, 4 cfm inner. All pictures are time exposures.

Air/Air

Air/Argon

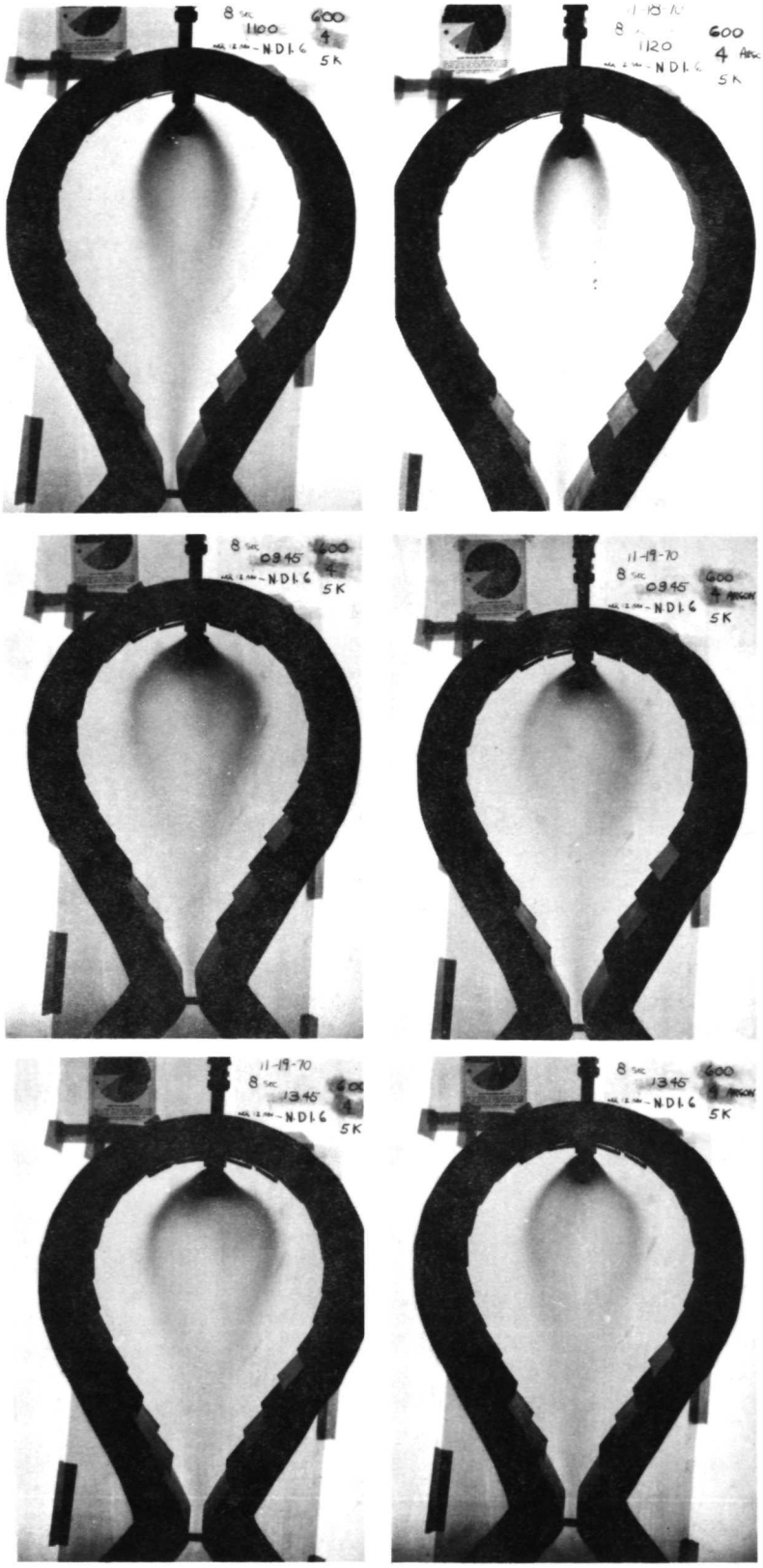

No foam restrictions

Foam on surface of top two louvers

Foam on top two louvers and extra 1-3/4" flow directing louver installed at very top of cavity

Fig. 5.31(b) Comparison of air vs argon as central gas. All flows 600 cfm outer, 4 cfm inner. All pictures are time exposures.

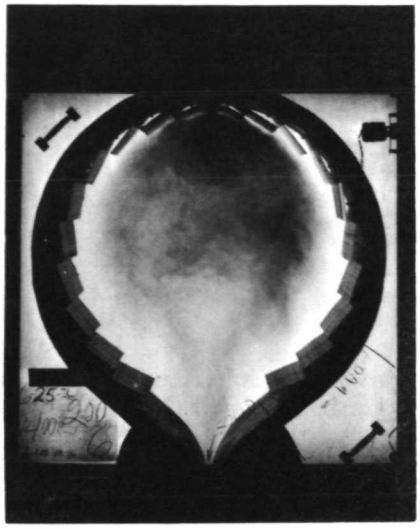

Air/Air

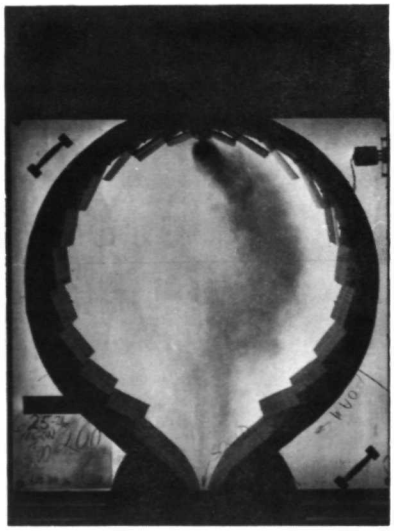

Air/Argon

Fig. 5.32 Comparison of Air vs Argon as central gas. Large 36-inch diameter cavity. Flow rates in cfm are 550 on outside, 6 on inside.

Tests were made with freon as the inner gas, giving a density ratio of approximately 4 to 1 between the inner and outer gases. Gravitational forces were more obvious in the freon tests than in the argon tests. However, photographs of the flow patterns were generally of poor quality because of the difficulty in darkening the freon entering through the injection nozzle. Thus, it must suffice for this report to merely comment that the visible flow patterns with freon and air obtained to date were generally unacceptable from a nuclear criticality point of view.

5.9 Coupling Effects of Flow and Reactivity

Using the critical experiment data[4],[5] as a calibration base for diffusion theory calculations, a number of criticality calculations were done on idealized spherical geometry models of the density configuration measured in the non-nuclear flowing experiments. The models used were spherical, with various shells containing different volume fractions of the uranium fuel and hydrogen propellant. A range of shell thicknesses and volume fractions were selected. In general, these were chosen such that the outer mixed layer was approximately 50% fuel, followed by a thin inner layer of somewhat higher fuel density, and the major central cavity region diluted to approximately 50% fuel. In all cases, the outermost layer adjacent to the cavity wall was pure hydrogen gas, between 4 inches and 16 inches thick in the 8 ft diameter cavity. The inner radius of this pure hydrogen region defined the radius ratio of the fuel to cavity.

Figure 5.33 displays the general trend of these calculations which, though idealized, should give some indication of the effects of fuel distribution on the criticality conditions. Fundamentally, the effects of inner region recirculation and mixing are noticeably not deleterious, in fact are nominally beneficial because of hydrogen moderation. The more important consideration is to expand the inner gas to as large a volume as is feasible. Figure 5.33 clearly shows these differences. Of course, there is the problem of leaving sufficient boundary layer of unfueled propellant gas to prevent melting of the walls. However, with the high extinction parameters obtainable in the seeded propellant[7], it appears that this is not a major problem.

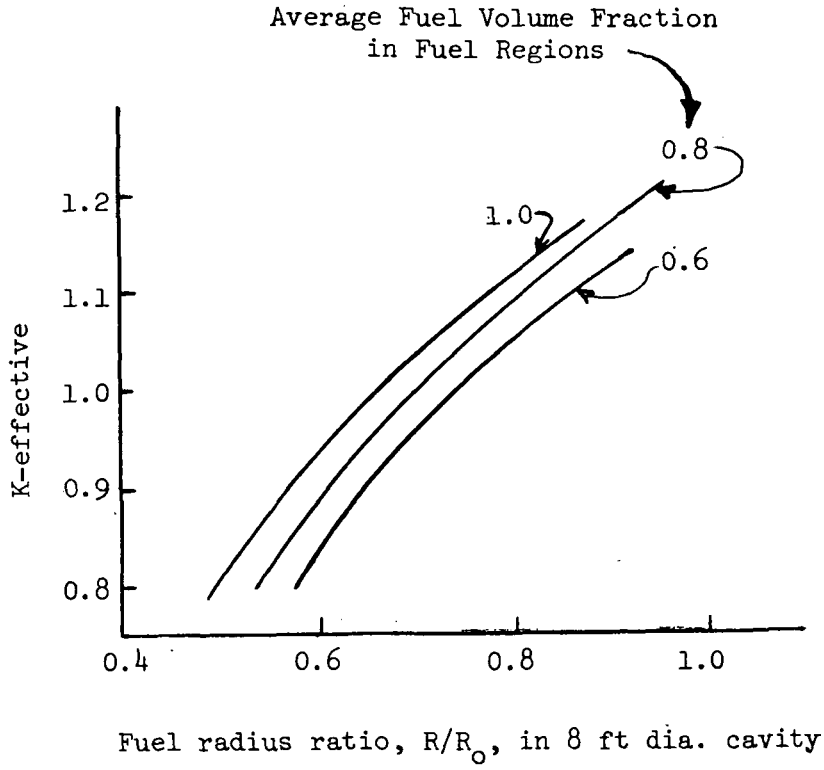

Fig. 5.33 Effect of fuel radius ratio and fuel volume fraction in fuel region on criticality

VI. CONCLUSIONS

The following conclusions can be drawn from the flow testing performed to date.

1. Obtaining the expansion with or without re-circulation of the inner gas into as large a volume as possible of the cavity is the major problem and goal.

2. Obtaining high volume flow rate ratios with high fuel volume fraction can be achieved by properly directing a high velocity outer gas flow stream tangentially along the cavity wall. The resulting high-shear, turbulent, high-velocity stream is nominally but a few inches thick (< 2 inches in the 18-inch diameter test, < 4 in the 36-inch diameter tests).

3. Expansion modes that have proven quite satisfactory for the inner gas are:

   a. High injection velocity--a condition that may not occur in the fuel vaporization process in the operating gas core.

   b. Expansion via velocity shear, by allowing the injected gas to contact the high velocity outer stream. Too much contact results in excessive mixing and dispersal; too little contact does not allow the heavier inner gas to become dispersed in the cavity interior before acceleration (gravity) causes the heavy gas to "fall out of" the exhaust nozzle.

4. Recirculation within the interior appears at present to be desirable and even necessary to assure good dispersal of the heavy inner gas throughout a large portion of the cavity.

5. The penalty of a low radius ratio (of inner gas radius/cavity radius) is more severe than the mixing of hydrogen and uranium in the cavity interior. The latter is in fact slightly beneficial except near the outer edge of the fuel region.

6. Recirculation patterns appear to be most obvious in the elongated cavities. Otherwise, cavity shape has little effect on flow patterns. The round shape is preferred for nuclear criticality conditions.

7. Exhaust nozzle pressure drop appears to have a slight effect on flow patterns and density distribution only in the lower regions of the cavity. The reason is not understood, and the observed effect is suspected of being one that may be the result of pressure leaks, and hence unreal. None of the tests to date have been conducted close to choked flow conditions.

8. Heavier gases as the central gas show a noticeable gravitational effect. They fill the cavity less easily, and tend to travel directly downward toward the exhaust nozzle. The direction of the gravitational force corresponds to the inertial force direction in an accelerating rocket. The reader needs to be cautioned in examining the photographic results in this report. The heavier gases were "colored" less darkly by the smoke than was the lighter air. Hence, only by referring to iso-density plots can one reliably obtain a measure of fuel volume fraction in the cavity.

9. The use of multiple injectors near the periphery of the desired outer fuel radius will not in itself guarantee better combination of volume fraction and radius ratio than the single injector model. Mechanisms for distributing the multiple injector feed material must be present, or else heavier inner gas will stream toward the exit nozzle in multiple streams.

10. Volume flow rate ratios of outer to inner gas of 100/1 to 200/1 can give very satisfactory uranium fuel distributions and volume fractions, the latter in the range of 33% for spherically shaped cavities. However, such desirable results were most readily obtained with gases of equal density. When gases of different densities were tested, not only were flow distribution patterns slightly less satisfactory, for the same volume flow rate ratios, but the mass flow rate ratio was automatically reduced by the ratio of the gas densities.

The above conclusions are with reference to the fundamental goal of achieving flow distributions in the cavity which will permit the gas core reactor to be critical with as low as possible cavity pressure, hence low atom densities in the cavity.

REFERENCES

1. F. E. Rom, "Comments on the Feasibility of Developing Gas Core Nuclear Rockets," NASA TM-X-52644, Conference on Frontiers of Power Technology, October 23-24, 1969.

2. J. C. Bennett and B. V. Johnson, "Experimental Study of One- and Two Component Low-Turbulence Confined Axial Flows," NASA CR-1851 (June 1971).

3. H. Weinstein, et al., "Turbulence in the Mixing Region Between Ducted Coaxial Streams," NASA CR-1335 (July 1969).

4. J. F. Kunze, G. D. Pincock and R. E. Hyland, "Cavity Reactor Critical Experiments," Nuclear Applications, 6, p. 104 (1969)

5. J. F. Kunze, J. H. Lofthouse, C. G. Cooper, and R. E. Hyland, "Benchmark Gas Core Critical Experiment," Nuclear Science and Engineering, 47, p. 59 (1972).

6. C. D. Lanzo, "A Flow Experiment on a Curved-Porous-Wall-Gas-Core Reactor Geometry," Nuclear Applications and Technology, 8, p. 6 (1970).

7. J. R. Williams, et al., "Thermal Radiation Absorption by Particle-Seeded Gases," Journal of Spacecraft and Rockets, 8, p. 339 (1971)

APPENDIX A

Flow Measurement Using Orifices

The standard methods of measuring flow by using a sharp edged, tapered orifice have been employed in the experiment. The basic reference for these methods is the ASME Research Report on Fluid Meters, 5th Edition, New York (1959) published by American Society of Mechanical Engineers.

The so-called "radius taps" were employed in both measuring circuits. These are installed so that the upstream tap is at 1.0 pipe diameter and the downstream is at 0.5 pipe diameter from the upstream orifice face. The upstream straight (unperturbed) pipe section was at least ten pipe diameters, and the downstream straight length was six pipe diameters. The basic equation is

$$V_2^2 - V_1^2 = 2gh$$

where h is the fluid head difference measured at the flange taps where the velocities are V_2 and V_1.

Since $q = Av$, it is easily shown that

$$q = A_o \sqrt{2gh} \left[\frac{1}{\sqrt{1 - (\frac{Ao}{Ap})^2}} \right] C_d$$

The term in parentheses is usually referred to as the "velocity-of-approach" factor, where Ao is the orifice area and Ap is the pipe area. The head is usually measured as a pressure difference:

$$h = \frac{\Delta p}{\rho}$$

where ρ is the fluid density and p the pressure.

The ratio of ρ for smoked air/argon/freon is 1.0/1.39/4.11.

The discharge coefficient of C_d is usually tabulated as a total flow coefficient:

$$K = \frac{C_d}{\sqrt{1 - (\frac{Ao}{Ap})^2}}$$

The values of K were obtained from Table 12 of the referenced document, as a function of Reynolds number and Ao/Ap. In general, $C_d \approx 0.6$.

APPENDIX B

Film Response

Density measurements of the smoked central gas were made by recording the back-lighted scene on film, and then making film density measurements using a sensitive, highly resolving, automatic-recording densitometer. The events were recorded on 35 mm film, with the cavity filling nearly the entire film frame (24 x 36 mm). The densitometer light beam was a slit of light 0.025 mm wide at the film plane. The slit height was generally varied between 1 and 10 times the slit width, depending on the vertical averaging desired.

The measured transmission is an exponential function of the smoke density, $T=T_o e^{-\mu\chi}$. Furthermore, most films have a nominal logarithmic response, i.e., film density is a logarithmic function of exposure. This relationship is true only over a portion of the density-exposure curve. To minimize or eliminate the number of needed corrections, it is desirable to operate the film in the logarithmic portion of this curve so that

$$D_{film} = \log T_o e^{-\mu\chi} = \log T_o + \mu\chi \log_{10} e$$

i.e., so that the density read on the film is proportional to the density of smoke, $\mu\chi$.

The exponential relationship for transmission of light is rigorous, if multiple scattering effects of light back into the beam are negligible. For the "two-dimensional" tests, such scatter buildup will be nominally uniform over the entire image, and corrections for or elimination of the scattering is not needed. For the three-dimensional tests, however, side directed light can reflect from the forward portion of the smoke surface into the transmitted light beam. Therefore, for the three-dimensional tests, the light source was confined ("collimated") to an area equal to the cross sectional area of the cavity, thus virtually eliminating the surface scattering problem. It was assumed that the multiple beam scattering would not significantly distort the transmission measurement.

The film response with respect to the smoke density was calibrated using the test box and the identical smoke mixing and flow apparatus used in the flow tests. A wedge shaped region, through which the smoke flowed, was photographed. The resulting wedge was then scanned for density. This was done for various exposures, and various smoke densities injected into the pipe leaving the smoke mixing box. Subsequently, a standard injection smoke density was adopted (reading of 10 K-ohm across the photo cell). Likewise a standard development, approximately as recommended by the manufacturer, was adopted. This was 12 minutes (at 70°F) in a 1:1 dilution of D-76 on Panatomic-X film.

Various curves for different exposures are shown in Figure B-1. All of these curves were obtained with a 5% transmitting neutral density filter. As can be seen, the

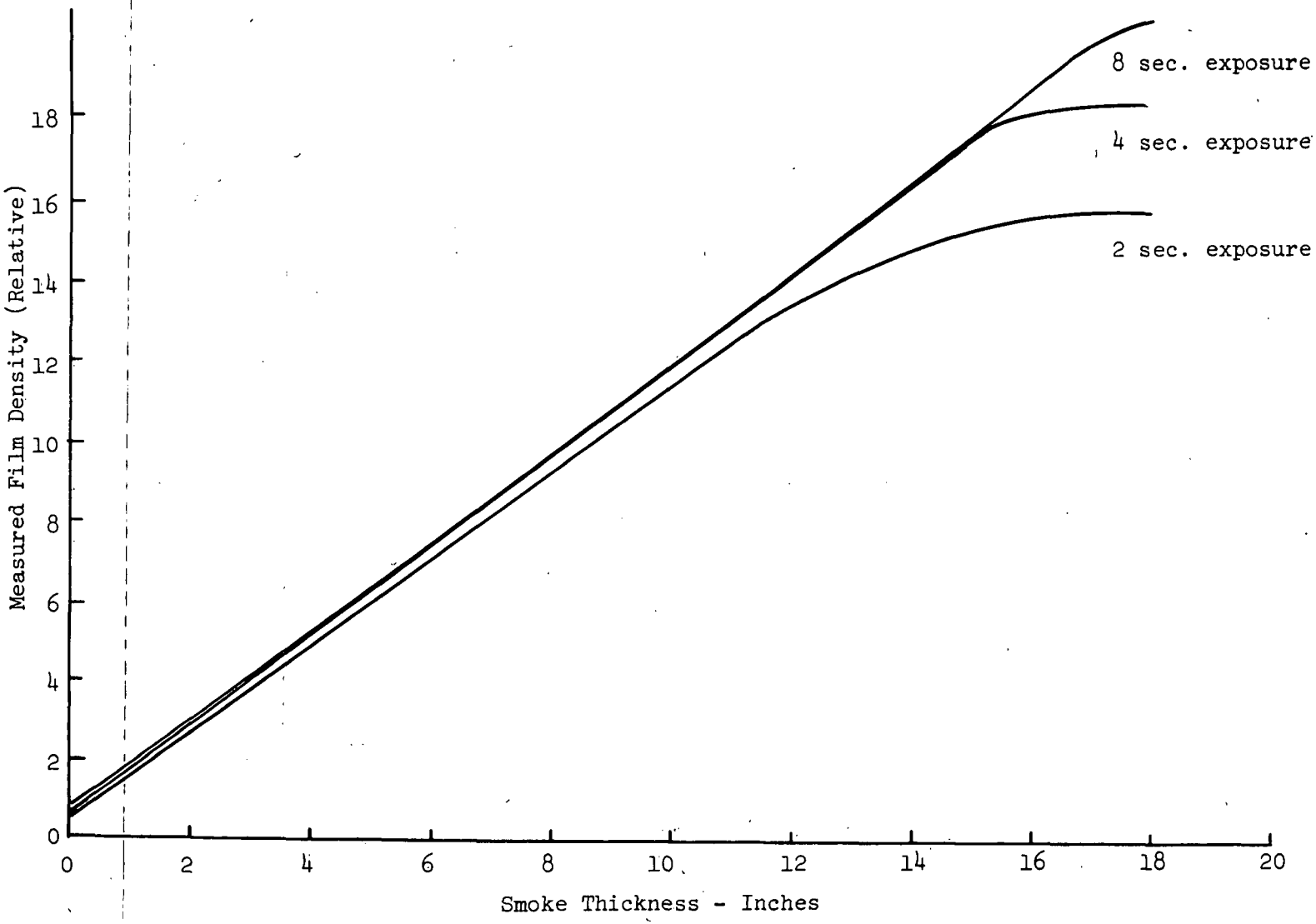

Fig. B-1 Results of Wedge Smoke Calibration Test, Panatomic-X film, D-76, 1:1 for 12 minutes Neutral Density Filter with 5% transmission

8-second exposure results gave a linear response over 0 to 18-inch smoke depth, which is the full range of the smoke density in the small scale tests. The 36-inch thick large scale tests showed slight loss of linearity at full density, 36-inch smoke thickness, using these same exposures. Hence, when densitometer readings are to be made from the 36-inch tests, exposure times are lengthened somewhat to retain more linearity over the entire range, particularly at the high end of the density-exposure curve.

APPENDIX C

Radial Density Function from Chordal Measurements*

The problem is simply one of:

Given: a radial density distribution with azimuthal symmetry, in a sphere or cylinder.

Problem: from measurements of the integrated density at a number of locations along a projected diameter, deduce the radial density function.

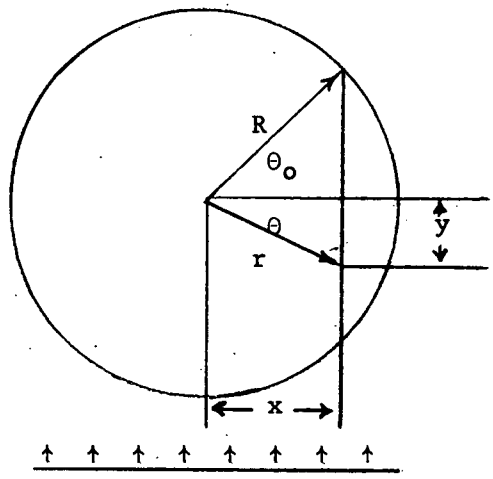

Density measurements at various locations along the diameter in the direction shown.

$$y = r \sin \theta$$
$$x = R \cos \theta_o$$

The linear absorption coefficient should be directly proportional to the density assuming that the buildup from scattered light is also linear with density

1) $\mu = B\rho(r)$, where B is a constant factor

The total absorption in the direction of the arrows is given by W(x), which is the sum of all the absorbing material in the chord.

---

* Contributed by R. C. Young

2) $$W(x) = 2B \int_0^{R \sin \Theta} \rho(r(x,y))dy = 2B \int_0^{\sqrt{R^2 - x^2}} \rho(\sqrt{x^2 + y^2})\, dy$$

The light transmission $t = t_o e^{-W}$, but the film density (D) is normally a logarithmic response to light; i.e.,

$$D = D_o + \gamma \log (t/t_o)$$

and $$t = t_o e^{-W}$$

3) $$D = D_o - \gamma W$$

For this relation to be valid, there must be a negligible amount of scattered light from regions with significantly different density from that of the chord being measured.

Equation 2 can be manipulated to give (noting rdr = ydy)

4) $$W(x) = 2B \int_x^R \rho(r) \frac{rdr}{\sqrt{r^2 - x^2}}$$

Equation (4) is the basic equation that must be inverted so as to solve for $\rho(r)$ when W(x) is known. Proceed as follows.

Multiply by $\frac{xdx}{\sqrt{x^2 - u^2}}$ and integrate from x = u to x = R, where u is a dummy variable, giving

5) $$\int_u^R \frac{W(x)\, xdx}{\sqrt{x^2 - u^2}} = 2B \int_u^R \int_x^R \rho(r) \frac{xdx}{\sqrt{x^2 - u^2}} \frac{rdr}{\sqrt{r^2 - x^2}}$$

$$= 2B \int_u^R \rho(r)\, r \int_u^r \frac{xdx}{\sqrt{x^2 - u^2}\sqrt{r^2 - x^2}}\, dr$$

The inner integral over dx has the value of $\frac{\pi}{2}$*. Therefore, we can now differentiate with respect to u, noting that $\rho(R) = 0$ (i.e., zero density at the outer radius of the cavity), to get (note dummy variable u has been switched to r).

$$6) \quad \frac{d}{dr} \int_r^R \frac{W(x)\ x\,dx}{\sqrt{x^2 - r^2}} = -B\pi r\rho(r)$$

Integrating the left hand side by parts gives:

---

* To evaluate

$$\int_u^r \frac{x\,dx}{\sqrt{x^2 - u^2}\sqrt{r^2 - x^2}}, \qquad \text{substitute} \quad x^2 = r^2 - (r^2 - u^2)\cos^2\phi$$

$$2x\,dx = (r^2 - u^2)2\cos\phi\sin\phi\,d\phi$$

$$\text{at } \phi = 0,\ x = u$$

$$\phi = \pi/2,\ x = r$$

$$r^2 - x^2 = (r^2 - u^2)\cos^2\phi$$

$$x^2 - u^2 = (r^2 - u^2)(1 - \cos^2\phi)$$

$$= (r^2 - u^2)\sin^2\phi$$

$$\int_o^{\pi/2} \frac{(r^2 - u^2)\,\mathrm{Cos}\,\phi\ \mathrm{Sin}\,\phi\,d\phi}{\sqrt{r^2 - u^2}\,\mathrm{Sin}\,\phi\sqrt{r^2 - u^2}\,\mathrm{Cos}\,\phi} = \int_0^{\pi/2} d\phi = \pi/2$$

7) $$\frac{d}{dr}\left\{\left[W(x)\sqrt{x^2 - r^2}\right]_r^R - \int_r^R \frac{dW}{dx}\sqrt{x^2 - r^2}\,dx\right\}$$

The first term is zero because $W(R) = 0$ and $\sqrt{x^2 - r^2} = 0$ at the lower limit of r.

8) $$B\pi r\rho(r) = + \frac{d}{dr}\int_r^R \frac{dW}{dx}\sqrt{x^2 - r^2}\,dx$$

$$= -\sqrt{x^2 - r^2}\left.\frac{dW}{dx}\right|_{x=r} - \int_r^R \frac{dW}{dx}\frac{d}{dr}\left(\sqrt{x^2 - r^2}\right)dx$$

8(a) $$B\pi r\rho(r) = -0 - r\int_r^R \frac{dW}{dx}\frac{dx}{\sqrt{x^2 - r^2}}$$

Finally, one obtains

9) $$\rho(r) = -\frac{1}{B\pi}\int_r^R \frac{dW}{dx}\frac{dx}{\sqrt{x^2 - r^2}} = -\frac{A}{\pi}\int_r^R \frac{dW}{dx}\frac{dx}{\sqrt{x^2 - r^2}}$$

Even though $\sqrt{x^2 - r^2} = 0$ at the lower limit, $\frac{dW}{dx} = 0$ also, and the integral converges. Note also, that the constant $\frac{1}{B}$ was replaced by A for convenience.

To evaluate the result (9) for experimental data, the approximation is used

10) $$\frac{1}{X}\frac{dW}{dX} = \frac{2}{X_{n+1} + X_n}\frac{W_{n+1} - W_n}{X_{n+1} - X_n} = \frac{2\,(W_{N+1} - W_n)}{X_{n+1}^2 - X_n^2}$$

11) for $X_n \leq X \leq X_{n+1}$ and $0 \leq n \leq N$; $\quad W_{n+1} \equiv 0$

This corresponds to the use of a parabola, coaxial with the experimental volume, for interpolating between the measured values.

12) $$\rho(r_k) = -\frac{A}{\pi}\sum_{n=k}^{N}\int_{X_n}^{X_{n+1}}\frac{1}{x}\frac{dW}{dx}\frac{xdx}{\sqrt{x^2 - r_k^2}}$$

$$= -\frac{A}{\pi}\sum_{n=k}^{N}\frac{2(W_{n+1} - W_n)}{X_{n+1}^2 - X_n^2}\int_{X_n}^{X_{n+1}}\frac{xdx}{\sqrt{x^2 - r^2}}$$

$$= \frac{2A}{\pi}\sum_{n=k}^{N}\frac{W_n - W_{n+1}}{X_{n+1}^2 - X_n^2}\left[\sqrt{X_{n+1}^2 - r_k^2} - \sqrt{X_n^2 - r_k^2}\right]$$

13) $r_k = k\frac{R}{N}$ and $X_n = n\frac{R}{N}$

Using (13), one can convert the X_n and r_n to forms as follow

$$X_{n+1}^2 - X_n^2 = \left(\frac{R}{N}\right)^2 (2n+1)$$

and $$\sqrt{X_{n+1}^2 - r_k^2} = \frac{R}{N}\sqrt{(n+1)^2 - k^2}$$

Finally, one obtains

14) $$\rho_K = \frac{2AN}{\pi R}\sum_{n=k}^{N}\frac{W_n - W_{n+1}}{2n+1}\left\{\sqrt{(n+1)^2 - k^2} - \sqrt{n^2 - k^2}\right\}$$

or with substitutions $D_n = \frac{W_n - W_{n+1}}{2n+1}$ and $h_n = \sqrt{n^2 - k^2}$

15) $$\rho_k = \frac{2A}{\pi\Delta X}\sum_{n=k}^{N} D_n (h_{n+1} - h_n)$$

Since $\frac{R}{N} = \Delta X$, the mesh interval.

The constant A is usually adjusted so that the maximum value of the smoke density ρ at the injection point is 1.0.

The containment ratio is calculated simply as

16) $$C.R. = \frac{\text{Total integrated density relative to 100\% for injection density}}{\text{Total Volume of Cavity}}$$

Integrated density is

17) $$U = \int_o^L dZ \int_o^R 2\pi r\rho(r)dr = 2\pi \sum_{i=1}^{M}\left(\frac{Z_{i+1}-Z_{i-1}}{2}(\Delta X_i)^2 \sum_{k=1}^{N} k\rho_k\right)$$

where there are M planes along which density traces were taken.

Likewise, the total volume is

18) $$V = \int_o^L dZ \int_o^R 2\pi r dr = \pi \sum_{i=1}^{M} \frac{Z_{i+1} - Z_{i-1}}{2}(N_i \Delta X_i)^2$$

19) $$C.R. = \frac{U}{V} \quad .$$

APPENDIX C
(Continued)

FORTRAN PROGRAM FOR REDUCING SCAN DATA TO DENSITY DISTRIBUTION

```
C       THIS PROGRAM READS VALUES OF INTEGRATED DENSITY ALONG CHORDS OF
C         A CIRCLE AND COMPUTES THE RADIAL DISTRIBUTION OF DENSITY AT
C         SEVERAL AXIAL POSITIONS.
C       THE CHORDS ARE TO BE AT EQUAL INTERVALS FROM THE AXIS.
C       CYLINDRICAL SYMMETRY IS ASSUMED.
C
C       THE MEASURED INPUT VALUES CORRESPOND TO THE INTEGRATED DENSITY
C             W(X) = 1/A INTEGRAL.DY RHO(R(X,Y))
C                  = 2/A INTEGRAL.DR R * RHO(R) / SQRT(R**2 - X**2)
C                           LIMITS X TO RMAX
C       THE PATH IS ALONG THE CHORD OF A CIRCULAR SECTION AT DISTANCE
C          X FROM THE CENTER, RMAX = RADIUS OF CIRCLE.
C
C       THIS INTEGRAL MAY BE INVERTED TO GIVE DIRECTLY THE RADIAL
C       DISTRIBUTION OF DENSITY --
C             RHO(R) = A/PI INTEGRAL.DX (-DW/DX) / SQRT(X**2 - R**2)
C                           LIMITS R TO RMAX
C       WHERE DW/DX IS THE DERIVATIVE OF W
C             A     IS A NORMALIZATION OR SCALE CONSTANT
C
C       FOR NUMERICAL EVALUATION, THE QUANTITY  D(X) = (1/X)*(-DW/DX)
C       IS ASSUMED TO BE SMOOTHLY VARYING AND IS TAKEN AS CONSTANT ACROSS
C       SUBINTERVALS OF THE INTEGRATION. THAT IS, INTERPOLATION BETWEEN
C       INPUT POINTS IS BY PARABOLAS WHOSE AXES COINCIDE WITH X=0.
C
C       THE INPUT DATA MAY BE SMOOTHED  BEFORE CALCULATION
C       BY FITTING COAXIAL PARABOLAS TO 3 INPUT POINTS.
C       IF KTRL(1) IS  0  DON'T SMOOTH DATA
C                      1  SMOOTH ALL INPUT DATA
C                     -N  SMOOTH 1ST N POINTS (AT EACH Z)
C
C       PLOTS MAY BE OBTAINED.  IP=KTRL(2)
C       IF  IP  IS ODD  CONTOUR PLOT OF RHO VS RADIUS
C         IP/2   "      PLOTS OF RHO VS R AT Z
C         IP/4   "      PLOTS OF W VS X AT Z
C         IP/8   "      PLOTS OF D
C
      DIMENSION W(57),D(50),RHO(50,50),RR(50),CALX(100),CALY(100)
      DIMENSION ACON(5),KTRL(4),X(50),Y(50),NR(50)
      EQUIVALENCE (ACON(2),DELT)
      EQUIVALENCE (KTRL(1),ISM)
      EQUIVALENCE (KTRL(2),IPC)
      REAL*8 TITLE(9),DUM8,TTL/'TITLE'/,FIVE/'    5'/
      COMMON /TITLE/ TITLE
      REAL*8 CALIB/'CALIBRAT'/ ,BLANK /' '/
      LOGICAL CALSW /T/
      DATA L,LC /2*0/
      DATA ZERO/0.0/
C
   20 CONTINUE
C                                          READ TITLE
      READ 1,DUM8,TITLE
    1 FORMAT (10A8)
      IF (DUM8.EQ.FIVE) STOP
      IF (DUM8.NE.CALIB) GO TO 22
```

```
C                                                    CALIBRATION TABLE
C       CALIBRATE 3(SMOKE-PATH-LENGTH,FILM-DENSITY)
        CALL INFILQ(TITLE,72)
        READ 17,(CALY(I+LC),CALX(I+LC),I=1,3)
   17   FORMAT (2X,6F10.0)
        IF (LC.GT.0 .AND. CALX(LC+1).LE.CALX(LC) ) GO TO 21
        LC=LC+1
        IF(CALX(LC+1).EQ.0.) GO TO 16
        IF (CALX(LC+1).LE.CALX(LC) ) GO TO 21
        LC=LC+1
        IF(CALX(LC+1).EQ.0.) GO TO 16
        IF (CALX(LC+1).LE.CALX(LC) ) GO TO 21
        LC=LC+1
   16   IF (CALSW) GO TO 18
        PRINT 2,DUM8,TITLE
    2   FORMAT (4H0     ,10A8)
        GO TO 20
   18   CALSW=.FALSE.
        DO 19 I=1,9
   19   TITLE(I)=BLANK
        CALL PAGEIT(0)
        PRINT 116,CALIB,(CALY(I),CALX(I),I=1,LC)
  116   FORMAT (1H0,A11,6F10.2)
        GO TO 20
   21   PRINT 115
  115   FORMAT ('0    DENSITY VALUES NOT INCREASING.  OPTION IS CANCELED')
        CALSW=.TRUE.
        CALIB=FIVE
        GO TO 20
C
   22   CONTINUE
        IF (DUM8.NE.TTL) GO TO 20
        MM=50
        CALL PAGEIT(0)
C                                                    INITIALIZE
        DO 24 I=1,2500
   24   RHO(I,1)=-.015625
        RHO(1,1)=0.
        RHOMAX=0.
        X(1)=0.
        Y(1)=0.
        RR(1)=0.
        Z1=0.
        U=0.
        V=0.
        J=1
        NR(1)=1
        KMAX=1
C       TYPE 1                                       READ MAIN CONTROL CARD
        READ 3,KTYP,ACON,KTRL
    3   FORMAT (I5,5X,5F10.0,4I5)
        IF(KTYP.NE.1) GO TO 30
        ANORM=ACON(1)
        IF (ANORM.EQ.0.) ANORM=1.0
        IF(DELT.EQ.0.) DELT=1.0
        PRINT 5,ACON,KTRL
```

```
    5  FORMAT ('0  CARD 1  A=',F8.2,'      DELT=',4F8.2,7X,'IS =',I2,
     &  7X,'IP =',I3,2I5)
       CALL PAGEIT(2)
C                       SET PLOT SWITCHES
       IPD=IPC/8
       IPC=IPC-IPD*8
       IPW=IPC/4
       IPC=IPC-IPW*4
       IPR=IPC/2
       IPC=IPC-IPR-IPR
C                       SET X ARRAY
       DO 26 K=2,50
       X(K)=X(K-1)+DELT
       IF (X(K).GE.10.) GO TO 28
   26  CONTINUE
   28  X(K)=10.
       NN=K
       GO TO 40
C      CARD 1 IS OMITTED, MOVE DATA & USE DEFAULTS.
   30  Z=ACON(1)
       R=ACON(2)
       DEL=ACON(3)
       ACON(1)=0.
       ANORM=1.0
       DELT=1.0
       NN=11
       DO 32 K=2,NN
   32  X(K)=X(K-1)+1.
       GO TO 42
C      TYPE 2                                READ FOR SLICE AT HEIGHT Z
   40  READ 6,KTYP,Z,R,DEL
    6  FORMAT (I5,5X,7F10.0)
   42  IF (DEL.EQ.0.) DEL=DELT
       PRINT 7,KTYP,Z,R,DEL
    7  FORMAT ('0 CARD',I2,4X,'Z =',F8.2,8X,'R =',F8.2,8X,'DEL =',F8.3)
       CALL PAGEIT(2)
       IF (KTYP.NE.2) GO TO 72
       IF (Z.NE.0.) J=J+1
       Y(J)=Z
       IF(DEL.EQ.DELT .OR.IPC.EQ.0) GO TO 43
       IF (J.EQ.1) GO TO 45
       PRINT 107
       IPC=0
  107  FORMAT ('-***',3('****'),'REQUEST FOR CONTOUR PLOT DELETED.'/
     &  T18,'REQUIRES SAME DEL FOR ALL Z' / 1H0 )
       CALL PAGEIT(6)
       IF (IPR+IPD+IPW.EQ.0) GO TO 43
   45  DO 46 K=2,50
       X(K)=X(K-1)+DEL
       IF (X(K).GE.10.) GO TO 47
   46  CONTINUE
   47  X(K)=10.
       IF (J.EQ.1) DELT=DEL
   43  CONTINUE
       RR(J)=R
       IF (R.GT.0.) GO TO 50
```

```
   44 Z1=Z
      NR(J)=1
      RHO(1,J)=0.
      GO TO 40
C     TYPE 3                                  READ DATA AT HEIGHT Z
   50 CALL PAGEIT(2)
      PRINT 8
    8 FORMAT (1HO,T15,'INPUT DATA W(N)')
      N=0
   52 L=1+N
      N=L+6
      READ 6,KTYP,(W(I),I=L,N)
      IF (KTYP.NE.3) GO TO 60
      PRINT 101,(W(I),I=L,N)
  101 FORMAT (8X,7F12.4)
      CALL PAGEIT(1)
      GO TO 52
   60 N=L-1
      TSUM=0.
      IF(N.LE.0) GO TO 70
C                              SEARCH FOR LAST POINT
      DO 58 I=1,N
   58 IF(W(I+1).EQ.0.)N=I
      NNL=-(3+N/7)
      IF (CALSW) GO TO 96
C                                        APPLY CALIBRATION TO W
      IC=2
      DO 94 I=1,N
C                    FIND INTERVAL
   90 IF (W(I).LE.CALX(IC)) GO TO 91
      IF (IC.GE.LC) GO TO 94
      IC=IC+1
      GO TO 90
   91 IF (W(I).GE.CALX(IC-1)) GO TO 92
      IC=IC-1
      IF (IC.GT.1) GO TO 91
      IC=2
      GO TO 93
C                                    INTERPOLATE
   92 W(I)=(W(I)-CALX(IC-1))*(CALY(IC)-CALY(IC-1))
     &   /(CALX(IC)-CALX(IC-1)) +CALY(IC-1)
   93 IF (W(I).LT.0.) W(I)=0.
   94 CONTINUE
      CALL PAGEIT(NNL)
      PRINT 113
  113 FORMAT (1HO,T15,'CORRECTED DATA')
      PRINT 101,(W(I),I=1,N)
C
   96 CONTINUE
      IF (ISM.EQ.0) GO TO 99
C                                        SMOOTH INPUT DATA
      IF (N.LE.2) GO TO 99
      DO 120 K=1,ISM
      F=W(1)
      W(1)=(17.*F +12.*W(2) -3.*W(3) )/26.
      TWON=0.
```

```
      DO 97 I=2,N
      IF (I.EQ.N) GO TO 98
      TWON=TWON+2.
      TNS=TWON*TWON
      H=3.*TNS+1.
      G=(TNS+TWON)*F +(TNS+1.)*W(I) +(TNS-TWON)*W(I+1)
      F=W(I)
      W(I)=G/H
   97 CONTINUE
C
   98 CONTINUE
      W(I)=(0.5*(1.-TNS)*W(I-2) +(TNS-TWON)*F
     &        +(2.5*TNS+TWON+0.5)*W(I) )/H
      CALL PAGEIT(NNL)
      PRINT 114,K
  114 FORMAT (1HO,T15,'SMOOTHED VALUES',I4)
      PRINT 101,(W(I),I=1,N),ZERO
  120 CONTINUE
C
C                                          CALCULATE DIFFERENCES
   99 CONTINUE
      CON=-1.
      DO 62 I=1,N
      CON=CON+2.
      D(I)=(W(I)-W(I+1))/CON
   62 CONTINUE
C     SET N TO INCLUDE FINAL ZERO.
      N=N+1
      NR(J)=N
      KMAX=MAXO(N,KMAX)
      D(N-1)=W(N-1)/CON
      D(N)=0.
      CALL PAGEIT(NNL)
      PRINT 9
    9 FORMAT (1HO,T15,'D(N) = DERIVATIVE-OF-W = (W(N)-W(N+1)) / (2N+1)'
     &  ,10X,'---SHOULD BE SMOOTH---')
      PRINT 102,(D(I),I=1,N)
  102 FORMAT (14X,7F12.4)
C     C=(2./PI)*A/DEL                          CALCULATE RHO
      CON=ANORM*.63662/DEL
      AK=0.
      DO 68 K=1,N
      AKK=AK*AK
      AI=AK
      RSUM=0.
      HH=0.
      DO 66 I=K,N
      AI=AI+1.
      H=SQRT(AI*AI-AKK)
      RSUM=RSUM + D(I)*(H-HH)
      HH=H
   66 CONTINUE
      RHO(K,J)=CON*RSUM
      TSUM=TSUM + AK*RHO(K,J)
      RHOMAX=AMAX1(RHO(K,J),RHOMAX)
      AK=AK+1.
```

```
   68  CONTINUE
       CALL PAGEIT(NNL)
       PRINT 103,Z
  103  FORMAT ('0  RADIAL DISTRIBUTION RHO(R) AT Z=',F10.2 )
       PRINT 101,(RHO(I,J),I=1,N)
C         FINISH RADIAL INTEGRALS AND ACCUMULATE AXIAL SUMS
   70  TSUM=TSUM*6.283185*(DEL*DEL)
       AREA=3.1415925E0*R*R
C      NEXT Z VALUE IS IN W(L),  PREVIOUS IN Z1
       CON=0.5*(W(L)-Z1)
       U=U+TSUM*CON
       V=V+AREA*CON
       RAT=TSUM/AREA
       PRINT 104,TSUM,AREA,RAT
  104  FORMAT ('0  RADIAL DENSITY INTEGRAL =',F10.2,8X,'AREA =',F10.2/
     &  '0   LOCAL RATIO =',F9.4/)
       CALL PAGEIT(5)
       Z1=Z
       Z=W(L)
C                                        CHECK NEXT CARD TYPE
       IF (KTYP.NE.2) GO TO 72
C                                  MORE, SHIFT THINGS
       R=W(L+1)
       DEL=W(L+2)
       GO TO 42
C                                  PRINT FINAL
   72  CONTINUE
       PRINT 106, KTYP,Z
  106  FORMAT ('0  CARD',I2,'  FINAL Z =',F12.4)
       J=J+1
       JMAX=J
       NR(J)=1
       Y(J)=Z
       RHO(1,J)=0.
       CALL PAGEIT(0)
       IF (ACON(1).NE.0.) GO TO 76
C                                        NORMALIZE TO 100% MAX
       ANORM=100./RHOMAX
       U=U/RHOMAX
       PRINT 111
  111  FORMAT ('0     DENSITY IS NORMALIZED TO 100% AT MAXIMUM VALUE.')
       MM=JMAX
       DO 74 J=1,JMAX
       K=NR(J)
       DO 74 I=1,K
       RHO(I,J)=RHO(I,J)*ANORM
   74  CONTINUE
C
   76  CONTINUE
       RAT=U/V
       PRINT 105,U,V,RAT
  105  FORMAT('0  VOLUME DENSITY INTEGRAL =',F10.2,8X,'VOLUME =',F10.2,
     &   6X,'CONTAINMENT RATIO =',F8.4/)
C                                        SUMMARY PRINT
       IF (DELT.EQ.DEL) GO TO 79
       DO 78 K=1,NN
```

```
   78  X(K)=X(K-1)+DELT
   79  CONTINUE
       PRINT 108,(X(K),K=1,KMAX)
  108  FORMAT('-    RADIUS',20F6.1/(7X,20F6.1) )
       PRINT 109
  109  FORMAT ('0     Z  /',22X,'RADIAL DENSITY RHO(R)' /
     &  7X,1H/,22(' - -') )
  110  FORMAT (T10,1H|,T1,F7.1,T11,20F6.1/(6X,20F6.1) )
       MULT=50/INT(Z)
       IF (MULT.LE.0) MULT=1
       N=0
       L=-1
       DO 82 J=1,JMAX
       IF(N.GT.20) L=L+(N-1)/20
       N=NR(J)
       LCOMP=INT(Y(J)+0.5)*MULT
   80  L=L+1
       IF (L.GE.LCOMP) GO TO 82
       PRINT 110
       GO TO 80
   82  PRINT 110,Y(J),(RHO(I,J),I=1,N)
C                                          CONTOUR PLOT
       IF (IPC.EQ.0) GO TO 88
       PRINT 112
  112  FORMAT ('-     A CONTOUR PLOT OF THE DENSITY HAS BEEN DRAWN.')
       CALL CONPLT(X,50,Y,MM,RHO,50,50,10,1, NN ,1,JMAX,8HRADIUS R,8,
     &  16HAXIAL POSITION Z,16,TITLE,72)
   88  CONTINUE
       IF (KTYP.EQ.5) STOP
       IF (KTYP.EQ.4) GO TO 20
   10  PRINT 11
   11  FORMAT ('0 INVALID CARD SEQUENCE, SKIPPING REST OF THIS SET.')
       GO TO 20
       END
```

SUBROUTINE FOR MAKING CONTOUR PLOTS OF DENSITY DATA

```
C       SUBROUTINE GENERATES CONTOUR MAP OF A FUNCTION OF TWO VARIABLES  CNTR0040
C       CONTAINS SPECIAL MODIFICATIONS FOR CAVITY-REACTOR FLOW-MODEL SEP 71
        REAL X(1),Y(1),XL(1),YL(1),TTL(1)
        INTEGER NX,NY,NXD,NYD,N,L,R,T,B,NXL,NYL,NTTL                     CNTR0060
      DIMENSION Z(NXD,NYD)
        REAL F(6),XS(4),YS(4),LS,SZ(4)                                   CNTR0070
        INTEGER IS(4),LP1,RM1,TP1,BM1                                    CNTR0080
        REAL AND,OR                                                      CNTR0090
        LOGICAL S1,S2,S3,S4                                              CNTR0095
        DATA F/1.0,2.0,2.5,5.0,10.0,20.0/                                CNTR0100
        DATA SX,SZ /4.0,8.0,8.5,3.2,10./                                 CNTR 105
        DATA MSK0/ZFFFFFFF8/,MSK1/Z00000001/,MSK2/Z00000002/,            CNTR0110
     * MSK4/Z00000004/,MSK3/ZFFFFFFFA/                                   CNTR0120
        DATA SUP/Z00000000/,SDN/Z0F000000/                               CNTR0130
C                                                                        CNTR0140
C       CHECK INTEGER INPUT PARAMETERS                                   CNTR0150
        IF (NX .LE. 1  .OR.  NXD .LE. 1  .OR.  NX .GT. NXD) GO TO 1001   CNTR0160
        IF (NY .LE. 1  .OR.  NYD .LE. 1  .OR.  NY .GT. NYD) GO TO 1001   CNTR0170
        IF (L .LE. 0  .OR.  L .GE. R  .OR.  R .GT. NX) GO TO 1001        CNTR0180
        IF (T .LE. 0  .OR.  T .GE. B  .OR.  B .GT. NY) GO TO 1001        CNTR0190
        IF (N .LT. 2) GO TO 1001                                         CNTR0200
        IF (NXL .LT. 0  .OR.  NXL .GT. 60) GO TO 1001                    CNTR0210
        IF (NYL .LT. 0  .OR.  NYL .GT. 60) GO TO 1001                    CNTR0220
        IF (NTTL .LE. 0  .OR.  NTTL .GT. 75) GO TO 1001                  CNTR0230
C                                                                        CNTR0240
C       GET INDEX QUANTITIES                                             CNTR0250
        LP1 = L + 1                                                      CNTR0260
        RM1 = R - 1                                                      CNTR0270
        TP1 = T + 1                                                      CNTR0280
        BM1 = B - 1                                                      CNTR0290
C                                                                        CNTR0300
C       CHECK GRID DATA                                                  CNTR0310
   10   DO 11 I = LP1,R                                                  CNTR0320
        IF (X(I) .LE. X(I-1)) GO TO 1002                                 CNTR0330
   11   CONTINUE                                                         CNTR0340
        DO 12 I = TP1,B                                                  CNTR0350
        IF (Y(I) .LE. Y(I-1)) GO TO 1002                                 CNTR0360
   12   CONTINUE                                                         CNTR0370
C                                                                        CNTR0380
C       FIND MINIMUM AND MAXIMUM OF Z                                    CNTR0390
        ZMIN = Z(L,T)                                                    CNTR0400
        ZMAX = ZMIN                                                      CNTR0410
        DO 14 J = T,B                                                    CNTR0420
        DO 13 I = L,R                                                    CNTR0430
        IF (Z(I,J) .LE. ZMAX) GO TO 16                                   CNTR0440
        ZMAX = Z(I,J)                                                    CNTR0450
        GO TO 13                                                         CNTR0460
   15   IF (Z(I,J) .LT. ZMIN) ZMIN = Z(I,J)                              CNTR0470
   13   CONTINUE                                                         CNTR0480
   14   CONTINUE                                                         CNTR0490
        GET CONTOUR LEVEL INTERVAL                                       CNTR0500
        XS(1) = ZMAX - ZMIN                                              CNTR0510
```

```
      IF (XS(1) .EQ. 0.0) GO TO 1003                                    CNTR0520
      IF (NY.EQ.NYD) GO TO 9                                            CNTR 521
      KL=1                                                              CNTR 522
      DZ=10.                                                            CNTR 523
      SC=1.                                                             CNTR 524
      ZMON=0.                                                           CNTR 524
      IF (ZMIN+.02.LT.0.) ZMON=-DZ                                      CNTR 525
      XMIN=0.                                                           CNTR 526
      YMIN=20.                                                          CNTR 527
      DX=2.5                                                            CNTR 528
      DY=2.5                                                            CNTR 529
      GO TO 19                                                          CNTR 530
C                                                                       CNTR 532
    9 CONTINUE                                                          CNTR 538
      XS(1) = XS(1)/FLOAT(N)*0.6                                        CNTR0540
      DZ = ALOG10(XS(1))                                                CNTR0550
      IF (DZ .LT. 0.) DZ = DZ - 1.0                                     CNTR0560
      SC = 10.0**INT(DZ)                                                CNTR0570
      XS(1) = XS(1)/SC                                                  CNTR0580
      DO 17 I = 1,6                                                     CNTR0590
      IF (XS(1) .LE. F(I)) GO TO 18                                     CNTR0600
   17 CONTINUE                                                          CNTR0610
   18 KL = 2                                                            CNTR0620
      IF (I .LT. 5) GO TO 20                                            CNTR0621
      I = I - 4                                                         CNTR0622
      SC = SC*10.0                                                      CNTR0623
   20 DZ = F(I)*SC                                                      CNTR0630
      IF (N .GT. 15) GO TO 15                                           CNTR0635
      IF (I .NE. 3) KL = 1                                              CNTR0637
C                                                                       CNTR0640
C     GET SUITABLE MINIMUM LEVEL                                        CNTR0650
   15 ZMON = AINT(ZMIN/SC*0.01)                                         CNTR0660
      IF (ZMON .LT. 0.0) ZMON = ZMON - 1.0                              CNTR0670
      ZMON = ZMON*SC*100.0                                              CNTR0680
C                                                                       CNTR0690
C     SCALE GRID DATA                                                   CNTR0700
      XMIN = X(L)                                                       CNTR0710
      CALL DXDY (X(R),XMIN,DX,SX)                                       CNTR 720
      YMIN = Y(T)                                                       CNTR0730
      CALL DXDY (Y(B),YMIN,DY,SZ(1))                                    CNTR0740
      IF (DX - DY) 21,22,23                                             CNTR0750
   21 IF (DX/DY .GE. 0.5) DX = DY                                       CNTR0760
      GO TO 22                                                          CNTR0770
   23 IF (DY/DX .GE. 0.5) DY = DX                                       CNTR0780
   22 YMIN = YMIN + SZ(1)*DY                                            CNTR0790
   19 CONTINUE                                                          CNTR 798
      DO 24 I = L,R                                                     CNTR0800
   24 X(I) = (X(I) - XMIN)/DX                                           CNTR0810
      DO 25 I = T,B                                                     CNTR0820
   25 Y(I) = (YMIN - Y(I))/DY                                           CNTR0830
C                                                                       CNTR0840
C     DRAW AXES AND TITLE                                               CNTR0850
      CALL PLOTS (0.0,-12.0,-3)                                         CNTR0860
      CALL PLOT (0.5,1.5,-3)                                            CNTR0870
      CALL AXIS (0.0,0.0,XL,NXL,SX,0.0,XMIN,DX,1)                       CNTR0880
      CALL AXIS (0.0,0.0,YL,NYL,SZ,90.0,YMIN,-DY,1)                     CNTR0890
```

```
      YS(1) = Y(B)                                                      CNTR0900
      YS(2) = YS(1) + 0.1                                               CNTR0910
      CALL PLOT (X(L),YS(1),3)                                          CNTR0920
      DO 26 I = L,R                                                     CNTR0930
      CALL PLOT (X(I),YS(1),0)                                          CNTR0940
      CALL PLOT (X(I),YS(2),0)                                          CNTR0950
   26 CALL PLOT (X(I),YS(1),0)                                          CNTR0960
      XS(1) = X(R)                                                      CNTR0970
      XS(2) = XS(1) - 0.1                                               CNTR0980
      J = B                                                             CNTR0990
      DO 27 I = TP1,B                                                   CNTR1000
      J = J - 1                                                         CNTR1010
      CALL PLOT (XS(1),Y(J),0)                                          CNTR1020
      CALL PLOT (XS(2),Y(J),0)                                          CNTR1030
   27 CALL PLOT (XS(1),Y(J),0)                                          CNTR1040
      YS(1) = Y(T)                                                      CNTR1050
      YS(2) = YS(1) - 0.1                                               CNTR1060
      J = R                                                             CNTR1070
      DO 28 I = LP1,R                                                   CNTR1080
      J = J - 1                                                         CNTR1090
      CALL PLOT (X(J),YS(1),0)                                          CNTR1100
      CALL PLOT (X(J),YS(2),0)                                          CNTR1110
   28 CALL PLOT (X(J),YS(1),0)                                          CNTR1120
      CALL SYMBL4 (-.5,SZ(2),0.14,TTL,0.0,NTTL)                         CNTR1121
      CALL SYMBL4 (0.5,SZ(3),0.10,18HCONTOUR INTERVAL =,0.0,18)         CNTR1122
      CALL NUMBER (2.14,SZ(3),0.10,DZ,0.0,0)                            CNTR1123
      IF (SC.EQ.1.0) GO TO 97                                           CNTR1124
      CALL SYMBL4 (3.0,SZ(3),0.10,18HMULTIPLY LEVELS BY,0.0,18)         CNTR1125
      CALL NUMBER (4.64,SZ(3),0.10,SC,0.0,0)                            CNTR1126
   97 XS(1)=X(L)                                                        CNTR1130
      XS(2) =XS(1) + 0.1                                                CNTR1140
      CALL PLOT(XS(1),Y(T),3)                                           CNTR1146
      DO 29 I = TP1,B                                                   CNTR1150
      CALL PLOT (XS(1),Y(I),0)                                          CNTR1160
      CALL PLOT (XS(2),Y(I),0)                                          CNTR1170
   29 CALL PLOT (XS(1),Y(I),0)                                          CNTR1180
                                                                        CNTR1240
      CLEAR STATUS BITS OF Z ARRAY                                      CNTR1250
      DO 31 J = T,B                                                     CNTR1260
      DO 30 I = L,R                                                     CNTR1270
      Z(I,J) = AND(Z(I,J),MSK0)                                         CNTR1280
   30 CONTINUE                                                          CNTR1290
   31 CONTINUE                                                          CNTR1300
                                                                        CNTR1310
      SET PRINT BITS IN OUTER ROWS AND COLUMNS                          CNTR1320
      DO 32 I = L,R                                                     CNTR1330
      Z(I,T) = OR(Z(I,T),MSK2)                                          CNTR1340
      Z(I,B) = OR(Z(I,B),MSK2)                                          CNTR1360
   32 CONTINUE                                                          CNTR1372
      DO 33 I = TP1,BM1                                                 CNTR1380
      Z(L,I) = OR(Z(L,I),MSK2)                                          CNTR1390
      Z(R,I) = OR(Z(R,I),MSK2)                                          CNTR1410
   33 CONTINUE                                                          CNTR1422
                                                                        CNTR1430
      PLOT POSITION AND POSSIBLY VALUE OF LOCAL MIN AND MAX OF Z        CNTR1442
      DO 34 J = TP1,BM1                                                 CNTR1450
```

```
      DO 35 I = LP1,RM1                                                  CNTR1460
      IF (Z(I,J) .LE. Z(I-1,J)) GO TO 36                                 CNTR1470
      IF (Z(I,J) .LE. Z(I+1,J)  .OR.  Z(I,J) .LE. Z(I,J-1)  .OR.         CNTR1480
     * Z(I,J) .LE. Z(I,J+1)) GO TO 35                                    CNTR1490
      XS(1) = SUP                                                        CNTR1500
      GO TO 37                                                           CNTR1510
   36 IF (Z(I,J) .EQ. Z(I-1,J)  .OR.  Z(I,J) .GE. Z(I+1,J)  .OR.         CNTR1520
     * Z(I,J) .GE. Z(I,J-1)  .OR.  Z(I,J) .GE. Z(I,J+1)) GO TO 35        CNTR1530
      XS(1) = SDN                                                        CNTR1540
   37 CALL SYMBL4(X(I),Y(J),0.28,XS(1),0,1)                              CNTR1550
      IF (AND(Z(I,J),MSK2) .NE. 0.0) GO TO 35                            CNTR1560
      Z(I,J) = OR(Z(I,J),MSK2)                                           CNTR1565
      IF ( ABS((X(I)-X(I-1))/(Z(I,J)-Z(I-1,J))*DZ) .LT. .50  .OR.        CNTR1567
     *ABS((Y(J)-Y(J-1))/(Z(I,J)-Z(I,J-1))*DZ) .LT. .50) GO TO 35         CNTR1569
      Z(I-1,J) = OR(Z(I-1,J),MSK2)                                       CNTR1571
      Z(I+1,J) = OR(Z(I+1,J),MSK2)                                       CNTR1572
      CALL NUMBER (X(I)-0.18,Y(J)+0.07,0.07,Z(I,J)/SC,0.0,1)             CNTR1580
   35 CONTINUE                                                           CNTR1590
   34 CONTINUE                                                           CNTR1600
                                                                         CNTR1610
      GET FIRST LEVEL AND INITILIZE LABEL SWITCHES                       CNTR1620
      K = 0                                                              CNTR1625
   39 ZMON = ZMON + DZ                                                   CNTR1630
      K = K + 1                                                          CNTR1635
      IF (ZMON .LE. ZMIN) GO TO 39                                       CNTR1640
      K = KL - MOD(K,KL)                                                 CNTR1650
      S1=K.EQ.KL                                                         CNTR1660
      KN = (R-L+B-T)/2                                                   CNTR1666
      GO TO 40                                                           CNTR1670
                                                                         CNTR1680
      TURN OFF SCAN BIT                                                  CNTR1690
   38 DO 41 J = TP1,B                                                    CNTR1700
      DO 41 I = LP1,R                                                    CNTR1710
   41 Z(I,J) = AND(Z(I,J),MSK3)                                          CNTR1720
                                                                         CNTR1730
      SET LEVEL TO BE DIFFERENT FROM Z                                   CNTR1740
   40 LS = OR(AND(ZMON,MSK3),MSK4)                                       CNTR1750
      S2 = .FALSE.                                                       CNTR1755
      IF (S1) ZMONP = ZMON/SC                                            CNTR1756
      S4 = .FALSE.                                                       CNTR1757
                                                                         CNTR1760
      SEARCH AND SCORE CROSSINGS                                         CNTR1770
      IN = 0                                                             CNTR1780
      IP = 0                                                             CNTR1790
      J = TP1                                                            CNTR1800
   43 I = LP1                                                            CNTR1810
                                                                         CNTR1814
      SKIP IF SCAN BIT SET                                               CNTR1815
   44 IF (AND(Z(I,J),MSK1) .NE. 0.0) GO TO 59                            CNTR1820
   42 IF (IN .EQ. 1) GO TO 45                                            CNTR1830
      IF (Z(I-1,J-1).GT.LS .AND. Z(I-1,J).GT.LS  .OR.                    CNTR1840
     * Z(I-1,J-1).LT.LS .AND. Z(I-1,J).LT.LS) GO TO 45                   CNTR1850
      IP = IP + 1                                                        CNTR1860
      XS(IP) = X(I-1)                                                    CNTR1870
      YS(IP) = (LS-Z(I-1,J-1))/(Z(I-1,J)-Z(I-1,J-1))*(Y(J)-Y(J-1))       CNTR1880
     * + Y(J-1)                                                          CNTR1890
```

```
      IS(IP) = 3                                                        CNTR1900
   45 IF (IN .EQ. 2) GO TO 46                                           CNTR1910
      IF (Z(I-1,J-1).GT.LS .ANC. Z(I,J-1).GT.LS  .OR.                   CNTR1920
     * Z(I-1,J-1).LT.LS .AND. Z(I,J-1).LT.LS) GO TO 46                  CNTR1930
      IP = IP + 1                                                       CNTR1940
      XS(IP) = (LS-Z(I-1,J-1))/(Z(I,J-1)-Z(I-1,J-1))*(X(I)-X(I-1))      CNTR1950
     * + X(I-1)                                                         CNTR1960
      YS(IP) = Y(J-1)                                                   CNTR1970
      IS(IP) = 4                                                        CNTR1980
   46 IF (IN .EQ. 3) GO TO 47                                           CNTR1990
      IF (Z(I,J-1).GT.LS .AND. Z(I,J).GT.LS  .OR.                       CNTR2000
     * Z(I,J-1).LT.LS .AND. Z(I,J).LT.LS) GO TO 47                      CNTR2010
      IP = IP + 1                                                       CNTR2020
      XS(IP) = X(I)                                                     CNTR2030
      YS(IP) = (LS-Z(I,J-1))/(Z(I,J)-Z(I,J-1))*(Y(J)-Y(J-1)) + Y(J-1)   CNTR2040
      IS(IP) = 1                                                        CNTR2050
   47 IF (IN .EQ. 4) GO TO 48                                           CNTR2060
      IF (Z(I-1,J).GT.LS .AND. Z(I,J).GT.LS  .OR.                       CNTR2070
     * Z(I-1,J).LT.LS .AND. Z(I,J).LT.LS) GO TO 48                      CNTR2080
      IP = IP + 1                                                       CNTR2090
      XS(IP) = (LS-Z(I-1,J))/(Z(I,J)-Z(I-1,J))*(X(I)-X(I-1)) + X(I-1)   CNTR2100
      YS(IP) = Y(J)                                                     CNTR2110
      IS(IP) = 2                                                        CNTR2120
                                                                        CNTR2124
      IF NO CROSSINGS, ADVANCE MESH RETANGLE                            CNTR2125
   48 IF (IP .EQ. 0) GO TO 59                                           CNTR2130
      IF (IP .EQ. 4) GO TO 55                                           CNTR2140
                                                                        CNTR2144
      STANDARD TWO CROSSING     TEST IF START OF CONTOUR PLOT (PEN UP)  CNTR2145
      IF (IN .NE. 0) GO TO 49                                           CNTR2150
                                                                        CNTR2154
      START OF CONTOUR PLOT                                             CNTR2155
      I1 = I                                                            CNTR2160
      J1 = J                                                            CNTR2170
      IF (S1) S2 = .TRUE.                                               CNTR2180
      IG = IS(2)                                                        CNTR2190
                                                                        CNTR2194
      CHECK AGAINST DEADEND                                             CNTR2195
      GO TO (51,52,53,54),IG                                            CNTR2200
   51 IF (I .EQ. R) GO TO 58                                            CNTR2210
      IF (AND(Z(I+1,J),MSK1) .EQ. 0.0) GO TO 61                         CNTR2220
      GO TO 58                                                          CNTR2230
   52 IF (J .EQ. B) GO TO 58                                            CNTR2240
      IF (AND(Z(I,J+1),MSK1) .EQ. 0.0) GO TO 61                         CNTR2250
      GO TO 58                                                          CNTR2260
   53 IF (I .EQ. LP1) GO TO 58                                          CNTR2270
      IF (AND(Z(I-1,J),MSK1) .EQ. 0.0) GO TO 61                         CNTR2280
      GO TO 58                                                          CNTR2290
   54 IF (J .EQ. TP1) GO TO 58                                          CNTR2300
      IF (AND(Z(I,J-1),MSK1) .EQ. 0.0) GO TO 61                         CNTR2310
   58 XS(3) = XS(1)                                                     CNTR2320
      XS(1) = XS(2)                                                     CNTR2330
      XS(2) = XS(3)                                                     CNTR2340
      YS(3) = YS(1)                                                     CNTR2350
      YS(1) = YS(2)                                                     CNTR2360
      YS(2) = YS(3)                                                     CNTR2370
```

```
      IS(2) = IS(1)                                                    CNTR2380
                                                                       CNTR2384
      POSITION TO FIRST POINT (PEN UP)                                 CNTR2385
   61 CALL PLOT (XS(1),YS(1),3)                                        CNTR2390
                                                                       CNTR2394
      DRAW CONTOUR THRU MESH RECTANGLE                                 CNTR2395
   49 CALL PLOT (XS(2),YS(2),0)                                        CNTR2400
      IN = IS(2)                                                       CNTR2410
                                                                       CNTR2415
      CHECK IF LABEL SHOULD BE WRITTEN                                 CNTR2416
      IF (S4) GO TO 95                                                 CNTR2419
      IF (S2) GO TO 94                                                 CNTR2420
      IF (.NOT.S1) GO TO 80                                            CNTR2425
      KNP = KNP - 1                                                    CNTR2426
      IF (KNP .GT. 0) GO TO 93                                         CNTR2427
      S2 = .TRUE.                                                      CNTR2428
                                                                       CNTR2429
      WRITE IF ROOM                                                    CNTR2424
   94 IF (AND(Z(I-1,J-1),MSK2) .NE. 0.0  .OR.  AND(Z(I-1,J),MSK2) .NE. CNTR2430
     *0.0  .OR.  AND(Z(I,J-1),MSK2) .NE. 0.0  .OR.  AND(Z(I,J),MSK2)   CNTR2440
     * .NE. 0.0) GO TO 93                                              CNTR2450
      S3 = .FALSE.                                                     CNTR2455
      A = 0.0                                                          CNTR2460
      XS(4) = 0.50                                                     CNTR2465
      YS(4) = 0.50                                                     CNTR2466
      XS(3) = Z(I,J)-Z(I-1,J)                                          CNTR2467
      IF (XS(3) .NE. 0.0) XS(4) = ABS((X(I)-X(I-1))/XS(3)*DZ)          CNTR2470
      YS(3) = Z(I,J)-Z(I,J-1)                                          CNTR2475
      IF (YS(3) .NE. 0.0) YS(4) = ABS((Y(J)-Y(J-1))/YS(3)*DZ)          CNTR2480
      IF (XS(4) .GE. .50  .AND. YS(4) .GE. .15) GO TO 90               CNTR2490
      A = 90.0                                                         CNTR2500
      IF (YS(4) .GE. .50  .AND.  XS(4) .GE. .15) GO TO 90              CNTR2510
      YS(3) = (X(I)-X(I-1) + Y(J-1)-Y(J))*DZ                           CNTR2512
      XS(3) = Z(I,J-1)-Z(I-1,J)                                        CNTR2518
      XS(4) = 0.50                                                     CNTR2514
      YS(4) = 0.50                                                     CNTR2516
      IF (XS(3) .NE. 0.0) XS(4) = ABS(YS(3)/XS(3))                     CNTR2520
      XS(3) = Z(I,J)-Z(I-1,J-1)                                        CNTR2522
      IF (XS(3) .NE. 0.0) YS(4) = ABS(YS(3)/XS(3))                     CNTR2524
      IF (XS(4) .LT. .50  .OR.  YS(4) .LT. .15) GO TO 64               CNTR2526
      A = 45.0                                                         CNTR2527
      IF (YS(2)-YS(1) .LE. XS(2)-XS(1)) S3 = .TRUE.                    CNTR2528
      GO TO 65                                                         CNTR2529
   64 IF (YS(4) .LT. .50 .OR. XS(4) .LT. .15) GO TO 93                 CNTR2530
      A = -45.0                                                        CNTR2535
      IF (YS(1)-YS(2) .LE. XS(2)-XS(1)) S3 = .TRUE.                    CNTR2536
      GO TO 65                                                         CNTR2537
   90 IF (YS(2) .GT. YS(1)) S3 = .TRUE.                                CNTR2540
   65 IF (XS(1) .GT. XS(2)) S3 = .NOT.S3                               CNTR2550
      XS(3) = XS(2)                                                    CNTR2560
      YS(3) = YS(2)                                                    CNTR2570
      IF (A .LE. 0.0) GO TO 91                                         CNTR2580
      IF (S3) GO TO 92                                                 CNTR2590
      XS(3) = XS(3) + 0.10                                             CNTR2600
      GO TO 92                                                         CNTR2610
   91 IF (.NOT. S3) GO TO 92                                           CNTR2620
```

```
      YS(3) = YS(3) - 0.10                                              CNTR2630
   92 CALL NUMBER (XS(3),YS(3),0.07,ZMONP,A,0)                          CNTR2640
      Z(I-1,J-1) = OR(Z(I-1,J-1),MSK2)                                  CNTR2650
      Z(I-1,J) = OR(Z(I-1,J),MSK2)                                      CNTR2660
      Z(I,J-1) = OR(Z(I,J-1),MSK2)                                      CNTR2670
      Z(I,J) = OR(Z(I,J),MSK2)                                          CNTR2680
      CALL PLOT (XS(2),YS(2),3)                                         CNTR2690
   95 S2 = .FALSE.                                                      CNTR2693
      KNP = KN                                                          CNTR2695
      GO TO 80                                                          CNTR2700
   93 XS(1) = XS(2)                                                     CNTR2710
      YS(1) = YS(2)                                                     CNTR2720
      GO TO 80                                                          CNTR2725
C                                                                       CNTR2730
C     FOUR CROSSINGS                                                    CNTR2740
   55 IF (IN .NE. 0) GO TO 63                                           CNTR2750
      I1 = I                                                            CNTR2760
      J1 = J                                                            CNTR2770
      IF (S1) S2 = .TRUE.                                               CNTR2780
      CALL PLOT (XS(1),YS(1),3)                                         CNTR2790
      GO TO 62                                                          CNTR2800
   63 GO TO (62,87,88,62),IN                                            CNTR2810
   87 IS(4) = IS(3)                                                     CNTR2820
   88 IN = 4 - IN                                                       CNTR2830
      XS(1) = XS(IN+1)                                                  CNTR2840
      XS(IN+1) = XS(IN+2)                                               CNTR2850
      XS(IN+2) = XS(1)                                                  CNTR2860
      YS(1) = YS(IN+1)                                                  CNTR2870
      YS(IN+1) = YS(IN+2)                                               CNTR2880
      YS(IN+2) = YS(1)                                                  CNTR2890
   62 CALL PLOT (XS(3),YS(3),0)                                         CNTR2900
      CALL PLOT (XS(2),YS(2),3)                                         CNTR2910
      CALL PLOT (XS(4),YS(4),0)                                         CNTR2920
      IN = IS(4)                                                        CNTR2930
      IF (.NOT.S1) GO TO 80                                             CNTR2940
      XS(1) = XS(4)                                                     CNTR2950
      YS(1) = YS(4)                                                     CNTR2960
C                                                                       CNTR2965
C     FOLLOW CONTOUR IF NOT AT BOUNDARY OR PREV. DRAWN AREA             CNTR2966
   80 IP = 1                                                            CNTR2970
      Z(I,J) = OR(Z(I,J),MSK1)                                          CNTR2980
      GO TO (71,72,73,74),IN                                            CNTR2990
   71 I = I + 1                                                         CNTR3000
      IF (I .LE. R) GO TO 77                                            CNTR3010
C                                                                       CNTR3015
      GO TO 76                                                          CNTR3020
   72 J = J + 1                                                         CNTR3030
      IF (J .LE. B) GO TO 77                                            CNTR3040
      GO TO 76                                                          CNTR3050
   73 I = I - 1                                                         CNTR3060
      IF (I .GT. L) GO TO 77                                            CNTR3070
      GO TO 76                                                          CNTR3080
   74 J = J - 1                                                         CNTR3090
      IF (J .LE. T) GO TO 76                                            CNTR3100
   77 IF (AND(Z(I,J),MSK1) .EQ. 0.0) GO TO 42                           CNTR3110
C     RESTART SCAN FROM WHERE LAST CONTOUR STARTED                      CNTR3116
```

```
   76  I = I1                                                          CNTR3120
       J = J1                                                          CNTR3130
       IP = 0                                                          CNTR3140
       IN = 0                                                          CNTR3150
       S4 = .TRUE.                                                     CNTR3155
       GO TO 96                                                        CNTR3156
   59  S4 = .FALSE.                                                    CNTR3157
   96  I = I + 1                                                       CNTR3160
       IF (I .LE. R) GO TO 44                                          CNTR3170
       J = J + 1                                                       CNTR3180
       IF (J .LE. 8) GO TO 43                                          CNTR3190
C                                                                      CNTR3195
C      ADVANCE LEVEL AND RESTART IF NOT ABOVE ZMAX                     CNTR3196
       ZMON = ZMON + DZ                                                CNTR3200
       IF (ZMON .GE. ZMAX) GO TO 81                                    CNTR3210
       S1 = .FALSE.                                                    CNTR3215
       K = K - 1                                                       CNTR3220
       IF (K .NE. 0) GO TO 38                                          CNTR3230
       S1 = .TRUE.                                                     CNTR3240
       K = KL                                                          CNTR3250
       GO TO 38                                                        CNTR3260
C                                                                      CNTR3270
C      RESTORE X AND Y ARRAYS, MOVE TO NEXT PLOT, AND RETURN           CNTR3280
   81  DO 82 I = L,R                                                   CNTR3290
   82  X(I) = X(I)*DX + XMIN                                           CNTR3300
       DO 83 I = T,B                                                   CNTR3310
   83  Y(I) = YMIN - Y(I)*DY                                           CNTR3320
       CALL PLOT (SZ(4),0.0,-3)                                        CNTR3330
       RETURN                                                          CNTR3340
C                                                                      CNTR3350
C      ERROR PRINTOUT                                                  CNTR3360
 1001  WRITE (6,2001)                                                  CNTR3370
 2001  FORMAT (33HOERROR IN INTEGER INPUT TO CONPLT)                   CNTR3380
       RETURN                                                          CNTR3390
 1002  WRITE (6,2002)                                                  CNTR3400
 2002  FORMAT (35HOERROR IN COORDINATE DATA TO CONPLT)                 CNTR3410
       RETURN                                                          CNTR3420
 1003  WRITE (6,2003)                                                  CNTR3430
 2003  FORMAT (15HONO Z VARIATION)                                     CNTR3440
       RETURN                                                          CNTR3450
       END                                                             CNTR3460
```

```
ISN 0002              SUBROUTINE PAGEIT(N)
ISN 0003              COMMON /TITLE/ TITLE(9)
ISN 0004              REAL*8 TITLE,DAT
ISN 0005              LOGICAL SW/F/
ISN 0006              DATA LINE,NPAGE /2*0/
ISN 0007              IF (SW) GO TO 5
ISN 0009              CALL DATE(DAT)
ISN 0010              SW=.TRUE.
                C
ISN 0011             5  IF (N.EQ.0) GO TO 10
ISN 0013              LINE=LINE+IABS(N)
ISN 0014              IF (LINE.LE.56) GO TO 15
                C
ISN 0016            10  NPAGE=NPAGE+1
ISN 0017                PRINT 12,DAT,TITLE,NPAGE
ISN 0018            12  FORMAT ('1 CHORDAL ABSORPTION DATA REDUCTION', T86,A8/
                      &  T10,9A8, T86,'PAGE',I4/)
ISN 0019                LINE=0
ISN 0020                IF(N.LT.0) LINE=-N
                C
ISN 0022            15  RETURN
ISN 0023                END
```